

6-26-2023 9:30 AM

Effects of High Glucose on Autophagy and Apoptosis in Preimplantation Mouse Embryo Culture

Virginia Wolfe, *Western University*

Supervisor: Watson, Andrew J., *The University of Western Ontario*

Co-Supervisor: Betts, Dean H., *The University of Western Ontario*

A thesis submitted in partial fulfillment of the requirements for the Master of Science degree in Physiology and Pharmacology

© Virginia Wolfe 2023

Follow this and additional works at: <https://ir.lib.uwo.ca/etd>



Part of the [Cell and Developmental Biology Commons](#)

Recommended Citation

Wolfe, Virginia, "Effects of High Glucose on Autophagy and Apoptosis in Preimplantation Mouse Embryo Culture" (2023). *Electronic Thesis and Dissertation Repository*. 9414.

<https://ir.lib.uwo.ca/etd/9414>

This Dissertation/Thesis is brought to you for free and open access by Scholarship@Western. It has been accepted for inclusion in Electronic Thesis and Dissertation Repository by an authorized administrator of Scholarship@Western. For more information, please contact wlsadmin@uwo.ca.

Abstract

Maternal diabetes increases congenital malformations due to teratogenic effects of glucose on the developing embryo. High glucose culture alters preimplantation embryo development and is associated with increased oxidative stress. Apoptosis and autophagy are programmed cell death and cell survival mechanisms induced by oxidative stress, but their role in preimplantation diabetic embryopathy is poorly elucidated. It was hypothesized in this study that high glucose culture would alter autophagic and apoptotic responses, and that they are dependent on the timing of high glucose culture initiation. High glucose culture impaired blastocyst development and total cell number but did not result in changes in apoptotic measures. Autophagic assessments showed increased autophagosome formation and maturation in hyperglycemic embryos, when cultured from the early 2-cell stage, but not the late 2-cell stage. Overall, high glucose exposure appears to induce autophagy, but not apoptosis in embryos cultured under diabetically relevant glucose concentrations in the mouse embryo. These results increased the knowledge of mechanisms involved in the etiology of diabetic embryopathy.

Keywords

Diabetes, Preimplantation embryo development, apoptosis, autophagy, embryopathy

Summary for Lay Audience

Maternal diabetes, particularly type 1 and type 2 diabetes, is associated with increased fetal malformations or stillbirth during pregnancy. The levels of glucose in the mother's blood affect uterine levels and increase embryo stress, negatively affecting embryonic development. My research exposed mouse preimplantation embryos to elevated concentrations of glucose and analyzed cell death (apoptosis) and cell survival (autophagy) mechanisms in response. Apoptosis mechanisms are initiated by extracellular / intracellular signaling and represent a controlled and sequential process that results in nucleus and cell membrane disintegration and cellular demise. Sometimes this occurs because of cell damage, but it can also be a normal part of controlling cell number and health during embryo development. Autophagy mechanisms promote cell survival by packaging unnecessary or damaged cellular material into a vesicle called an autophagosome, which contains specific tags for degradation. The molecules are released and can be reused as building blocks for other cellular functions. In my research I found that an elevated glucose stimulus in the embryo culture medium does not affect apoptosis, but it does induce autophagy mechanisms. This is important because it suggests the early embryo can employ autophagy to promote survival under the stressful diabetic environment. However, it is still possible the embryo is permanently altered. Additional research employing the high glucose stimulus throughout pregnancy is required to determine if elevated glucose exposure and altered autophagy leads to permanent alterations in the developing fetus.

Co-Authorship Statement

Experiments and designed, performed, and analyzed by Virginia Wolfe in consultation with Dr. Andrew Watson and Dr. Dean Betts, except for assistance from friend and fellow research assistant Zuleika Leung, whose advice and protocols for autophagy measurement were used, and who helped determine primer efficiency for GLUT1 and GLUT3 measurements.

Acknowledgment

First and foremost, I would like to thank my grandpa for being my biggest fan and continual support every day (or mostly night) that I came home from lab. You always wanted to hear about my day and tried your best to understand the work I do. You always provided a listening ear, wise advice, fresh coffee, and a chance to wind down by playing cards or watching a sports game. If there is one thing I didn't think I would learn during my thesis it was that the Packers are factually the best football team and what are the hometowns of each Maple Leaf player. It's been awesome living with you the past two years and getting to know you better as my grandpa and my friend.

Zuleika – I honestly don't know if I would have finished this thesis without you. Thanks for being my continual support and best friend every day both inside and outside the lab. You taught me almost everything I know, from the first embryo I flushed to your secret methods for LC3 analysis. Your positivity, selflessness and logical input while coming along side me when I was stressed has helped me get through some of my toughest days and you have been an invaluable support system in my life. We have made so many memories together, whether it was our late nights working in lab, or other things like getting ice cream or coffees, planning trips, snowboarding, and camping, and going to the beach together and with friends. I am so blessed to have met you and I know that even when we live farther away we are still going to be friends for a very long time.

Thank you to my family also for your support especially in the last few months of my thesis writing. My dad for checking in on me while I was burrowed away in my room, pushing me through my writing blocks, and my mom for all the things you do as well. Thanks for telling me what I need to hear, encouraging me always, and believing me in and my ability to do whatever I set my mind to.

To my amazing supervisors Dr. Watson and Dr. Betts, your mentorship and guidance has been a huge part of bringing me where I am today. Thank you for your dedication to my project and personal development, for your patience, and for helping me have confidence when I didn't believe in myself. Thanks for allowing me independence in pursuing a project of my choosing – and the lessons I learned from doing that. Looking back on who I was when I stepped into the lab

versus who I am today, you have helped me grow in many ways and become a better scientist and researcher.

Thanks to Michele and Hailey for training me and all the mouse work we did together – Michele with your lifelong experience working with embryos, and to Hailey for showing me new techniques and how to oversee a mouse breeding colony.

Thank you also to other members of the DDT lab - Dave, Alex, Andrew, Kendrick, for your friendship and advice – having a good community is so important in the lab environment and I couldn't have asked for better.

Also, thank you to my peers and members of the PPGSC who became my close friends, comic relief, and huge supporters in my extracurricular endeavors to develop leadership skills and play a contributing part in the grad student community.

Finally, a big thank you to the funding sources that supported my M.Sc. journey: the Children's Health Research Institute, Obstetrics and Gynecology Graduate Scholarship (Western University) and WSRG.

Abbreviations

AJ	Adherens junction
AMBRA1	Activating molecule in Beclin-1-regulated autophagy protein 1
AMOT	Angiomotin
APAF-1	Apoptotic protease activating factor-1
aPKC	Atypical protein kinase C
AR	Aldose reductase
ATG	Autophagy-related gene
ATP	Adenosine triphosphate
CAD	Caspase-activated deoxyribonuclease
CAT	Catalase
CDX2	Caudal type homeobox 2
CMA	Chaperone-mediated autophagy
COX	Cytochrome c oxidase
DFF40	DNA fragmentation factor 40
DISC	Death inducing signaling complex
DNA	Deoxyribonucleic acid
ECM	Extracellular matrix
Epi	Epiblast
ER	Endoplasmic reticulum
ESCRT	Endosomal sorting complex required for transport
FADD	Fas-associated death domain
FBP	Fructose 1,6-biphosphate
FGF	Fibroblast growth factor
G6P	Glucose 6-phosphate
G6PD	Glucose 6-phosphate dehydrogenase
GATA3	GATA binding protein3
GATA6	GATA binding protein 6
GLUT	Glucose transporter
GPx	Glutathione peroxidase
GSH	Glutathione
GSSG	Oxidized glutathione
H ₂ O ₂	Hydrogen peroxide
HBP	Hexosamine biosynthetic pathway
HOCl	Hypochlorous acid
hpi	Hours post fertilization
ICM	Inner cell mass
IGF-1	Insulin growth factor 1
LATS	Large tumor suppressor
MII	Second meiotic division
MMP	Matrix metalloproteinase
MOMP	Mitochondrial outer membrane permeabilization
mTOR	Mammalian target of rapamycin
mTORC1	mTOR complex 1
NANOG	Nanog protein homeobox
NBR1	Neighbor of BRCA1 gene 1

NF2	neurofibromin 2
NO•	Nitric oxide radical
NOS	Nitrous oxide synthase
O ₂ ^{•-}	Superoxide radical
OCT4	Octamer-binding transcription factor 4
O-GlcNAc	O-linked N-acetylglucosamine
O-GlcNAcyclation	O-linked-N-acetylglucosaminylation
OGT	O-GlcNAc transferase
OH•	Hydroxyl radical
ONOO ⁻	Peroxynitrite
PCD	Programmed cell death
PE	Phosphatidylethanolamine
PI	Phosphatidylinositol
PI3K	Phosphoinositide 3-kinase
PI3P	Phosphatidylinositol triphosphate
PPP	Pentose phosphate pathway
PrE	Primitive endoderm
R5P	Ribose 5-phosphate
RNA	Ribonucleic acid
ROS	Reactive oxygen species
SAF	Site of autophagosome formation
SOD	Superoxide dismutase
SOX2	SRY-box transcription factor 2
TAZ	Taffazin
TCA	Tricarboxylic
TE	Trophectoderm
TEAD	Transcriptional enhanced associate domain
TNF	Tumor necrosis factor
TRADD	TNF-associated death domain
TUNEL	Terminal transferase-mediated dUTP nick-end labelling
UDP-GlcNAc	Uridine diphosphate N-acetylglucosamine
ULK1	Unc-51-like autophagy activating kinase 1
VEGF	Vascular endothelial growth factor
VPS34	Vacuolar protein sorting 34
WIPI	WD repeat domain phosphoinositide-interacting protein
YAP	Yes-associated protein
ZP3	Zona pellucida 3

Table of Contents

Abstract	ii
Summary for Lay Audience	iii
Co-Authorship Statement	iv
Acknowledgment	v
Abbreviations	vii
Table of Contents	ix
List of Figures	xii
List of Appendices	xiv
Chapter 1	1
1 Introduction	1
1.1 Preimplantation embryo development	1
1.1.1 From fertilization to blastocyst stage	1
1.1.2 Cell differentiation and organization during embryo development	2
1.1.3 Critical period	5
1.2 High glucose during pregnancy	6
1.2.1 Glucose as a teratogen	6
1.2.2 The maternal environment of the preimplantation embryo	6
1.2.3 Impacts in diabetic pregnancy	7
1.3 Glucose metabolism in the preimplantation embryo	8
1.3.1 Glucose transport	8
1.3.2 Glucose metabolism through development	9
1.3.3 Hexosamine biosynthesis pathway	10
1.3.4 Pentose phosphate pathway	10
1.3.5 Glycolysis	11
1.4 Embryonic cellular response to high glucose	12
1.4.1 Development of oxidative stress	14
1.5 Apoptosis	15
1.5.1 Apoptosis initiation	15
1.5.2 Morphological changes	17
1.5.3 Apoptosis in the preimplantation embryo	20
1.6 Autophagy	21
1.6.1 Autophagy initiation	22
1.6.2 Autophagosome elongation	25
1.6.3 Autophagosome maturation	30
1.6.4 Autophagosome degradation	32
1.7 Autophagy in the preimplantation embryo	33
1.7.1 High glucose induction of embryonic autophagy	34
1.8 Methods of measuring autophagy in scientific research	35
1.9 Rationale	36
1.10 Hypothesis	36
1.10.1 Specific Aims	36
Chapter 2	38
2 Materials and Methods	38
2.1 Animals and Ethics Approval	38

2.2	Mouse Superovulation and Mating	38
2.3	Embryo Collection	38
2.4	Media Preparation	39
2.5	Embryo Culture and Experimental Design	40
2.6	Developmental Stage Analysis	41
2.7	Immunofluorescence Techniques	42
2.8	TUNEL Staining to Assess Embryo Apoptosis	43
2.9	Confocal Microscopy	43
2.10	Image Analysis.....	44
2.10.1	Total Cell Number	44
2.10.2	LC3-II Puncta Counts	44
2.10.3	P62 Fluorescence Analysis	45
2.10.4	LC3-II/Lysotracker Colocalization	45
2.11	RNA Extraction and Reverse Transcription (RT)	45
2.12	Quantitative Polymerase Chain Reaction (qPCR)	46
2.13	Statistical Analysis.....	46
Chapter 3	48
3	Results	48
3.1	Effects of high glucose on preimplantation development.....	48
3.1.1	Effects of glucose dose response on preimplantation development when starting at 48 hpi.....	48
3.1.2	Effects of combined high glucose and high O ₂ on development.....	51
3.1.3	Effects of onset timing of high glucose treatment on preimplantation development.....	52
3.1.4	Effects of high glucose treatment beginning at 36 hpi on blastomere proliferation.....	54
3.2	Effects of high glucose on apoptosis and autophagy	55
3.2.1	Effects of high glucose treatment on preimplantation embryo apoptosis.....	55
3.2.2	Effects of high glucose treatment on LC3-II puncta.....	57
3.2.3	Determination of the onset timing of increased LC3-II puncta after 36 hpi glucose treatment	59
3.2.4	Effects of high glucose treatment on p62 immunofluorescence	60
3.2.5	Effects of high glucose treatment on autophagosome formation during preimplantation development.....	61
3.2.6	Effects of high glucose treatment on GLUT1 and GLUT3 mRNA transcript abundance	63
Chapter 4	64
4	Discussion	64
4.1	Effects of high glucose on preimplantation development.....	65
4.2	Effects of high glucose on apoptosis	68
4.3	Effects of high glucose on autophagy	70
4.4	Glucose transporter roles in the embryonic hyperglycemic response	73
4.5	Limitations	74
5	Conclusion and future directions	76
References	77
Appendices	108

Appendix A: Canadian Council on Animal Care and Western University's Animal Care and Use Policies	108
Appendix B: Supplementary Figure	109
Curriculum Vitae	111

List of Figures

Figure 1. Stages and cell fate specification in mouse preimplantation embryonic development. ..	3
Figure 2. Apoptosis via the intrinsic and extrinsic pathways.	19
Figure 3. Autophagy initiation.	24
Figure 4. Phagophore membrane synthesis.	26
Figure 5. Autophagosome elongation and cargo sequestration.	29
Figure 6. Autophagosome maturation.	31
Figure 7. Representative images of mouse preimplantation embryo stages.	42
Figure 8. Blastocyst formation and total cell number after 48 hours of culture under increasing glucose concentrations.	49
Figure 9. Blastocyst formation and hatching after 72 hours of culture under increasing glucose concentrations.	50
Figure 10. Blastocyst formation after combined high (25mM) glucose and high (20%) oxygen exposure.	51
Figure 11. Blastocyst formation and total cell number after high glucose exposure to early and late 2-cell embryos.	53
Figure 12. Ki-67 positive nuclei in blastocysts exposed to high glucose at the early 2-cell stage.	54
Figure 13. TUNEL-positive nuclei in blastocysts exposed to high glucose at the early 2-cell stage.	56
Figure 14. LC3I-II puncta per cell in embryos exposed to high glucose at the early and late 2-cell stage.	58

Figure 15. Developmental series of LC3-II puncta in embryos cultured in high glucose.	59
Figure 16: p62 fluorescence in embryos exposed to high glucose at the early 2-cell stage.	60
Figure 17: Colocalization of LC3-II puncta with Lysotracker Red in embryos treated with high glucose at the early 2-cell stage.	62
Figure 18. Relative mRNA expression of GLUT1 and GLUT3 in blastocyst, morulae (delayed) and arrested embryos.	63

List of Appendices

Appendix A: Canadian Council on Animal Care and Western University's Animal Care and Use Policies	108
---	-----

Chapter 1

1 Introduction

In this introduction I discuss normal preimplantation embryo development and important events during the first week of early embryonic morphological progression. I then present an overview of the physiology of glucose metabolism of the preimplantation embryo, and how this metabolism changes throughout that first week of development. Next, I discuss how high glucose levels affect the preimplantation embryo as we know today, including the composition of the maternal micro-environment, glucose uptake mechanisms, induction of oxidative stress in response to a high glucose environment, and how this may affect apoptosis and autophagy. I conclude this section discussing my objectives, rationale, and hypothesis for this thesis.

1.1 Preimplantation embryo development

1.1.1 From fertilization to blastocyst stage

During ovulation, the oocyte completes first meiotic division and proceeds to metaphase II, creating a mature ovum and a polar body (De La Fuente, 2006; Strączyńska et al., 2022). Sperm enters the oocyte by binding to zona pellucida 3 (ZP3) receptors on the zona surface and then breaking through the zona via an acrosome-mediated reaction. A sharp increase in intra-cellular levels of calcium occurs upon spermatozoa entry, which triggers the second (MII) meiotic division, which creates a second polar body and a female pronucleus ready for gamete fusion (Clift & Schuh, 2013). The goal of preimplantation development is for the fertilized zygote to form a uterine implantation competent blastocyst with a fluid filled cavity, consisting of 3 distinct cell lineages – epiblast (Epi), primitive endoderm (PrE), and Trophectoderm (TE). Embryonic stage progression and cell differentiation are two phenomenon that orchestrate this process. The cell divisions seen during preimplantation are known as “cleavages”, where due to short growth phases, each cell division creates smaller volume cells, while the total embryo volume remains relatively the same (Aiken et al., 2004; Płusa & Piliszek, 2020). The mammalian zygote first cleaves into 2 cells, then 4 cells, then 8 cells, all which appear as identical round

spheres known as blastomeres. The 8-16 cell embryo will begin compaction, where the cell membranes undergo cytoskeleton modifications which increase the contact between adjacent blastomeres, effectually “flattening” the cells until individual blastomeres cannot be distinguished (Maître et al., 2015). At this stage, the mouse embryo is roughly 72 hours post fertilization (hpi) and is referred to as a morula. Around this stage, some blastomeres will become intracellularly polarized due to orientation of the mitotic spindle during cleavage (Zenker et al., 2018). Apical-polarized blastomeres will position to the outer layer of cells in the embryo (TE) and undergo a process known as “actin zippering” where actin rings will extend to cell perimeters and form tight junctions that create a fluid tight epithelial barrier (Ducibella et al., 1975; Zenker et al., 2018). At around 96 hpi, a combination of intracellular and extracellular transcription, signaling, and growth factors will spearhead cavitation, thus forming a blastocyst (Watson, 1992). Na^+/K^+ ATPases and aquaporins in the trophectoderm will support the active transport of ions and passive water diffusion into the embryo, which will allow for increased hydrostatic pressure between cells, creating small spaces called “microlumen” that will lead to the beginning of the embryo cavity and subsequent blastocyst expansion (Zenker et al., 2018). Just prior to implantation, a combination of trypsin-like digestive enzyme release from the trophectoderm cells, along with the outward pressure of the expanding cavity, will weaken and force open the zona (Leonavicius et al., 2018; Sharma et al., 2006). In a process known as “hatching”, trophectoderm cells then proliferate and migrate out through the gap in the zona, allowing them to encounter and initiate implantation into the maternal uterine endometrium.

1.1.2 Cell differentiation and organization during embryo development

The morphological shape and stage progression of preimplantation embryo development occurs in concert with cell differentiation into key lineages of inner cell mass (ICM), primitive endoderm (PrE), and trophectoderm (TE) (Figure 1). During the first few cell divisions, the embryo cells are totipotent stem cells, meaning they can give rise to any of the future cell types in the embryo and its supporting tissue (Cockburn & Rossant, 2010; Yao et al., 2016). The first lineage specification in mouse embryos begins in the compacted 8-16 cell morula, where the cells will differentiate into either the extra-embryonic TE or the pluripotent ICM. Trophectoderm

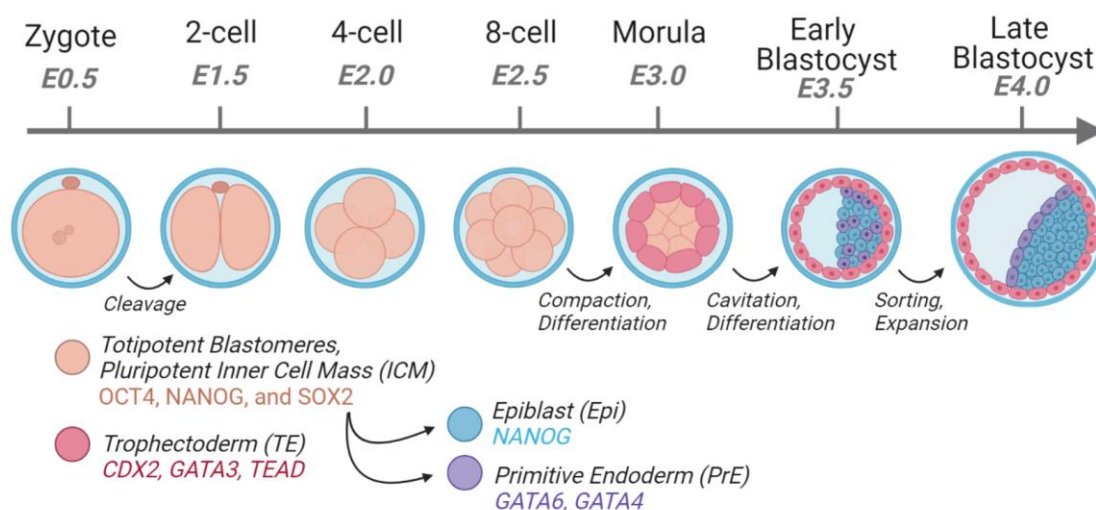


Figure 1. Stages and cell fate specification in mouse preimplantation embryonic development.

Preimplantation embryo development in the mouse occurs from day E0.5 – E4.0. The fertilized mouse zygote progresses through cleavage stages as totipotent blastomere cells until the 8-cell stage. It undergoes compaction and the first cell fate specification, forming the pluripotent inner cell mass and trophectoderm cells. The second cell fate specification occurs in the cavitating early blastocyst, where ICM cells differentiate into epiblast or primitive endoderm cells. Cavity expansion and sorting of the epiblast or primitive endoderm cells results in a mature blastocyst ready for zona pellucida hatching and implantation. Image created with BioRender.com

cells orient to the periphery of the circular embryo and will become trophoblasts, the first embryo-sourced cells of the developing placenta. ICM cells are precursors to the embryonic and extraembryonic tissues and comprise the inner cells of the embryo. This segregation is initiated based on a combination of cell polarity and localization at cell division (Korotkevich et al., 2017), which differentially activates the canonical hippo signaling pathway, effectively creating a mechanism that translates positional information into signaling information (Hirate et al., 2013). Specifically, the protein angiomin 1 (AMOT) is localized to adherens junctions (AJ) between the inner embryonic cells and binds to neurofibromin 2 (NF2) and large tumor suppressor (LATS) to form a protein complex NF2:AMOT:LATS. LATS phosphorylates AMOT, which phosphorylates yes-associated protein (YAP) to signal its degradation. In the polarized outer cells of the compacted embryo, the Par- atypical protein kinase C (aPKC) complex sequesters AMOT to the apical domain, disrupting the AJ complex, thus turning off Hippo signaling (Hirate et al., 2013). In the absence of Hippo signaling, YAP is expressed ubiquitously, and binds to tazzin (TAZ) to form a complex that travels to the nucleus and interacts with transcriptional enhanced associate domain (TEAD) factors. (Hirate et al., 2013). TEAD is a transcription factor for caudal type homeobox 2 (CDX2) and GATA binding protein 3 (GATA3), key genes in the specification of the TE lineage (Nishioka et al., 2008, 2009). In the inner cells, activated hippo signaling prevents CDX2 transcription, which allows octamer-binding transcription factor 4 (OCT4) signaling due to the mutually exclusive inhibitory effect of CDX2 and OCT4 on each other. OCT4, NANOG, and SRY-Box Transcription Factor 2 (SOX2) expression will eventually specify the inner cell mass (Strumpf et al., 2005).

During the second cell-fate specification, which occurs in the early-cavitating blastocyst, ICM cells will differentiate into PrE and Epi fates. PrE cells will then sort into a single layer surrounding the epiblast cells on their basolateral side and facing the blastocyst cavity on their apical side. The mechanisms driving ICM to Epi and PrE differentiation have been long contemplated, and many theories attribute this lineage separation to be driven by cell position (Rossant, 1975), polarized cell divisions (Morris et al., 2010), exposure to TE signaling factors (Mihajlovic et al., 2015), and fibroblast growth factor (FGF) signaling. As seen in Figure 1, the current understanding is that in the E3.0-E3.25 stage embryo (cavitation stage), a randomized

“salt-and-pepper” distribution of cells expressing the (mutually co-inhibitory) genes Nanog protein homeobox (NANOG; Epi-specific) and GATA binding protein 6 (GATA6; PrE-specific) begins to form (Chazaud et al., 2006). It is thought that reciprocal NANOG/GATA6 ratios act in coordination with levels of FGF4 and FGF2 signaling to create a gene-regulatory network that is sufficient for cell fate specification (Goldbeter et al., 2014). The origins of the Nanog/Gata6 ratio and mechanisms controlling it are multifactorial, however many studies point to FGF signaling as the probable initiator. How FGF signaling is regulated is currently unknown, though some theories suggest that FGF4 signaling is heterogeneously distributed in the ICM cells through stochastic “transcriptional noise” (i.e. intrinsic variation between cells; Ohnishi et al., 2013), or through inherited bias during the 8-16 and 16-32 cell division (Morris et al., 2010). In summary, FGF signaling, in combination with the NANOG/GATA6 ratio drive cell differentiation to Epi or PrE fates. A diagram depicting the stages of mammalian preimplantation development and associated cell differentiation can be seen in Figure 1 below.

1.1.3 Critical period

Successful embryo development requires the fulfillment of sequential growth checkpoints. Alterations to the early patterns in embryo growth can affect the developmental trajectory of the organism, causing detrimental effects to the later fetus or individual. Teratogens are substances which have the capacity to alter the embryonic developmental trajectory, causing birth defects (Coles, 1994). Teratogens are classified into four types: physical agents, metabolic conditions, infection, and chemicals (Dutta, 2015). Embryos are especially susceptible to teratogenic effects during the “critical periods” in preimplantation development – windows of time associated with specific developmental checkpoints during which the developmental trajectory can be affected by a specific teratogen (Coles, 1994). As organ development occurs during the post-implantation period of the first trimester, weeks 3-8 of human embryo development are considered a critical period. The preimplantation period of the first trimester is generally considered an “all-or-none” period as the embryo can either recover from less severe exposures without congenital abnormalities or else terminate itself under severe exposures, thereby preventing the birth of an

organism with severe defects (Coles, 1994; Dutta, 2015). However, this is not always the case, and studies have shown that some teratogens can disturb embryo development during the preimplantation period without causing embryo death (Akar et al., 2019; Fabro et al., 1984; Legault et al., 2021). Therefore, it is important to study such teratogens to further understand the etiology of congenital diseases and disorders.

1.2 High glucose during pregnancy

1.2.1 Glucose as a teratogen

Implicated in diseases such as maternal diabetes and other metabolic disorders, high glucose exposure can alter embryonic development causing congenital malformations in limbs and neural development of the fetus, pregnancy loss, and other conditions (Hawthorne et al., 1997). Although a strong link between high glucose and malformations is established (Schaefer et al., 1997), the precise mechanism by which it occurs is not known. In the next section, I introduce the importance of normo-glucose concentrations in embryonic development and metabolism, and the effects of hyper-glucose concentrations on embryo development and cellular function in other cellular systems.

1.2.2 The maternal environment of the preimplantation embryo

During mammalian preimplantation development, a delicate relationship between the embryo and its micro-environment supports the simultaneous embryonic development and transport from the oviduct to the uterine tube. The early mouse embryo is present in the oviduct from days 1-3, entering the uterine tube at the morula stage and beginning implantation and endometrial decidualization at the end of day 4 (Matsumoto, 2017; Paria et al., 1993; Yoshinaga, 2013). Oviductal fluid contains nutrients, growth factors, antioxidants, sex hormones, proteases, signaling factors, and embryonic feedback secretions (Li & Winuthayanon, 2017). It maintains temperature, pH levels, and oxygen levels, and acts as a source for blastocyst fluid (Li & Winuthayanon, 2017). The concentration of glucose in the mouse follicular fluid, oviductal fluid, and uterine fluid have been measured at approximately 0.46, 1.09, and 0.61 mmol/L,

respectively, with plasma levels around 11.71 mmol/L (Harris et al., 2005). Other studies report basal oviductal glucose concentrations of 3.4 mmol/L (Gardner & Leese, 1990) and blood glucose concentrations reported ranging from 3.5-9.7mmol/L (Han et al., 2008; Harris et al., 2005). Reports from Jackson Laboratories state the oviductal concentration ranges from 4.4-5.6 mmol/L (Danielle Fontaine, 2019). Overall, serum glucose levels are slightly higher than that of follicular and oviductal fluids, though they increase and decrease proportionally to each other (Gardner & Leese, 1990). Bovine studies show there is a direct association between concentrations of energy substrates in oviduct fluid and in plasma. Oviduct glucose, lactate, and pyruvate levels were all positively associated with plasma glucose, lactate, and pyruvate, respectively ($P < 0.01$) (Dean, 2019; Hugentobler et al., 2008). The reproductive tract must maintain glucose concentrations within an optimal level in both a temporal and spatial manner as the embryo moves into the uterus, and changes in plasma glucose levels can alter these levels.

1.2.3 Impacts in diabetic pregnancy

Gestational, type 1, and type 2 diabetes can cause alterations from fertilization throughout pregnancy and beyond. It can predispose the fetus to many congenital malformations in organogenesis, growth restriction, or insulin resistance causing macrosomia (abnormally large infant body size) (Negrato et al., 2012). The highest risk for fetal malformations is reported for women with type 1 or type 2 diabetes. An intermediate risk is reported for overweight or prediabetic women developing gestational diabetes, while otherwise healthy pregnant women with gestational diabetes experience perinatal outcomes similar to the general population (Castori, 2013). In offspring of mothers with type 1 diabetes, a study in the Netherlands found that despite glycemic control and folic acid supplementation, increased rates of pre-eclampsia (12.7%), preterm delivery (32.2%), caesarean section (44.3%), congenital malformations (8.8%), perinatal mortality (9; 2.8%) and macrosomia (45.1%) were seen compared to the general population, and neonatal morbidity was increased by 80.2% (Evers et al., 2004). The degree of high glucose that the fetal tissues are exposed to has a significant effect on the embryo. In type 1 and type 2 diabetic women the embryo is exposed from the earliest stages and is more likely to affect primordial organ development or cease development altogether. The major congenital

malformations seen include cardiovascular, central nervous system, gastrointestinal, urinary tract, or limb and extremity effects such as caudal regression or a cleft palate (Negrato et al., 2012). Gestational diabetes develops during the second or third trimester of pregnancy, bypassing effects to organogenesis and instead leading to hypertrophy of insulin-sensitive tissues, macrosomia, and metabolic issues later in life (Canadian Diabetes Association, n.d.).

1.3 Glucose metabolism in the preimplantation embryo

The importance of glucose during mammalian preimplantation embryo development is undisputed, as the embryonic transition from pyruvate to glycolytic energy metabolism during the cavitation stages is well known (Sutton-McDowall & Thompson, 2015). Glucose metabolism plays a role in cumulus cell expansion during oogenesis (Sutton-McDowall et al., 2010) and in cell differentiation and commitment to ICM vs TE cell fate (Chi et al., 2020). Mouse preimplantation embryos cultured devoid of glucose form small and cellular-deficient morulae without progression to the blastocyst stage (Chatot et al., 1994; Pantaleon et al., 2008), but even 1-minute pulses of glucose exposure at specific time points can rescue this phenotype and restore standard cavitation rates (Chatot et al., 1994). Therefore, mouse embryos require glucose exposure for normal proliferative, differentiative, and metabolic development to the blastocyst stage (Pantaleon et al., 2008).

1.3.1 Glucose transport

In the mouse embryo, glucose is taken up through glucose transporters (GLUTs). Out of the 14 currently known GLUTs (Pantaleon & Kaye, 1998), GLUT1 and GLUT3 are considered the main transporters involved in glucose uptake and metabolism in the preimplantation embryo, though other GLUTs are implicated in various studies (Pantaleon & Kaye, 1998). In early studies, GLUT1 was found in all preimplantation stages of the mouse and localized throughout both the trophectoderm and ICM cells, GLUT2 was expressed from the 8-cell stage and preferentially localized to the trophectoderm membranes facing the blastocyst cavity, while GLUT4 presence was not detected up to the blastocyst stage. Based on its cellular localization, GLUT1 was considered the primary transporter of glucose up to the blastocyst stage (Aghayan et

al., 1992; Hogan et al., 1991). Later studies rejected this theory and put forward that GLUT3 (first expressed around the compaction stage), rather than GLUT1, was primarily responsible for glucose uptake by blastocysts (Pantaleon et al., 1997). This theory was based on subcellular GLUT3 localization to the outer TE cells during compaction and cavitation (indicating access to maternal glucose supply), while GLUT1 is nuclear during early cleavage stages, it is then localized on the basolateral membrane of TE cells after cavitation (Pantaleon et al., 2001). GLUT3 also has a lower K_m value for glucose transport, meaning it is more efficient and better suited to the low glucose concentrations in uterine fluid. Further, the initiation of glucose-dependent metabolism occurs around the time of GLUT3 expression, and inhibition of GLUT3 protein expression with antisense oligodeoxynucleotides prevents blastocyst formation (Pantaleon et al., 1997). Later studies have implicated the co-ordination of GLUT1 and GLUT3 in glucose uptake (Pantaleon & Kaye, 1998). In TE cells, GLUT1 provides both efflux and influx methods of glucose transport, with a low K_m value ($1\text{--}2\text{ mmol l}^{-1}$) for influx and a higher K_m value ($20\text{--}30\text{ mmol/L}$) for efflux (Thorens, 1996). Thus, consistent with its kinetic characteristics, the polarized expression of GLUT3 (apical) and GLUT1 (basolateral) across the TE cells facilitates the influx of glucose into trophectoderm cells from the uterine fluid and subsequent efflux into the blastocyst cavity as a glucose reservoir. This reservoir could then provide glucose for the glycolytic activity of the ICM by influx through GLUT1 in the ICM cells in its low K_m mode (Pantaleon & Kaye, 1998). In addition, GLUT1 is an insulin growth factor-1 (IGF-1) responsive transporter, and its expression is increased in response to culture in low glucose conditions. This allows an embryo to positively respond to its outer environment and increase glucose uptake in response to growth and proliferative stimuli within the ICM (Pantaleon & Kaye, 1998).

1.3.2 Glucose metabolism through development

Preimplantation embryonic development is associated with a change in preference of energy metabolism pathways. During the earliest cleavage stages, exogenous pyruvate is the major energy substrate, metabolized through the Krebs cycle to maintain a redox state (Chi et al., 2020). At the morula stage, glucose uptake becomes necessary for biosynthesis and

differentiation signaling, while pyruvate continues to be the major nutrient utilized for energy production (Chi et al., 2020). As the embryo transitions from the morula to the blastocyst stage, glucose uptake, oxygen utilization and glycolysis increase sharply, preparing the embryo for invasion into the maternal endometrium (Sharpley et al., 2021). The mechanisms that govern this sequence of events balance the redox control, bioenergetics, and biosynthesis within the developing preimplantation embryo, and are discussed below, with a special emphasis on the role of glucose.

1.3.3 Hexosamine biosynthesis pathway

The three major arms of glucose metabolism throughout embryo development are glycolysis, the pentose phosphate pathway (PPP) and hexosamine biosynthetic pathway (HBP) (F. Chi et al., 2020). The HBP uses 2-5% of the environmental glucose supply in embryos (Marshall et al., 1991), diverging from glycolysis at fructose-6-phosphate. The HBP plays key roles in sensing the nutritional environment in the cell. It integrates molecules coming from carbohydrates, fatty acids, amino acids and nucleotides into an activated amino sugar and an energy substrate called uridine diphosphate N-acetylglucosamine (UDP-GlcNAc) (Denzel & Antebi, 2015). The GlcNAc portion is used in protein modifications such as N- and O-linked glycosylation in the endoplasmic reticulum (ER) and Golgi apparatus, and for single sugar conjugation to proteins catalyzed by O-GlcNAc transferase (OGT) in the cytoplasm, nucleus, and mitochondria (Akella et al., 2019; Butkinaree et al., 2010). These processes allow changes in cell signaling (growth, survival, and homeostasis), metabolism, gene regulation, and cellular reorganization processes (Akella et al., 2019).

1.3.4 Pentose phosphate pathway

The proportion of glucose uptake directed towards the PPP ranges from 10-15% in cleavage stages of the preimplantation embryo to 1-5% in the blastocyst stages in all of mouse, bovine and sheep embryos (Javed & Wright, 1991; O'Fallon & Wright, 1986; Wales & Du, 1993). Despite the altered proportion of glucose throughput, PPP activity is still elevated in the blastocyst due to increases in the total amount of glucose uptake during this time (Javed & Wright, 1991; O'Fallon

& Wright, 1986; Wales & Du, 1993). The PPP diverges after the first step glucose 6-phosphate (G6P) of glycolysis and plays key roles in regulation of cellular reduction-oxidation (redox) homeostasis and biosynthesis (Ge et al., 2020). It consists of both oxidative branches and non-oxidative branches, which occur in the cytosol. Glucose 6-phosphate dehydrogenase (G6PD) is the rate-limiting enzyme of the oxidative PPP, the first of a series of enzymes that convert G6P into ribose 5-phosphate (R5P) and associated NADPH production. NADPH and R5P are two metabolites vital for the survival and proliferation of cells. R5P is a building block for nucleotide biosynthesis which is essential for DNA replication and damage repair (Wamelink et al., 2008). NADPH is the reducing power required for the synthesis of fatty acids, sterols, nucleotides, and non-essential amino acids (Patra & Hay, 2014). Furthermore, NADPH reduces oxidized glutathione (GSSG) to glutathione (GSH), an important cellular antioxidant. Controversially, it also acts as a substrate for NADPH oxidases to produce reactive oxygen species (ROS) (Yen et al., 2020). The PPP is the largest contributor to cytosolic NADPH, important in maintaining the cell's redox state (Ge et al., 2020). When the PPP is blocked during cleavage stages, mouse embryos are blocked at compaction, failing to form blastocysts due to redox disruption and the inability to form ribose-based nucleotides (Chi et al., 2020).

1.3.5 Glycolysis

While the cleavage-stage embryo is largely reliant on exogenous pyruvate for energy metabolism and ATP generation, a metabolic switch occurs at the morula to blastocyst cavitation stage, resulting in high levels of glucose uptake and a utilization of anaerobic glycolysis as the largest portion of glucose metabolism in the embryo. Cleavage stage embryos exhibit quiet embryo metabolism, with mitochondria functioning at a minimal level needed to supply the embryo's energy requirements (Leese & Barton, 1984). This maintains low reactive oxygen species production which benefits preimplantation embryo development by maintaining a low stress environment (Leese & Barton, 1984). As first noted by Otto Warburg, in cancer cells, aerobic glycolysis is the preferential conversion of glucose into lactate in the presence of available oxygen and mitochondrial activity (Warburg, 1956). Blastocysts also make use of this effect to support their metabolic requirements and rapid cell proliferation phenotype, converting from

34% up to 90% of glucose uptake in mouse and human blastocysts into lactate as the blastocyst readies for implantation (Gardner & Leese, 1987; Gott et al., 1990). While mammalian somatic cells utilize glucose for oxidative phosphorylation and extensive ATP production, lactate generation through aerobic glycolysis serves the embryonic system as a crucial signaling molecule, a fuel source, and a redox buffer between the glycolytic and oxidative phosphorylation systems in the embryo (Gardner, 2015). Specifically, extensive lactate levels create lactic acid, which decreases the pH of the embryonic micro-environment. This activates proteases such as the matrix metalloproteinases (MMPs), allowing controlled degradation of the extracellular matrix (ECM) of the endometrium to facilitate trophoblast invasion. It also stimulates cytokine signaling and angiogenesis via vascular endothelial growth factor (VEGF) induction (Gardner, 2015). Besides mediating embryonic implantation, lactate can modulate the redox state of the embryo, altering the ratio of $\text{NAD}^+:\text{NADH}$ ratio through its conversion to pyruvate with the lactate dehydrogenase (LDH) enzyme. While the early embryo is highly dependent upon pyruvate, changes in redox control ability with the maturing blastocyst allow for metabolic plasticity through lactate-pyruvate conversion (Sharpley et al., 2021). This contributes to the differential transcriptional reprogramming of later-stage embryos during homeostasis or upon adaptation to environmental changes (Sharpley et al., 2021).

1.4 Embryonic cellular response to high glucose

High glucose exposure is associated with perturbed preimplantation embryo development in both murine and bovine models, decreasing embryo quality and implantation rates (Cagnone et al., 2012; Fraser et al., 2007). Preimplantation embryos are sensitive, yet adaptive to changes in their environment that may compromise homeostasis. The general understanding is that high glucose induces a primary response of sustained generation of ROSs and depletion of antioxidants in the preimplantation embryo, which may lead to a plethora of effects. Some cell types are more vulnerable to high glucose levels than others due to their ability to reduce glucose transport such that their internal glucose concentration remains constant (Brownlee, 2005). For example, smooth muscle cells adapt to changes in extracellular glucose concentrations by modifying their hexose-transport activity, while vascular endothelial cells lack this autoregulatory mechanism.

(Kaiser et al., 1993). Preimplantation embryos are also unique in their ability to respond to glucose levels. It was first shown in 1998 that there were decreased concentrations of free glucose in preimplantation embryos of diabetic mice at 96 and 48 hours, associated with decreases in glucose transporter GLUT1, GLUT2 and GLUT3 expression (Moley, Chi, & Mueckler, 1998).

High glucose levels cause changes in glucose allocation to various metabolic pathways, which can lead to the production of ROS, as described below. The polyol pathway reduces glucose into polyols such as sorbitol and galactitol using NADPH. Polyol accumulation leads to oxidative stress and is the center of diabetic pathologies such as retinopathy, nephropathy and neuropathy (Fu et al., 2007). Increased intracellular levels of polyols are detected in preimplantation embryos exposed to high glucose (Eriksson et al., 1989; Moley et al., 1996). This increases NADH/NAD⁺ ratios, which leads to abnormal cellular redox levels, removing the primary reducing power for the synthesis of the important cellular antioxidants such as glutathione (N. Xie et al., 2020). Hexosamine signaling is implicated in a negative preimplantation embryonic response to glucose. UDP-GlcNAc, produced by the HBP, is a substrate for O-linked protein glycosylation (O-GlcNAcylation), of regulatory proteins, altering their activity in a manner similar to phosphorylation (Pantaleon et al., 2009). The enzymes involved are sensitive to UDP-GlcNAc levels, and therefore depend on glucose flux through the HBP pathway (Pantaleon et al., 2009). Excess HBP flux is associated with reduced cell proliferation and blastocyst formation, depletion of GSH (Horal et al., 2004), and alteration of the regulation of embryonic cellular proliferation and survival PI 3-kinase/Akt pathway (Pantaleon et al., 2009). Interestingly, nutrient deprivation induces HBP flux similarly as does nutrient excess, as it was found that following glucose or essential amino acid shortage, activation of the GCN2-eIF2 α -ATF4 stress pathway increases glutamine--fructose-6-phosphate transaminase (GFAT1) production, stimulating HBP flux and increased protein O-GlcNAcylation in mouse fibroblasts and epithelial cells (Chaveroux et al., 2016). In wildtype preimplantation embryos cultured from the 2-cell stage with 25 or 55mM of glucose, mitochondrial mass and gene expression of the mitochondrial cytochrome c oxidase genes (COX-1 and COX-2) were decreased significantly. COX plays major roles in cellular oxygen consumption and aerobic ATP generation. The simultaneous

deregulation of GLUT1 and GLUT3 in these embryos suggests that decreased glucose flux induces mitochondrial demise, which may, in turn, affect other cellular mechanisms (Shen et al., 2009). In other studies, decreased glycolysis, increased pyruvate uptake, inability to oxidize pyruvate, and a slowing of the Krebs cycle occurs in response to a hyperglycemic uterine environment, which may also lead to the apoptotic effects often associated with high glucose levels (M. Chi et al., 2002; Dumollard et al., 2007). With multiple studies showing a decrease in glucose transporter protein and expression under high glucose culture, the possibility of embryopathy due to nutrient deprivation must be considered (Dumollard et al., 2007). The categorically increased levels of ROS found in hyperglycemic embryo studies may just as well be a result of increased oxidative phosphorylation and ROS production in overly functioning mitochondria, as the inability to reduce ROS levels in the embryo.

1.4.1 Development of oxidative stress

Oxidative stress is a state of cellular physiology caused by an imbalance between production and accumulation of ROS in cells and tissues, and the inability of a biological system to detoxify these reactive products. This can be caused by factors that increase ROS production, decrease the efficacy of ROS removal, or both (Pizzino et al., 2017). ROS can be produced from a variety of sources in the preimplantation embryo, such as mentioned above. Superoxide radical ($O_2^{\bullet-}$) is generated by NADPH oxidase, xanthine oxidase, and peroxidases. Once formed, it is involved in several reactions that generate hydrogen peroxide, hydroxyl radical (OH^{\bullet}), peroxynitrite ($ONOO^-$), hypochlorous acid ($HOCl$), and so on. Hydrogen peroxide (H_2O_2 ; a nonradical) is produced by multiple oxidase enzymes, that is, amino acid oxidase and xanthine oxidase. OH^{\bullet} , the most reactive among all the free radical species in vivo, is generated by reaction of $O_2^{\bullet-}$ with H_2O_2 , with Fe^{2+} or Cu^+ as a reaction catalyst (Fenton reaction) (Pizzino et al., 2017). Nitric oxide radical (NO^{\bullet}), which plays important physiological roles, is synthesized from arginine-to-citrulline oxidation by nitric oxide synthase (NOS). These can act as signaling factors or substrates and alter cellular processing. Cells deploy an antioxidant defensive system based mainly on enzymatic components, such as superoxide dismutase (SOD), catalase (CAT), and

glutathione peroxidase (GPx), to protect themselves from ROS-induced cellular damage (Pizzino et al., 2017).

In embryos, oxidative stress left untreated can lead to lipid peroxidation, RNA and DNA rupture, and oxidation of proteins including inactivating many different enzymes, ultimately resulting in cellular demise (Ornoy, 2007). Oxidative distress also disrupts metabolic and signaling pathways, which can alter the expression of cell fate genes, thus affecting the bioenergetics and epigenetic landscape of the embryo. Finally, oxidative stress can induce cell death pathways such as apoptosis and autophagy in the embryo (Hardy et al., 2021).

1.5 Apoptosis

Apoptosis is a highly conserved and necessary cellular process that executes the protease-mediated termination and phagophore clearance of a cell following the activation of apoptotic signals. The cell detaches from surrounding tissue and compartmentalizes into shrunken “blebs” of organelles and cytoplasm for removal by phagocytosis, all while avoiding damage to the surrounding tissues (Obeng, 2021). Apoptosis is an essential programmed cell death (PCD) pathway – under normal conditions it is critical for tissue homeostasis, tissue growth control during embryonic development, and immune system development (Jacobson et al., 1997). Alternatively, apoptosis can be activated in response to a damaging or stressful cellular environment, and its dysregulation can lead to the development of pathologies such as embryonic maldevelopment, cancer (lack of sufficient functioning apoptosis), degenerative diseases such as Alzheimer’s, acquired immune deficiency syndrome, aplastic anemia, and myocardial infarction (excessive apoptosis) (D’arcy, 2019).

1.5.1 Apoptosis initiation

Cellular apoptosis is initiated through extrinsic or intrinsic signaling mechanisms. The extrinsic pathway is mediated through the interaction of death ligands with death receptors. As illustrated in Figure 2, death receptors are members of the tumor necrosis factor (TNF) family, which includes TNFR1, FAS, DR3 TRAIL-R1, TRAIL-R2. Death ligands (TNF, FAS-L, TLIA,

TRAIL) are released from natural killer cells, or macrophages, and correspond to their specific death receptor (Bossen et al., 2006). Ligand and receptor interactions transmits an extracellular death signal to the Fas-associated death domain (FADD) or TNF-associated death domain (TRADD) in the cytoplasm, which activate caspase-8 or caspase-10 to form the death inducing signaling complex (DISC) (Goldar et al., 2015; Obeng, 2021). This in turn activates executioner caspases -3, -7 and -9, the last step of apoptosis, which are discussed below (Elmore, 2007).

Intrinsic signaling involves activation arising from stimuli such as cell damage, DNA damage, oxidative stress, endoplasmic reticulum stress, hypoxia, and other insults (Elmore, 2007; Zhang et al., 2021). It is activated intracellularly and controlled through the Bcl-2 protein family, which contains both pro-apoptotic and anti-apoptotic members (Peña-Blanco & García-Sáez, 2018). The pro-apoptotic members are the Bax family (Bax, Bok and Bak) and the BH3-only proteins, Bid, Bad, and Bim. The anti-apoptotic members include Bcl-2, Bcl-xL, Bcl-w, Mcl1, and A1. As shown in Figure 2, a key event in intrinsic apoptosis is the release of cytochrome c into the cytosol from the mitochondria – an initiator of the caspase-mediated apoptotic cascade (Martinou & Youle, 2011). Under normal stress levels, anti-apoptotic Bcl-2 proteins dimerize with and inhibit the pro-apoptotic proteins to prevent apoptosis (Peña-Blanco & García-Sáez, 2018), and Bax is largely cytosolic and inactive. Under apoptotic signaling, BH3-only proteins are activated, escaping from Bcl-2 protein inhibition. Bax accumulates at the mitochondria and activates upon joining to BH3-only proteins. This interaction induces a conformational change that allows Bax to insert itself into the hydrophobic membrane, which in turn displaces BH3 proteins. Transient exposure of the BH3 domain allows an adjacent Bax or Bak molecule to bind in this groove, creating a symmetric dimer and pore (Peña-Blanco & García-Sáez, 2018). This is known as mitochondrial outer membrane permeabilization (MOMP) (Peña-Blanco & García-Sáez, 2018). An alternative path to achieve MOMP is through apoptotic stimulation of p53, the “tumor suppressor” gene, that is induced specifically in response to DNA damage. p53 is normally present in the cytosol at low levels, but under genomic stress it accumulates in the nucleus and temporarily arrests the cell cycle in the G1 phase, allowing it time for DNA repair (Amaral et al., 2010). If DNA is not repaired, p53 binds directly Bcl-2 family apoptotic targets (Bax, Noxa or PUMA) induce intrinsic mitochondrial cell death (Ozaki & Nakagawara, 2011; J. Yu & Zhang,

2008). P53 has the capability to execute its functions through intrinsic or extrinsic pathways, depending on its phosphorylation pattern, cell type, and the specific kinases that activate it (Amaral et al., 2010).

After MOMP, cytochrome C is released from the mitochondrial intermembrane space through Bax:Bak pores and binds to APAF-1 (apoptotic peptidase activating factor 1). Multiple APAF-1 subunits form an apoptosome complex, which provides an activation platform for the caspase-9 apoptosis initiating protease (Würtle & Rehm, 2014) (Figure 2). Apoptotic protease activating factor-1 (APAF-1) contains a caspase recruitment domain, a nucleotide binding and oligomerization domain and a COOH-terminal WD40 repeat domain. Cytochrome c binds to the WD domain, activating APAF-1, which then oligomerizes into a homo-heptameric apoptosome backbone (Reubold et al., 2011; Würtle & Rehm, 2014). Inactive cytoplasmic procaspase-9 is activated upon binding to the APAF-1 backbone, completing formation of the apoptosome. Both intrinsic and extrinsic pathways converge at the executioner proteases (caspase-3 and -7) which execute the morphological breakdown of the cell (Elmore, 2007).

1.5.2 Morphological changes

Apoptosis is characterized by cellular shrinkage and condensation of the nuclear chromatin, followed by nuclear karyorrhexis and cellular detachment from surrounding tissue. The cell becomes convoluted, forming extensions. Some extensions separate from the main body into small, compacted apoptotic bodies containing densely packed organelles, nuclear parts, and mitochondria (Saraste, 2000). Many of these changes are induced by the actions of caspase proteases, largely by caspase-3 and caspase-7, which target proteins such as actin, beta-catenin, laminin, MEKK-1, keratins, and many other structural and adhesion proteins involved in maintaining cellular membrane, nuclear lamina, nuclear envelope, chromatin structure, and cell-cell integrity (Cardone et al., 1997; Nicholson & Thornberry, 1997; Orth et al., 1996; Saraste, 2000; Takahashi et al., 1996; Wen et al., 1997). Caspases are cysteine proteases that are activated by cleaving their substrate proteins beside aspartate residues (Thornberry & Lazebnik, 1998). DNA disintegration is completed by endogenous DNases (DNA fragmentation factor 40 (DFF40), and caspase-activated deoxyribonuclease (CAD)), which cut through double stranded

DNA, leaving fragmented ends (Saraste, 2000). Apoptotic clearance requires the phagocytosis of the apoptotic cell by macrophages, parenchymal cells, and neighboring cells. It is signaled by the release of cell surface markers (phosphatidylserine) from the cell membrane. Failure in this process would cause apoptotic cell accumulation, leading to inflammation or secondary necrosis (Savill and Fadok, 2000; Kurosaka et al., 2003). Therefore, timely and effective clearance of apoptotic cells in multicellular organisms is important for the homeostasis of the organism (Doran et al., 2020). There are many research methods used to detect apoptosis. Some of the most common methods are by the expression of relative concentrations of pathway components such as (1) Bcl-2 family members at the mRNA or protein level (Ludwig et al., 2019), (2) analyzing annexin V, a marker of phosphatidylserine surface marker translocation (van Engeland et al., 1998), (3) activation of caspases, often through fluorescence microscopy or western blot (Amstad et al., 2001), and (4) detection of cleaved marker proteins such as PARP (X. Li & Darzynkiewicz, 2000), and through the terminal transferase-mediated dUTP nick-end labelling (TUNEL) assay of cleaved DNA by fluorescent labelling of 3'OH ends generated during apoptosis (Kyrylkova et al., 2012). A diagram of the discussed apoptotic pathways is depicted in Figure 2.

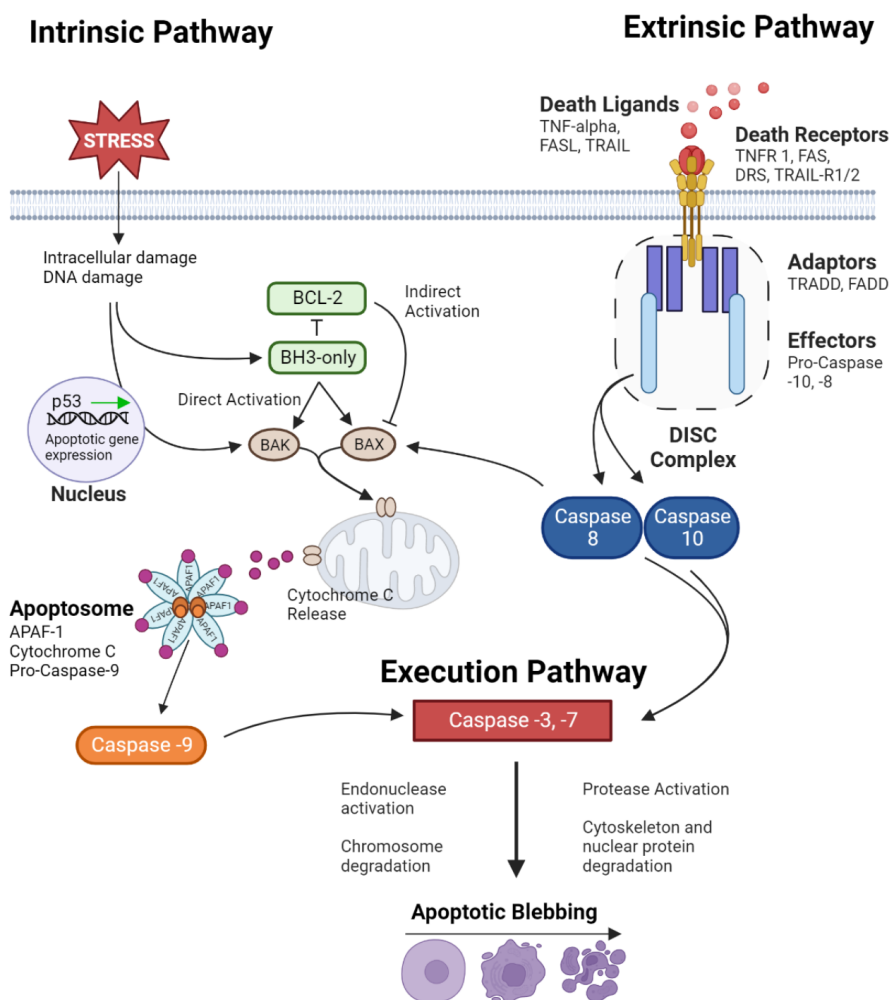


Figure 2. Apoptosis via the intrinsic and extrinsic pathways.

The intrinsic pathway is initiated intracellularly by the cell itself in response to damage. This activates the BH3-only proteins, releasing them from Bcl-2 inhibition and allowing them to bind to Bax or Bak proteins which dimerize and form a pore in the mitochondrial membrane. Cytochrome c is released and facilitates formation of the apoptosome with APAF1 protein and caspase-9 activation. In the extrinsic pathway, death ligands activate death receptors, leading to the formation of the DISC complex and Caspase -8, -10 activation. Caspase-8 can also contribute to mitochondrial cytochrome c release by activating Bax proteins. Both pathways converge when caspase 3 or caspase 7 (executioner caspase) is activated, causing breakdown of cell, DNA and organelles and subsequent cell death. Image created with BioRender.com.

1.5.3 Apoptosis in the preimplantation embryo

Apoptosis is a normal mechanism in development and tissue homeostasis in many organisms (Brill et al., 1999; Brison, 2000). In the preimplantation embryo, it functions to remove damaged cells and regulate germline cell number. It also regulates cells that are no longer required due to tissue morphogenesis, inappropriate phenotype, or with genetic or chromosomal abnormalities (Brill et al., 1999; Brison, 2000). Apoptosis first appears in the 32- to 64-cell mouse embryo (Brill et al., 1999), and occurs primarily in the ICM cells with a 10%–20% amount of ICM cell removal by E4.0 (Copp, 1978). It is proposed that the apoptotic process in the ICM eliminates cells that failed to translocate to the correct position for their fate during the segregation of the PE and EPI cell populations (Meilhac et al., 2009). One example of apoptosis under normal conditions is its role in pre-amniotic embryo cavitation and tube morphogenesis (Orietti et al., 2021). In preimplantation embryos exposed to high glucose levels, increased levels of apoptosis are observed in multiple studies. In studies performed on mouse preimplantation embryos *in vitro*, apoptosis increased in glucose exposures between 25.5mM to 55mM (M. Chi et al., 2000, 2002; Fraser et al., 2007; Keim et al., 2001; Leunda-Casi et al., 2002; Moley, Chi, Knudson, et al., 1998; Pantaleon et al., 2009; Shen et al., 2009). Many of these studies also reported decreased cell number, proliferation, and blastocyst formation.

The complete mechanism by which glucose induces apoptotic effects on the embryo is still largely unknown, however the involvement of various signaling mechanisms have been studied. Some studies have shown an increase in Bax signaling through the intrinsic cell death pathway (M. Chi et al., 2000; Peña-Blanco & García-Sáez, 2018) and the involvement of the Bax inducer and DNA damage sensor p53, which was necessary for Bax upregulation (Keim et al., 2001). Other possibilities include alterations in glucose metabolic pathways, such as activation of the hexosamine pathways, which results in GSH depletion, oxidative stress, and the disruption of the embryonic gene expression (Horal et al., 2004). It has been hypothesized that decreased glucose transport may lead to insufficient embryonic levels of glucose, causing metabolic deficiencies, mitochondrial dysregulation, and ultimately triggering cell death (Leunda-Casi et al., 2002). Other hypothesis are that 1) glucose deprivation-induced ATP depletion and stimulation of the

mitochondrial death pathway cascade (Saikumar et al., 1999), 2) glucose deprivation-induced oxidative stress and triggering of BAX-associated events including the JNK/MAPK signaling pathways (Lin et al., 2000) and 3) hypoglycemia-regulated expression of HIF-1 α , stabilization of p53 leading to an increase in p53-associated apoptosis (Carmeliet et al., 1998; M. Chi et al., 2000). While glucose-induced apoptosis through the intrinsic pathways is reported frequently, extrinsic pathways are not commonly implicated and may not be a direct route of high glucose effects on the embryonic cells. It is possible that it is induced through external, or third-party signaling pathways, such as through ER stress or autophagic cell death. TNF is active as early as the 2-cell stage in mouse development (Kawamura et al., 2007), but it is not reported in association with high glucose during the preimplantation-specific period. TRAIL-induced apoptosis is also present in the murine blastocyst, but has not yet been correlated with hyperglucose exposure (Riley et al., 2004). In bovine embryos, caspase-8, FAS/FASL transcripts are at very low abundance or absent (Leidenfrost et al., 2011). This could prevent convergence of the intrinsic and extrinsic pathway to activate the effector caspases, since caspase-8 would be absent or inactive.

1.6 Autophagy

The propensity of a cell to undergo apoptosis is counterbalanced by genes that stimulate cell survival and proliferation. Autophagy, generally considered a pro-survival mechanism, is initiated as a protective response to oxidative stress, ER stress, metabolic stress, and nutrient deprivation (Higdon et al., 2012; Haberzetti and Hill, 2013). This process occurs through the activation of specific autophagic genes and proteins to regulate the formation of a double-membraned vesicle called an autophagosome, which sequesters and compartmentalizes cellular debris. It merges with a lysosome to degrade contents, which can later be recycled as materials for future anabolic processes (Ravikumar et al., 2010). There are three kinds of autophagy: (1) microautophagy, (2) chaperone-mediated autophagy (CMA), and (3) macroautophagy. In this study, I focused on macroautophagy (called “autophagy” hereafter), the most common form, which is the mass clearance of organelles and proteins at a much less specific level of control than the other two types. It is dynamically inducible and is a highly conserved mechanism in

eukaryotes (Ravikumar et al., 2010). Autophagy can be broken down into 4 steps: Initiation, elongation, maturation, and degradation (Mizushima et al., 2010).

1.6.1 Autophagy initiation

Autophagy initiation includes activation of genetic pathways and the structural assembly of the autophagosome vesicle. Important in this process are the autophagy-related genes (ATGs) which specify key proteins critical to autophagy machinery. ATGs are inducible genes, regulated both post-transcriptionally and post-translationally in response to autophagic inducers (Bernard et al., 2015; Y. Xie et al., 2015). Figure 3 (below) illustrates autophagy initiation as described in this section. Autophagy is turned on through the activation of the unc-51-like kinase (ULK1) complex, which often occurs through the inhibition of the mammalian target of rapamycin (mTOR) (Martina et al., 2012). mTOR is a preliminary sensor coordinating the cellular nutrient state (i.e., amino acids, glycogen, glucose) with the activation of the autophagy response. In nutrient-rich cells, the mTOR complex 1 (mTORC1) directly binds with and phosphorylates ULK1 (Hosokawa et al., 1981; Martina et al., 2012). In conditions of nutrient deprivation, mTORC1 is inhibited and thus dephosphorylates, releasing ULK1, which promptly autophosphorylates and binds with ATG13, ATG101 and FIP200 to form the ULK1 complex (Hosokawa et al., 1981). ULK1 can also be directly activated through phosphorylation by AMPK which is increased because of a high AMP-to-ATP ratio seen in cells experiencing glucose deprivation or mitochondrial dysfunction (Hardie et al., 2012). Some studies maintain that AMPK is the inhibitor of the mTORC-ULK1 interaction, releasing ULK1 under glucose deprivation (Figure 3). Other nutrient deprivation or stress may inhibit mTOR in an alternate manner. Activated ULK1 releases the autophagic phosphoinositide 3-kinase (PI3K) complex I from its cytoskeleton attachment and translocates to the ER membrane where colocalization of multiple autophagic complexes creates the site of autophagosome formation (SAF). Specifically, the PI3K complex is tethered to the cytoskeleton through an interaction between activating molecule in beclin-1-regulated autophagy protein 1 (AMBRA1) and dynein light chains 1/2 (Di Bartolomeo et al., 2010). It is composed of PI3K, vacuolar protein sorting 34 (VPS34), beclin-1, ATG14, AMBRA1, and a general vesicular transport factor p115 (Dikic & Elazar, 2018).

Activated ULK1 phosphorylates AMBRA1, releasing the PI3K complex from the dynein proteins. PI3K is recruited to the ER membrane and binds to transmembrane protein VMP1 (Figure 3). Here, the ULK1 complex associates with the PI3K complex and phosphorylates beclin-1, activating the VPS34 lipid kinase which converts circulating levels of phosphatidylinositol (PI) to phosphatidylinositol triphosphate (PI3P) (Axe et al., 2008; Russell et al., 2013). The local enrichment of PI3P acts as a signal for the accumulation of additional components of the autophagic machinery, creating the site of autophagosome formation (Axe et al., 2008). This site is a distinct section of membrane that reforms into a structure called an omegasome, resembling the Greek Omega symbol (Grasso et al., 2018; Ktistakis & Tooze, 2016). Some evidence shows that alternative donor membranes may be sourced from the mitochondria, Golgi, endosomes, or contact sites between them, though the ER is the most studied (Zhen & Stenmark, 2023). A diagram of these processes can be seen in Figure 3.

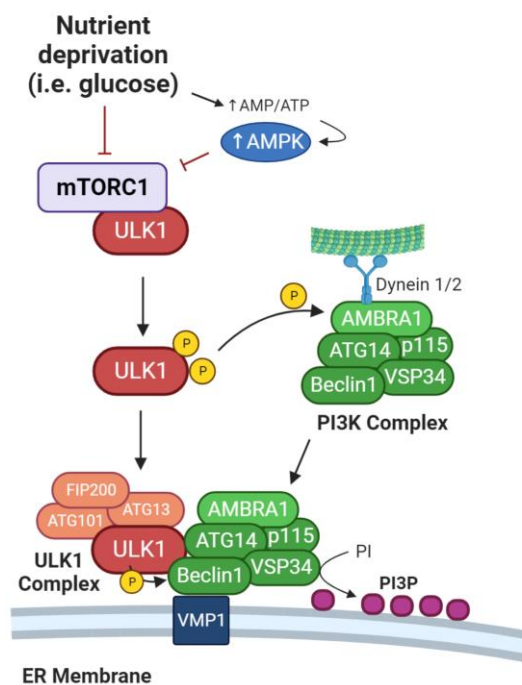


Figure 3. Autophagy initiation.

Nutrient deprivation triggers inhibition of mTORC1, dissociating it from ULK1, which subsequently auto-phosphorylates. ULK1 then phosphorylates AMBRA1 of the PI3K complex, releasing it from its hold to the cytoskeleton via dynein 1/2. ULK1 binds ATG13, FIP200 and ATG101 to form the ULK1 complex and is recruited to the ER membrane. The PI3K complex is recruited to the ER membrane where it associates with the ULK1 complex and binds to VMP1 transmembrane protein. VSP34 converts cytosolic phosphatidylinositol (PI) into phosphatidylinositol 3-phosphate (PI3P). Image created with BioRender.com.

1.6.2 Autophagosome elongation

Membrane expansion: At the omegasome, various structures accumulate to facilitate the construction of the phagophore membrane, including ATG proteins and additional tethering proteins, kinases, and phospholipids, as illustrated below in Figure 4. WD repeat domain phosphoinositide-interacting proteins (WIPIs) translocate to PI3P-enriched sites and will facilitate complex and protein recruitment at the initiation site. Phagophore membrane expansion is driven by local lipid synthesis and transfer at the ER membrane, and vesicular fusion from other donor membranes (Lamb et al., 2013). ATG2 and ATG9 proteins are important in this process. ATG9A is a transmembrane protein found endogenously in the Golgi complex (He et al., 2006). During autophagy induction, Golgi vesicles containing ATG9 shuttle to the site of autophagosome formation (SAF) on the ER membrane, where they act as seed vesicles from which mammalian autophagosome membranes will form (Olivas et al., 2022; Orsi et al., 2012). ATG9 trafficking and autophagy initiation is mediated by ULK1 phosphorylation and RAB2 recruitment (Ding et al., 2019; Zhou et al., 2017). RAB2 is a protein localized close to ATG9 on Golgi membrane structures and is activated upon autophagy initiation. It recruits ULK1 and ATG9+ Golgi vesicles to the SAF, where ULK1 phosphorylates ATG9, likely tethering the vesicles in this location (Ding et al., 2019). The ATG2 protein localizes to these contact sites and associates with ATG9 to promote autophagosome elongation. ATG9 proteins have lipid scramblase and lipid flipping abilities, and dock onto the ER by forming a complex with WIPI4 proteins and ATG2 (a lipid channel that is also bound to VMP1 in the ER membrane (Matoba et al., 2020; Valverde et al., 2019; van Vliet et al., 2022; Zhen & Stenmark, 2023). The complex allows lipid transfer across ER-autophagosome contact sites through the ATG2 and ATG9 channels, to feed phagophore membrane expansion (Valverde et al., 2019; Zhen & Stenmark, 2023). Figure 4 (below) depicts this process as described.

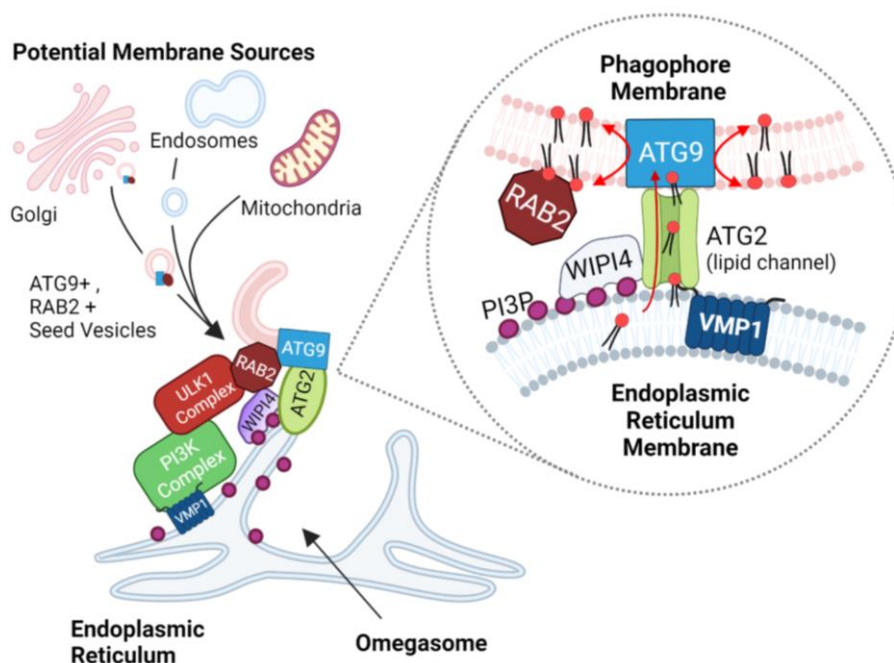


Figure 4. Phagophore membrane synthesis.

Association of the ULK1, RAB2, and the PI3K complex to the site of autophagosome causes omegasome formation and PI3P accumulation, which recruits WIPI4 and additional autophagy machinery. ATG2 binds to WIPI4 and VMP1 on the endoplasmic reticulum membrane, and to ATG9 on an ATG9-containing Golgi vesicle. ATG2 is a phospholipid channel, passing phospholipids from the endoplasmic reticulum membrane to the forming phagophore membrane. ATG9 works as a lipid scramblase and flippase to redirect the phospholipids equally to both sides of the phagophore bilayer. Image created with BioRender.com.

Cargo sequestration: As the autophagosome expands, the ATG proteins play a large role in its elongation and cargo sequestration. The mammalian homolog of the yeast ATG8 protein, LC3 (microtubule associated protein 1 light-chain 3), coordinates membrane proteins with ubiquitinated cargo destined for autophagosome-mediated degradation and is necessary for autophagy completion (Lee & Lee, 2016). At basal levels, the inactivated form of LC3 exists diffused through the cytoplasm and the nucleus. When autophagy is triggered, LC3 is cleaved in cytoplasm by ATG4 to form LC3-I and subsequently bound to by ATG7 and ATG3 (Grasso et al., 2018). Simultaneously, the WIPI2 protein is recruited to the forming autophagosome by PIP3 concentrates. WIPI2 acts as a binding target for the ATG16L1 protein, a member of the ATG12:ATG5:ATG16L1 complex, leading to association of this complex along the autophagosome membrane (Dikic & Elazar, 2018). Interaction of ATG12 with ATG3 at the membrane therefore specifies the site of LC3-I lipidation through its covalent bonding to phosphatidylethanolamine (PE) in the autophagosome membrane (Fujita et al., 2008). This lipidated form of LC3-I is called LC3-II, and decorates both outer and inner membranes of phagophores (Grasso et al., 2018). LC3-II enables protein sequestration as it is a ligand for autophagic cargo receptors to recruit tagged cellular cargo into aggregates at the autophagosome (Hansen & Johansen, 2011). The adaptor protein p62, is one well known protein to functionally link ubiquitinated protein aggregates or organelles with cleaved LC3-II on the assembling autophagosome (Runwal et al., 2019), allowing selective uptake of damaged or unneeded molecular cargo (Mukhopadhyay et al., 2014). The neighbor of BRCA1 gene 1 (NBR1) performs a similar function (Kirkin et al., 2009). The completed autophagosome is a double-layer intracellular membrane enclosing cytoplasmic materials and organelles (Lee & Lee, 2016). The final membrane closure of the autophagosomes is mediated by ESCRT (endosomal sorting complex required for transport) which melds the ends of the membranes together (S. Yu & Melia, 2017). The autophagosome is released from the ER through VMP1 depletion, leading to the destabilization of the ULK1 complex and resulting in decreased PI3P levels, which releases the association of ATG and WIPI proteins at the membranes (Zhao et al., 2017). Figure 5 (below) depicts these mechanisms.

The morphological and cellular location of the phagophore during membrane expansion is incompletely understood. Ultrastructural analysis in recent studies shows that the phagophore precursors emerge next to the ER as bud-like, highly curved membrane cisterns with a small opening to the cytosol (Gudmundsson et al., 2022). Phagophores then open to form more elongated structures as the membrane expands. The omegasome remains associated with the edge of the open end of the cup-shaped phagophore throughout expansion, maintained by WIPI and ATG2 proteins (Chowdhury et al., 2018). When the phagophore has expanded sufficiently, ATG2 and WIPI proteins dissociate from both membranes and the omegasome recedes as the phagophore is sealed (Chowdhury et al., 2018). Thus, the phagophore is formed and expanded while still associated with the omegasome, as seen in Figure 5.

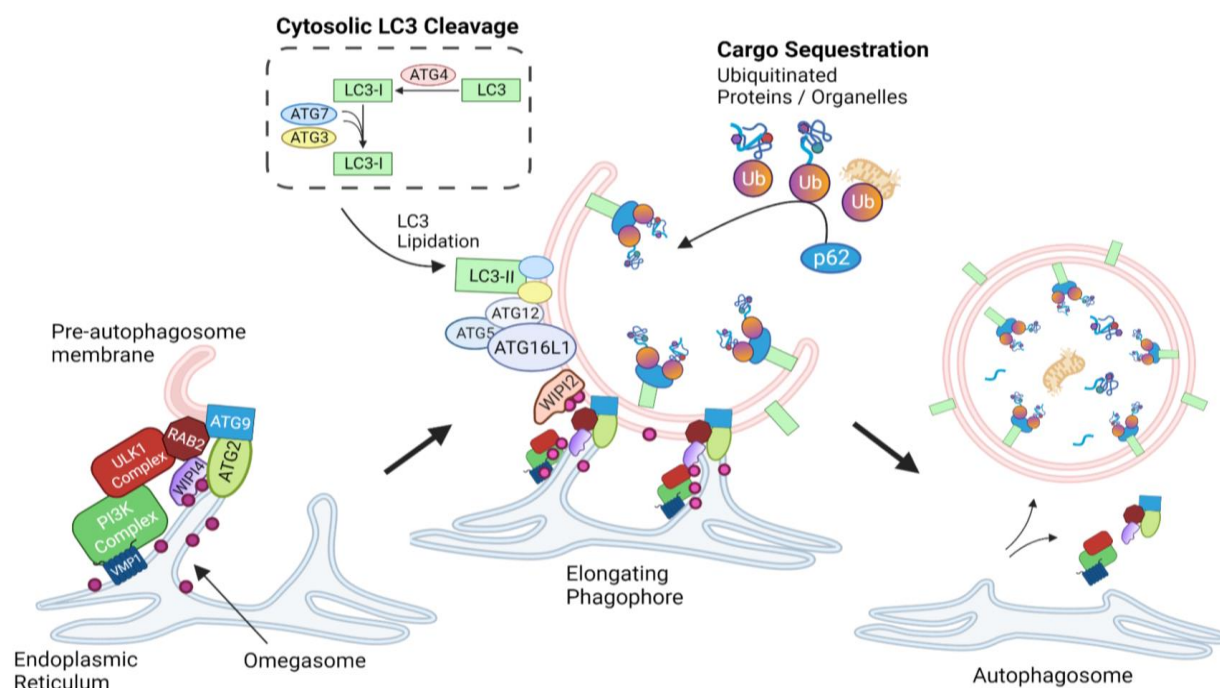


Figure 5. Autophagosome elongation and cargo sequestration.

ULK1 and PI3K association at the site of autophagosome formation produces PIP3 accumulation at the elongating phagophore membrane. This recruits WIP1, which associates with the ATG16L1, a member of the ATG12:ATG5:ATG16L1 complex. Meanwhile, LC3-I is cleaved by ATG4 in the cytoplasm and bound by ATG7 and ATG3. ATG3 then associates with ATG12 at the phagophore membrane, specifying the site of LC3-II lipidation. Ubiquitinated proteins, organelles and other cellular materials are bound by p62, which expresses a receptor for and subsequently attaches to membrane-bound LC3-II, effectively sequestering cargo to the autophagosome. After the autophagosome is formed, WIP1 depletion causes dissociation of autophagic machinery at the membrane, omegasome withdrawal, and autophagosome release. Image created with BioRender.com.

1.6.3 Autophagosome maturation

After dissociation from the ER, autophagosomes undergoing maturation will fuse with endosomes, forming an intermediate form of an autophagosome called an amphisome (Ganesan & Cai, 2021). These then fuse with lysosomes to form autophagolysosomes, as pictured in Figure 6 below. The fusion of these vesicles requires the formation of an anchoring SNARE complex and microtubule-based kinesin and dynein motors to transport autophagosomes and lysosomes near each other (Zhao & Zhang, 2019). Assembly of the SNARE complex proteins is spatiotemporally controlled by Rab7 GTPases and other tethering factors. The complex consists of two separate SNAP29 cytosolic proteins bound on either side by Q-SNARE and R-SNARE proteins, which are bound to the autophagosomal and endolysosomal membranes (Matsui et al., 2018). Rab7, situated on late endosome membranes, recruits additional tethering factors such as the homotypic fusion and protein sorting (HOPS) complex, essential autophagy gene (EPG5), and PLEKHM1. HOPS promotes the assembly of the SNARE complex and attaches to the membrane through Rab7 and PI3P binding (Stroupe et al., 2006). EPG5 and PLEKHM1 bind to LC3 on the autophagosome and Rab7 on the endosome or lysosome (Yim & Mizushima, 2020) (Figure 6). Vesicles are transported via microtubule motor proteins kinesin and dynein. Retrograde transport moves vesicles towards the “plus-end” of microtubules at periphery of the cell, and anterograde transport moves vesicles towards the “minus-end” of microtubules at center of the cell (Zhao & Zhang, 2019). Lysosomes undergo bidirectional transport to reach their targets, using retrograde movement to reach cell periphery during nutrient influx, and anterograde movement to reach autophagosomes during nutrient deprivation (Kendrick & Christensen, 2022). Autophagosomes (generally formed closer to the cell center) undergo retrograde movement towards lysosomes to reach proximity and enable their fusion (Zhao & Zhang, 2019). Recent theories postulate that direction of transport depends on the differential activation of motor proteins, which can be regulated by vesicle luminal pH (Hilverling et al., 2022). A more acidic vesicle alters its lipid composition, which in turn activates or deactivates motor proteins. The Rab7 protein, which is also important for maintaining the SNARE complex, is also thought to recruit dynein motors to promote lysosomal transport toward the nucleus (T. Wang et al., 2011).

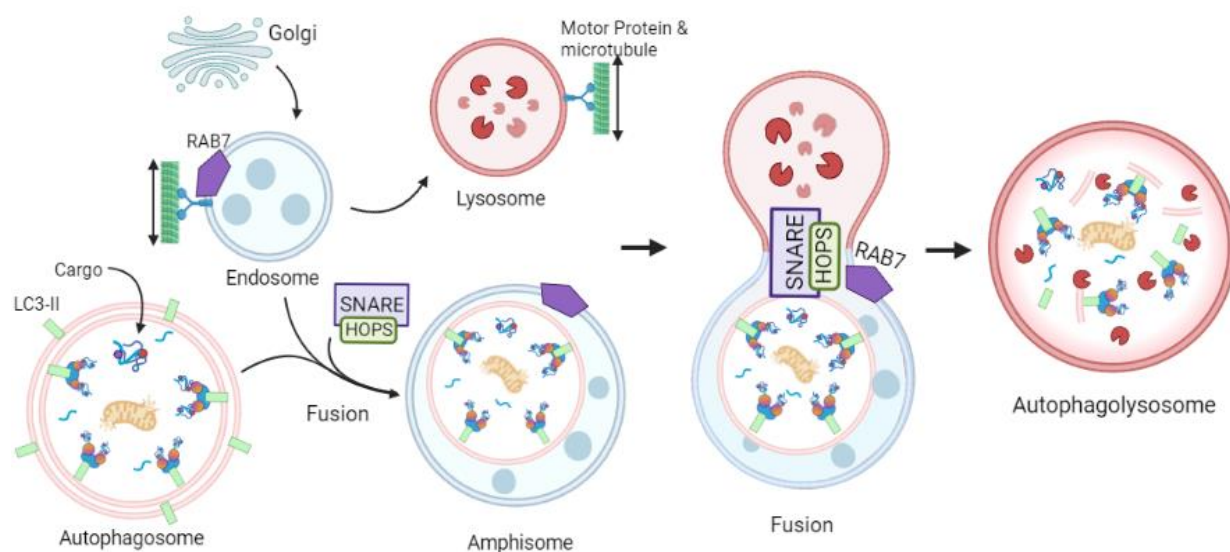


Figure 6. Autophagosome maturation.

After dissociation from the ER, autophagosomes undergoing maturation will fuse with endosomes, forming a hybrid intermediate called an amphisome. These then fuse with lysosomes to form autophagolysosomes. The fusion of these vesicles requires the formation of an anchoring SNARE complex, HOPS, and other proteins. Microtubule motor proteins transport autophagosomes, endosomes and lysosomes within proximity of each other to allow fusion. Rab7 is critical both in associating vesicles to motor proteins and recruiting additional tethering proteins to lysosomal-amphisome/autophagosome fusion. Image created with BioRender.com.

1.6.4 Autophagosome degradation

Lysosomal digestion of autophagic cargo and export of recycled metabolites back into the cell is essential in autophagy. When mammalian lysosomes fuse with the outer autophagosomal membrane (OAM), they supply acidic hydrolases that degrade the inner autophagosomal membrane (IAM) and contained material (Yim & Mizushima, 2020). More than 60 lysosomal hydrolases mediate the degradation of autophagosomal contents, which include protein aggregates, mitochondria, damaged lysosomes and bacteria (Schröder et al., 2010; Yim & Mizushima, 2020). Most of these enzymes require an acidic environment, which the lysosome maintains through proton pumping ATPases and associating Cl^-/H^+ antiporters (Mindell, 2012). Polypeptide chains are broken down by proteases, however little is known about precise content denaturation mechanisms due to an excess of protease activity and overlapping enzyme specificities (Winchester, 2005). Amino acids and peptides resulting from proteolysis are exported out of the lysosome by passive diffusion and specific transporters (Winchester, 2005). Over 10 amino acid transporters have been found in human cells, but only cystinosin, a cystine transporter (Town et al., 1998), and LYAAT-1, a transporter for small neutral amino acids have been fully characterized (Agulhon et al., 2003). O- and N- glycosidic linkages in glycan or monosaccharides are broken down through highly ordered and well specified pathways (Winchester, 2005). Three lysosomal monosaccharide transporters collectively transport all 11 monosaccharides produced in mammalian lysosomes by the digestion of glycol-conjugates (Lloyd, 1996; Winchester, 2005).

Lysosomes are critical for autophagy degradation and are rapidly consumed, thus maintaining an available lysosome population is essential. Autophagic lysosome reformation (ALR) is a pathway for lysosome regeneration by which existing outer membranes derived from autolysosomes are recycled to generate new lysosomes (McGrath et al., 2021). This happens by clathrin-coated buds forming on the lysosomal membranes and elongating using kinesin family member 5B (KIF5B), a microtubule motor, forming “reformation tubules” (McGrath et al., 2021). At the tips of these tubules, nascent lysosomes, called proto-lysosomes, are formed

through a scission/budding process performed by a large GTPase called dynamin 2 (DNM2) (McGrath et al., 2021).

1.7 Autophagy in the preimplantation embryo

Autophagy is a cellular and tissue homeostatic mechanism critically important in development. It arises in mammalian zygotes, triggered by fertilization and detectable by the two-cell stage. It functions to degrade maternally derived proteins and mRNA, into amino and nucleic acids for zygotic protein synthesis. Autophagy-null (ATG5-knockout) zygotes exhibit decreased protein synthesis and embryonic arrest by the 4-8 cell stage (Tsukamoto et al., 2008). This fertilization-induced autophagy in mouse embryos is independent of mTORC1, and is not affected by AMPK activators, suggesting an unknown mechanism induces this autophagy. Autophagy appears to be critical during zygotic genome activation (ZGA) specifically, as culturing 1-cell zygotes with 3-methyladenine (autophagy inhibitor) or rapamycin (autophagy inducer) displayed significantly reduced development, increased apoptosis, and altered ICM/TE specification, while treatment from the 2-cell to blastocyst stage did not have these effects (Lee et al., 2011). ICM cells must maintain pluripotency until their differentiation into embryonic lineages. Studies in mESCs show that autophagy helps maintain pluripotency by regulating mitochondrial homeostasis, and that Atg3 or ULK1 knockdown leads to damaged mitochondria and ROS production. Altered autophagy also affects the ICM:TE ratios of cells in mouse embryos, which may compromise embryo quality (Lee et al., 2011). No specific role for autophagy in blastocyst cavitation and expansion is currently known. Increased autophagy (particularly in the TE cells) is seen in dormant blastocysts waiting to implant (often due to maternal hormone fluctuations) (J. E. Lee et al., 2011). Injection of 3-MA (autophagy inhibitor) rendered these embryos more vulnerable to death via increased apoptosis. Autophagy gradually decreases from early cleavage to blastocyst stages, based on decreased ATG5, ATG6 transcript expression, and LC3-II (transcript and protein) quantification (Lee et al., 2011; Z. C. L. Leung et al., 2022). However, expression from the 1-cell to 2-cell stage likely represents maternal expression and represents the beginning of embryonic expression of autophagy components. Autophagy is still required throughout embryogenesis and provides the blastocyst with resilience to adapt to environmental stressors.

There is a great need for further studies investigating the role of autophagy during preimplantation development.

1.7.1 High glucose induction of embryonic autophagy

Studies investigating the hyperglycemic induction of autophagy in preimplantation embryos are scarce. One study has reported a co-increase in apoptotic and autophagic markers in mouse embryos after treatment of 5, 20, 35, and 52mM of glucose has been reported (Adastra et al., 2011) with autophagy increasing in a dose-dependent manner and apoptosis decreasing after 20mM. These embryos also showed alterations affecting cell lineage allocation, which may factor into future gestational malformations or fetal miscarriages (Adastra et al., 2011). In another study, porcine embryos were cultured from the 4-cell stage until the blastocyst stage at 5 and 55mM of glucose and showed a significant decrease in blastocyst formation and cell number, increased apoptotic cell counts and pro-apoptotic mRNA expression, mitochondrial disruption, and increased LC3 protein and mRNA levels (Xu et al., 2013). The researchers suggested that the high glucose levels in culture led to maladaptive changes in the mitochondrial transmembrane potential, causing increased ROS levels and cytochrome c release, thus inducing both apoptosis and autophagy (Xu et al., 2013). High glucose downregulates glucose transporters in many cells including early blastomeres which may induce a state of cellular nutrient deprivation (Moley, Chi, & Mueckler, 1998). Nutrient deprivation induced by ceramide in preimplantation mouse embryos decreased the expression of GLUT1, GLUT3, LAT-1 and 4F2hc (lysosomal amino acid transporters), increased apoptosis and decreased blastocyst formation, suggesting that ceramide-induced autophagy promotes apoptosis following downregulation of nutrient transporters during mouse embryogenesis. Additionally, an altered ratio of ICM:TE cells that occurs under increased glucose exposure may be a result of altered glucose metabolism through the hexosamine biosynthesis pathway (HBP) and the pentose phosphate pathway (PPP), which control TE-specific gene transcription (Chi et al., 2020). Autophagy therefore plays a role in glucose-induced embryopathy, and these effects start as early as the preimplantation stage. There is a dire need for more studies looking at diabetic embryopathy during this period of

development to understand the processes involved and best methods of prevention and intervention.

1.8 Methods of measuring autophagy in scientific research

Common challenges to assessing mammalian autophagy involve the capturing of a quickly changing dynamic process with static measurements. The number of autophagosomes observed at a specific time is a balance between the rate of their generation and the rate of their conversion into autolysosomes and subsequent degradation. Increased autophagosome measurements may represent either autophagy induction or impairment – such as the inability to fuse with lysosomes and degrade. Decreased autophagosome measurements could indicate lower induction but may also occur if the ability to form autophagosomes is impaired. A solution to this dilemma is to measure autophagic flux, which is the complete process of autophagosome formation, fusion with lysosomes, and clearance / degradation (Mizushima et al., 2010). Some methods of measuring autophagic flux include comparing treatments to in-culture autophagy activators (i.e. rapamycin) and inhibitors (i.e. chloroquine and hydroxychloroquine), lysosomal inhibitors, genetic knockout of certain ATG genes, and live cell imaging (Shen et al., 2015; Y. Yang et al., 2013).

Common markers in autophagy analysis include ATG proteins transcription and post-translation modifications. Often, ATG5, ATG7 and ATG3 and results of their inhibition are analyzed due to their recruitment during autophagosome-specific membrane elongation. The unique presence of LC3 on autophagosomes, but no other transient or permanent cellular organelle, plus its characteristic cleavage activation makes it a key target in autophagy studies. Degradation of p62 is another widely used marker to monitor autophagic activity because p62 directly binds to LC3 and is selectively degraded by autophagy (Pugsley, 2017). LAMP1/2 colocalization with LC3 also indicates the formation of an autophagolysosome (Pugsley, 2017). In live-cell imaging, LysoTracker Red fluorescence (a stain for the acidic environment of a lysosome) can be measured in association with p62 or LC3 fluorescence to determine autophagolysosome formation (L. Wang et al., 2013).

1.9 Rationale

Preimplantation embryonic development is a complex process that involves multiple cellular mechanisms, including routine apoptosis and autophagy. High glucose exposure, which occurs in individuals with diabetes and metabolic disorders, can disrupt embryonic development. Previous studies have shown that high glucose levels compromise blastocyst formation and quality, alters cell fate specification, and increases apoptosis. The involvement of autophagy in the hyperglycemic response of the preimplantation embryo, however, has yet to be thoroughly documented. There is also a lack of understanding in the initial cellular responses connecting the high glucose environment with programmed cell death mechanisms in question. Finally, much of the key knowledge in this area is still based on papers published many years ago, where research employs older culture techniques, media compositions and often treats embryos with glucose concentrations higher than physiological diabetic levels. More knowledge in this area is needed, which presents a significant opportunity for further research. Therefore, this thesis investigates the effects of a 25mM glucose treatment on preimplantation mouse embryo development, autophagy, and apoptosis. The findings from this study will provide valuable insights into the cellular mechanisms underlying diabetic embryopathy and may contribute to the development of targeted interventions to mitigate its impact.

1.10 Hypothesis

My primary hypothesis is that high glucose exposure would impair embryonic development to the blastocyst stage, induce both apoptosis and autophagy, and that the timing of hyperglycemic insult would have an influential impact in their induction.

1.10.1 Specific Aims

There are three main objectives for this work. First, to investigate effects to preimplantation embryo development under hyperglycemic conditions. Secondly, to investigate the activation of

autophagy and apoptosis in preimplantation embryos cultured in high glucose. Finally, to compare impacts of high glucose in the early vs late 2-cell embryo.

Chapter 2

2 Materials and Methods

2.1 Animals and Ethics Approval

All experiments were conducted using CD-1 mice from Charles River Laboratories (Senneville, QC). All mice were handled in accordance with the Canadian Council on Animal Care and Western University's Animal Care and Use Policies (Protocol # 2018- 075; Appendix E). Mice were housed in conventional housing with 12-hour light-dark cycle and access to food and water *ad libitum*.

2.2 Mouse Superovulation and Mating

For each experimental replicate, 20 CD1 female mice (4-6 weeks old) received 5.0 IU/ 0.1mL intraperitoneal (IP) injections of pregnant mare serum gonadotropin (PMSG, Merck Animal Health, Canada) and human chorionic gonadotropin (hCG, Merck Animal Health, Canada) to stimulate increased follicular development and timed ovulation, respectively. Immediately after hCG injection, females were housed 1:1 with male CD1 mice (6-12 weeks old) for overnight mating. Successful copulation was confirmed by presence of vaginal plug in the early AM. Female mice were returned to their original cage to await embryo collection.

2.3 Embryo Collection

Prior to embryo collection, culture dishes were prepared as per the following: 1x40uL droplet and 4x20uL droplets of the appropriate treatment media were evenly placed on a 4.5mm sterile untreated culture dish and blanketed with 3mL of embryo-tested mineral oil (Origio Inc., CT, USA; Cat# LGOL-500) to prevent evaporation. One wash dish (4x45uL droplets of KSOMaa, (Caisson Labs, UT, USA)) and 1 prep dish (1x40uL (per group) droplet of appropriate media) were also prepared. Starting January 2023, KSOMaa media was switched to a nearly identical EmbryoMAX KSOM media (Cat # MR-10; Sigma-Aldrich, Ontario Canada) due to

discontinuation of the KSOMaa provided by Caisson Labs. Dishes were pre-equilibrated at 37°C under a 5% CO₂, 5% O₂ and 90% N₂ culture atmosphere during collection process. Females with vaginal plugs were sacrificed via CO₂ asphyxiation followed by cervical dislocation at 36 or 48 hours post-hCG injection (hpi) depending on experiment, then immediately dissected for surgical oviduct removal. The oviducts from each female were placed in a 4.5mm sterile culture dish containing 1.5mL of M2 flushing medium (Sigma-Aldrich, ON, Canada; Cat# M7167) pre-equilibrated 1-2hr in an incubator at 37°C under a 5% CO₂, 5% O₂ and 90% N₂ culture atmosphere (unless otherwise specified). During dissection, a heat lamp and warmed water flask were used to maintain media temperature. Under a light microscope, pre-equilibrated M2 media and 2-cell embryos were flushed through the oviduct using a 3CC syringe and dulled 30G needle inserted and clamped at the infundibulum side of the oviduct. Embryos were collected using a modified 9" Pasteur pipette (Fisherbrand, Thermo Fischer Scientific, USA), flame treated to reduce the pipette tip diameter to approximately 200 µm and transferred through a series of KSOMaa wash droplets to filter out debris and poor-quality embryos (examples in Figure 7 below). Embryos were then pre-cultured in 40uL drops of treatment media before final rinse and distribution in 20uL culture drops at a density of 1 embryo per microliter. Embryos were cultured as described below.

2.4 Media Preparation

To prepare high-glucose media, D-(+)-glucose (Cat#G6152; Sigma-Aldrich, ON, Canada) was measured by weight and added to KSOMaa/EmbryoMAX medium in a 50mL falcon tube. To assist in glucose dissolution, media was vortexed and left in a 20-minute luc-warm water bath before incubation at 4°C overnight. The media was then filter-sterilized, measured for osmolarity and stored in aliquots at 4°C for use in embryo culture. For LysoTracker experiments, LysoTracker Deep Red (Cat#L12492; Invitrogen, Thermo Fischer, USA) was obtained at a stock concentration of 1mM in DMSO. Aliquots at concentrations of 500uM in DMSO were stored at -20°C. At time of use, LysoTracker was diluted to a concentration of 75nM in culture media and pre-equilibrated in incubator for 30 minutes prior to embryo culture with lysotracker.

2.5 Embryo Culture and Experimental Design

Determination of Glucose Treatment Concentration: To determine optimal glucose concentration for this study, the dose response effects of glucose exposure on mouse preimplantation development *in vitro* were measured. Embryos were flushed at late 2-cell stage (48hpi) and cultured in treatment groups included KSOMaa (optimized mouse embryo culture medium with 0.2mM D-glucose) as the control, 25mM L-glucose as the isomer control, 5mM D-glucose + 20mM L-glucose, 15mM D-glucose + 10mM L-glucose, and 25mM D-glucose until early blastocyst stage (96hpi) or zona hatching (118hpi). L-glucose (Cat# A17496-03; Thermo Fischer, MA, USA), a non-metabolized isomer of D-glucose (Cat# G6152; Sigma-Aldrich, Ontario, Canada), was a control for the effects of osmolarity. After dose response experiments with L-glucose, D-glucose was used exclusively for all remaining experiments. Outcome measures were blastocyst formation (BF), total cell number (TCN) and zona hatching percentage.

Effects of oxygen concentration in hyperglycemic embryo culture. To investigate the effects of low versus high oxygen culture environments on embryos in high glucose culture, embryos were cultured in KSOMaa media containing 0.2mM or 25mM of glucose in either low (a 5% CO₂, 5% O₂ and 90% N₂ culture atmosphere) or high (5% CO₂ in air atmosphere, 20% O₂) oxygen environment until blastocyst stage (96hpi). Developmental outcome measures of blastocyst formation (BF) and total cell number (TCN) were tested.

Effects of hyperglycemic exposure at early vs late 2-cell stage. To contrast the resilience of embryos exposed to hyper glucose at the early 2-cell stage (36hpi) vs the late 2-cell stage (48 hpi), embryos were flushed at these times post insemination and cultured in 0.2mM (control) and 25mM glucose in KSOMaa until the early blastocyst stage (96hpi). Outcome measures included morphological analyses of development (TCN, BF), transcriptional expression of glucose transporters GLUT1, GLUT2, and GLUT3 (36hpi only), and immunofluorescent analysis of cellular proliferation (Ki-67, early 2-cell only) autophagy (LC3 puncta counts, p62 expression) and apoptosis (TUNEL, cleaved caspase-3).

Determination of timing of autophagic induction. To investigate the time course during preimplantation development that hyperglycemic autophagic stimulation may first be observed, embryos were flushed at the early 2-cell stage (36hpi) and cultured in 0.2mM (control) and 25mM glucose in KSOMaa for 12, 24, 36, 48, and 60 hours (to 96hpi). Outcome measures included immunofluorescent analyses of LC3 puncta counts at each time point.

Determination of autophagolysosome formation. Embryos were flushed at the early 2-cell stage (36hpi) and cultured in 0.2mM (control) and 25mM glucose in KSOMaa until the blastocyst stage (96hpi). As previously determined in our lab, embryos were transferred to culture media containing LysoTracker Red at a concentration of 75nM for 30 minutes prior to the end of the incubation period, followed immediately with a rapid staining protocol for LC3 staining and confocal imaging (Leung, 2021).

2.6 Developmental Stage Analysis

Embryo developmental stage classification and quantification was performed under a dissecting light microscope. Embryos were classified as 1-cell, 2-cell, 4-cell, 8-cell, morula, blastocyst, and hatching blastocyst. Up to the 8-cell stage, individual blastomeres should be distinctly visible and have similar size and shape. Morulae were defined as embryos containing 8 cells or more, where distinct blastomeres could not be identified and no cavity was visible. Blastocysts were defined as an embryo with compacted cells and any visible fluid-filled cavity. An early blastocyst is defined by <50% of the total volume comprising the cavity. Hatching was determined by embryos that have (a) formed a blastocyst and (b) begun the process of outgrowth outside of the zona. Arrested embryos were defined by any embryo more than 1 stage behind what is expected at a given time point. Degenerated embryos were identified by a misshapen morphology, uneven cleavage, darkened granular blastomeres, or fuzzy debris within the embryo. Figure 7 depicts examples of embryos at each stage.

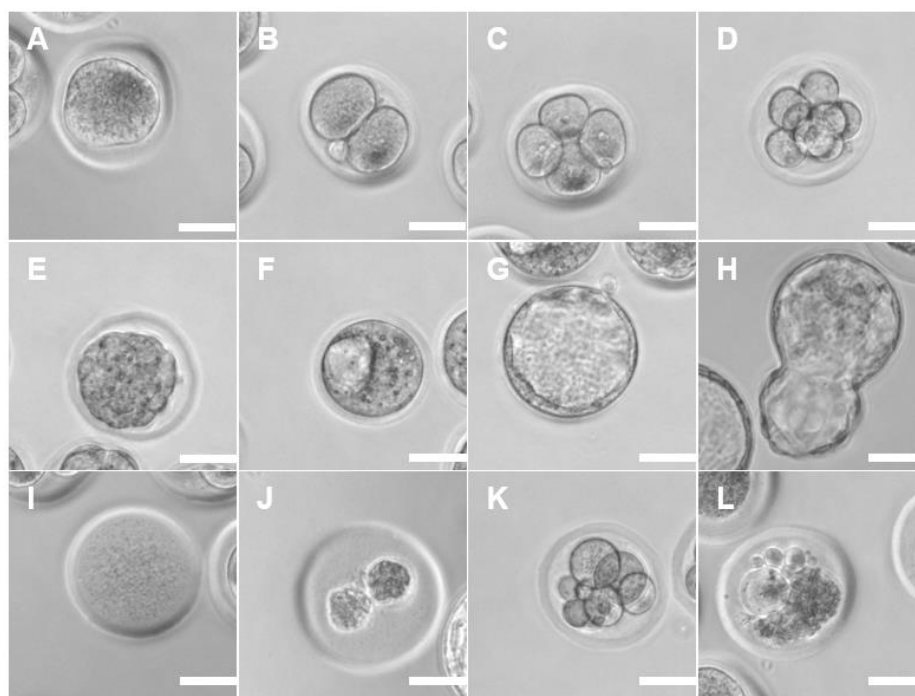


Figure 7. Representative images of mouse preimplantation embryo stages.

Representative images of mouse preimplantation embryos at the following stages: (A) unfertilized oocyte (no pronucleus or polar body), (B) 2-cell, (C) 4-cell, (D) 8-cell, (E) morula, (F) early blastocyst, (G) expanded blastocyst, (H) hatching blastocyst, (I) arrested oocyte (J) arrested and degenerated 2-cell, (K) uneven blastomere morphology (L) degenerated. Scale bars represent 50 μ m. Created with Quick Figures FIJI plugin.

2.7 Immunofluorescence Techniques

For immunofluorescent protein localization determination, embryos were fixed in glass-well dishes containing a 4% paraformaldehyde (PFA) in phosphate-buffer (PB) solution for 15 minutes (2-cell to 8-cell stage) or 30 minutes (morula and blastocyst stages) at room temperature. Embryos were stored overnight in a PHEM buffer containing PIPES (60 mM), HEPES (25 mM), EGTA (10 mM), and $\text{MgCl}_2 \cdot \text{H}_2\text{O}$ (1 mM) to preserve structural integrity of actin filaments (Schliwa & Van Blerkom, 1981). Fixed samples were simultaneously permeabilized and blocked at room temperature for 2 hours in PBS containing 5% donkey serum, and 0.1% Triton X-100,

then incubated overnight at 4°C in the following primary antibodies diluted in antibody dilution buffer (1X PBS containing 0.05% Triton X-100 and 1% normal donkey serum): rabbit LC3A/LC3B (Invitrogen #PA1-16931, 1:200), rabbit P62/SQStM1 (1:200; #AB_437085, Abcam), rabbit cleaved caspase-3 (Cell Signaling Technology #9661, 1:500). Samples were washed in antibody dilution buffer then incubated for 2 hr at room temperature in secondary antibodies conjugated to donkey anti-mouse IgG Alexa Fluor 488 (Abcam, #ab150073, 1:400) or 555 (Abcam or 555 Thermo Fisher Scientific; A24350, 1:400). Embryos were rinsed in a wash buffer, then incubated 1hr at room temperature in 4',6-diamidino-2-phenylindole (DAPI; 0.1 %; Sigma-Aldrich, St. Louis, MO, USA) for nuclear staining.

2.8 TUNEL Staining to Assess Embryo Apoptosis

For analysis of apoptosis, the TUNEL (terminal deoxynucleotidyl transferase dUTP nick end labeling) assay was performed. Fixed embryos were stored overnight in a PHEM buffer, then blocked in 5% donkey serum and 0.1% Triton X-100 for 1 hour at room temperature and permeabilized in 0.5% Triton X-100 and 0.1M SCC for 45 minutes at room temperature. The *In Situ* Cell Death Detection Kit (Fluorescein; Roche, Mannheim, Germany) was used according to the manufacturer's instructions, with slight modifications. Positive controls were treated with DNAase to induce DNA damage. Positive and experimental samples were incubated in the TUNEL reaction medium + labelling solution for 1hr at 37°C in a dark, humidified environment, while negative controls were incubated similarly but in labeling solution only. Embryos were transferred to a wash buffer to stop the reaction, then incubated in DAPI for nuclear staining.

2.9 Confocal Microscopy

Embryos were mounted on 34mm glass-bottom dishes in 2uL drops of KSOM media blanketed with 1.5mL of mineral oil. Due to changes in access, confocal microscopy was performed using a Zeiss LSM510 laser scanning confocal microscope, Dr Dale Laird Laboratory, Western University Ontario until April 2022, and a Nikon SP8 Confocal Laser, Robarts Imaging Center, Western University Ontario for the remaining experiments. Images with 19-21 z-sections taken every 6um through each blastocyst were taken at 25x magnification in the ZEISS confocal, and

40x magnification for the Nikon SP8 confocal (there was no 25x option here). For each experimental replicate, laser settings were kept consistent when detecting the same primary antibody between treatment groups. Laser compensation was used for imaging with the NIKON SP8 confocal microscope, where laser intensity and gain gradually increase by a predetermined amount with each z-stack layer to compensate for light diffusion in the dense cellular embryonic sphere. Laser compensation presets were kept consistent between all treatment groups of the same experimental replicate.

2.10 Image Analysis

2.10.1 Total Cell Number

Images of embryos with nuclear DAPI staining were visualized using FIJI (ImageJ) software (National Institutes of Health). Total cell number (TCN) was achieved via manual counting DAPI-positive nuclei of each cell within the embryo. Embryos were categorized by stage, allowing for filtration TCN counts based on desired stage analysis (usually blastocyst).

2.10.2 LC3-II Puncta Counts

Images were generated via the ZEISS software and confocal microscope in the Dr. David Laird Lab, Western University. Images were processed using FIJI (ImageJ). To quantify LC3-II puncta, 3D z-stack projections were exported as TIFF files and opened in ImageJ. A threshold for maximum puncta size (9 pixel^2) was set based on the reported size of mammalian autophagosomes (0.5 to $1.5 \mu\text{m}$ in mammals (Parzych & Klionsky, 2014) and bright LC3-II puncta were isolated using the “threshold” pixel brightness classification function on ImageJ. The “particle counter” tool was then used to quantify the number of particles per embryo. This number was then divided by the number of cells to achieve a final number of particles per cell for each embryo. Parameters were kept consistent between groups for each experimental replicate.

2.10.3 P62 Fluorescence Analysis

Images were generated via the ZEISS software and confocal microscope in the Dr. David Laird Lab, Western University. Images were processed using FIJI (ImageJ) and Ilastik software. For fluorescence intensity quantification, 3D z-stack projections were exported as TIFF files and opened in Ilastik. Background and foreground pixels were segregated, and average fluorescence intensity was measured in arbitrary units.

2.10.4 LC3-II/Lysotracker Colocalization

Images were generated via a NIKON software and confocal microscope in ROBARTS Imaging Core, Western University, and processed using FIJI (ImageJ) and IMARIS software. To measure colocalization of lysosomes and autophagosomes, images were converted to .ims files in imaris, then LC3 channels and Lysotracker channels were imported into the “Coloc” tool, where minimum threshold brightness values were set to create a new channel with colocalized pixels only. Images were imported into ImageJ, where the number of LC3 puncta and colocalized puncta were measured using the particle counter tool as previously described in section 2.10.2. As autolysosomes can range from 1-5 μm in size with mega-autolysosomes sometimes reaching to 10 μm (Rusten et al., 2004), a minimum pixel size restriction correlating to 0.5 μm was implemented for autolysosome quantification. All imaging and analysis parameters were kept consistent between all embryos within each experimental replicate.

2.11 RNA Extraction and Reverse Transcription (RT)

On the day of RNA extraction, embryos were collected after culture and processed according to manufacturer's instructions for the Power Cells-to-CT RNA extraction and qPCR kit (Invitrogen™ Cells-to-CT™ 1-Step Power SYBR™ Green, Lot #4402953). Specifically, embryos were dispensed into 2uL of lysis solution and the number of embryos per each group was recorded. DNaseI treatment was applied in a 1:100 dilution in lysis solution to reach a final concentration of 1embryo/uL. Lysates were stored at -80°C . 30uL reverse transcription (RT) reactions (including a no-RT control) were prepared according to kit directions and run under a thermocycler program of 37°C

for 60 minutes, then 95°C for 5 minutes to create cDNA and inactivate the RT enzyme. cDNA was stored at -20°C.

2.12 Quantitative Polymerase Chain Reaction (qPCR)

RT-qPCR reactions totaling 10µL were prepared using 2µL of cDNA, 1µL of forward and reverse primers at a final concentration of a 400-500nM, 5µL Power SYBR Green included in the previously mentioned “Cells-to-CT” kit, and 3µL RNase-free water. Each reaction was plated in triplicates into a 384-well plate. All reactions included a non-template control (NTC), no-RT control (NRT). The plate was centrifuged at 2000 rpm for 2 minutes prior to qPCR reaction. The BioRad CFX384 Touch Real-Time PCR Detection System was used to run the qPCR reaction with the following conditions: 95 °C for 5 minutes, then 45 cycles of: 95 °C for 15 seconds and 60 °C for 1 minute. A melt curve from 65°C- 95 °C was included following the reaction. mRNA transcript levels were measured in cycle threshold (Ct) values through the CFX Maestro 1.1 (Bio-Rad; USA). Relative mRNA abundance was quantified using the delta-delta cycle threshold (2-ddCt) method. H2A was used as a normalization control. Transcript analysis was performed on Excel (Microsoft, USA). The primer sequences are listed in Table 1.

Table 1. Sequence of primers used for RT-PCR studies.

Gene	Sense Primer (5' to 3')	Antisense Primer (3' to 5')
GLUT1	TACACCCAGAACCAATGGC	CCCGTAGCTCAGATCGTCAC
GLUT3	AATAGGTAGGCTGGGCTTCG	AGATGGGGTCACCTTCGTT
H2A	CGCAGAGGTACTTGAGTTGG	TCTTCCCGATCAGCGATTG

2.13 Statistical Analysis

The experimental design for this work included both multiple group and 2-group comparisons. All experiments were performed with a minimum of three biological replicates. When more than 1 group was analyzed, a standard one-way or two-way ANOVA was performed, where $p < 0.05$ were considered statistically significant. For 2-group comparisons, a one-sample t-test was performed where significance was denoted by $p < 0.033^*$, $p < 0.002^{**}$, $< 0.001^{***}$. All statistical

conclusions were calculated using Graphpad Prism 9, and figure panels were created using the Quick Figures plugin for FIJI recently developed by (Mazo, 2021).

Chapter 3

3 Results

3.1 Effects of high glucose on preimplantation development

3.1.1 Effects of glucose dose response on preimplantation development when starting at 48 hpi

In preliminary experiments, embryos were flushed in the late 2-cell stage (48hpi) and exposed to 0.2 mM (control), 5 mM, 15 mM, and 25 mM D-glucose, and 25mM L-glucose as an osmolarity control and cultured for 48 hours until the blastocyst stage (96hpi; E3.5). As seen in **Figure 8**, there were no significant differences ($p>0.05$) in blastocyst formation ($p=0.1264$) or in the average total cell number ($p=0.2540$) per blastocyst observed. Embryos were then cultured under the same conditions until the zona hatching stage (E4.5, 120hpi). Again, no significant differences ($p>0.05$) in the frequency of blastocyst formation ($p=0.1525$) or blastocyst zona hatching ($p=0.3026$) were observed (**Figure 9**).

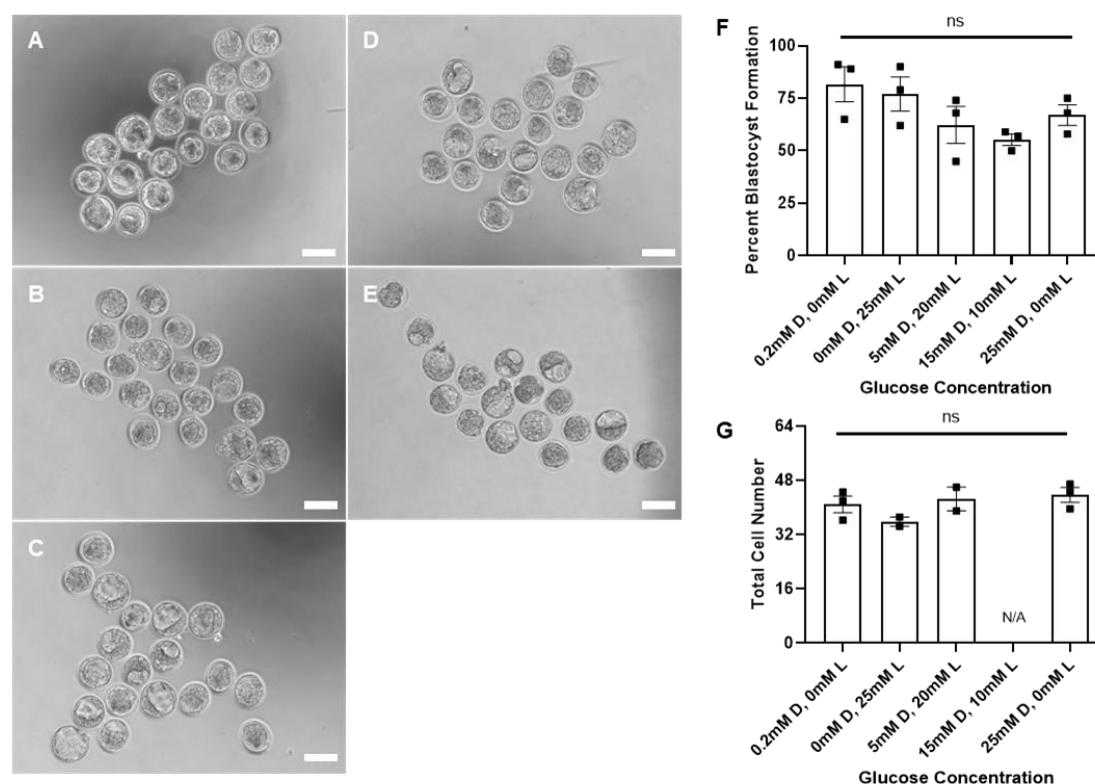


Figure 8. Blastocyst formation and total cell number after 48 hours of culture under increasing glucose concentrations.

Representative images show 2-cell embryos flushed at 48 hpi and cultured in (A) 0.2 mM D-glucose (control), (B) 25mM L-glucose (isomer control), (C) 5mM D-glucose + 20mM L-glucose, (D) 15mM D-glucose + 10mM L-glucose, and (E) 25mM D-glucose for to blastocyst stage (96hpi; E3.5). The scale bars represent 100 μ m. Data shows average (\pm SEM) values for (F) percent blastocyst formation ($n=3$ replicates) and (G) blastocyst total cell number ($n=3$ replicates). Replicates were a minimum of 20 embryos/treatment each. Statistics were calculated via an standard one-way ANOVA with significance indicated by $p<0.05$. Created with Quick Figures FIJI plugin.

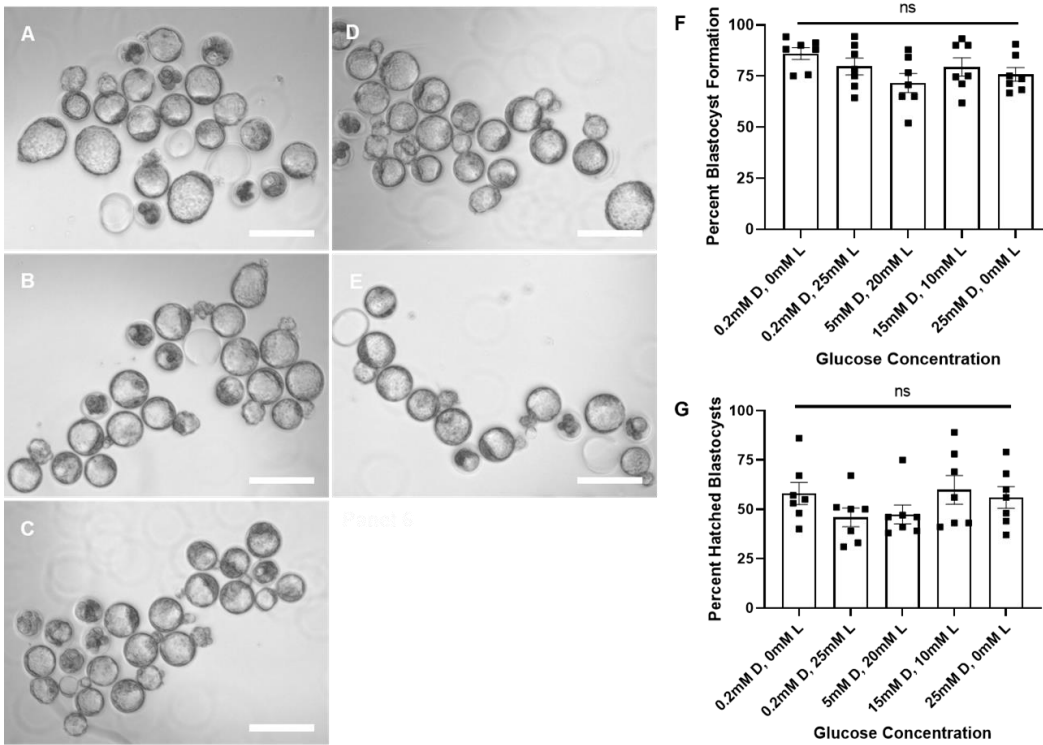


Figure 9. Blastocyst formation and hatching after 72 hours of culture under increasing glucose concentrations.

Representative images show 2-cell embryos flushed at 48 hpi and cultured in (A) 0.2 mM D-glucose (control), (B) 25mM L-glucose (isomer control), (C) 5mM D-glucose + 20mM L-glucose, (D) 15mM D-glucose + 10mM L-glucose, and (E) 25mM D-glucose to zona hatching stage (120 hpi; E4.5). The scale bars represent 200 μ m. Data shows average (\pm SEM) values for (F) percent blastocyst formation (N=7 replicates) and (G) hatching percent (N=7 replicates). Each replicate contained a minimum of 20 embryos. Statistics were calculated via standard one-way ANOVA with significance indicated by $p < 0.05$. Created with the QuickFigures FIJI plugin.

3.1.2 Effects of combined high glucose and high O₂ on development

Embryos were then subjected to a combination of high glucose treatments and high oxygen levels (20% O₂) with the intent that this combination would increase embryonic stress and unmask the effects of glucose on embryo development. Most earlier studies were also conducted under a culture atmosphere of 20% O₂ as this was the most prevalent culture atmosphere employed for mouse preimplantation embryo culture at the time. Results of a one-way ANOVA showed no significant differences ($p>0.05$) in blastocyst formation when embryos were cultured under high oxygen (20% O₂), high glucose (25 mM) or a combined environment (**Figure 10**).

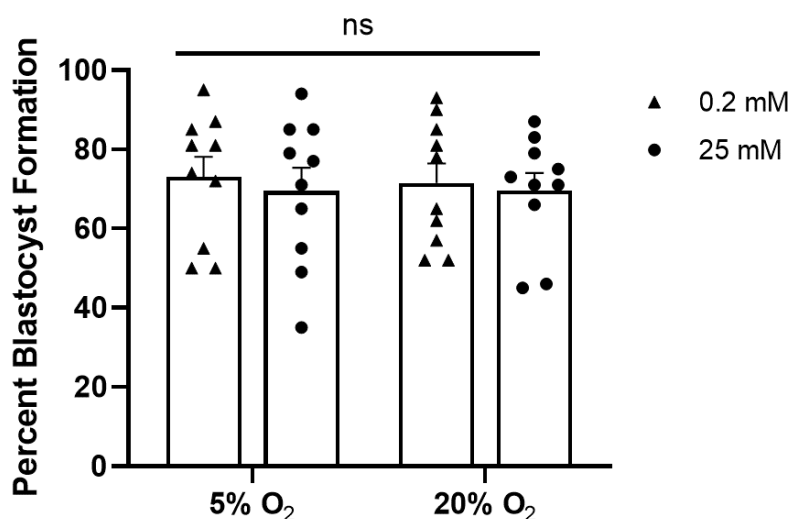


Figure 10. Blastocyst formation after combined high (25mM) glucose and high (20%) oxygen exposure.

2-cell embryos were flushed at 48 hpi and cultured in 0.2 mM (control) and 25 mM glucose under low (5%) or high (20%) oxygen levels for 48 hours to the cavitation (blastocyst) stage (E3.5). Data shows average (\pm SEM) values for percent blastocyst formation, for 10 experimental replicates ($n=10$) of a minimum of 20 embryos/group. Statistics were calculated via a two-way ANOVA with Tukey's post-hoc test, with significance indicated by $p<0.05$.

3.1.3 Effects of onset timing of high glucose treatment on preimplantation development

Subsequent experiments investigated increasing high glucose exposure by adjusting the timing of the onset of hyperglycemic treatment from the late 2-cell stage 48 hours post-hCG injection (48 hpi) to the early 2-cell stage (36 hpi). Early and late 2-cell embryos were exposed to control glucose levels (0.2 mM) or high glucose levels (25 mM) until the blastocyst cavitation stage, as seen in **Figure 11A**. Results show that when embryos are flushed and exposed to glucose 12 hours earlier (36hpi), the effects of high glucose on blastocyst formation and total cell number were significant. Blastocyst formation frequencies (shown as percent of controls) decreased significantly in embryos flushed at the early 2-cell stage ($p=0.009$), accompanied by a significant decrease in the average total number of cells per blastocyst ($p=0.0227$) (**Figure 11B**). In embryos flushed during the late 2-cell stage, the decrease in blastocyst formation was not significant between groups ($p=0.2090$), though a significant decrease in total cell number was observed ($p=0.0110$) (**Figure 11C**).

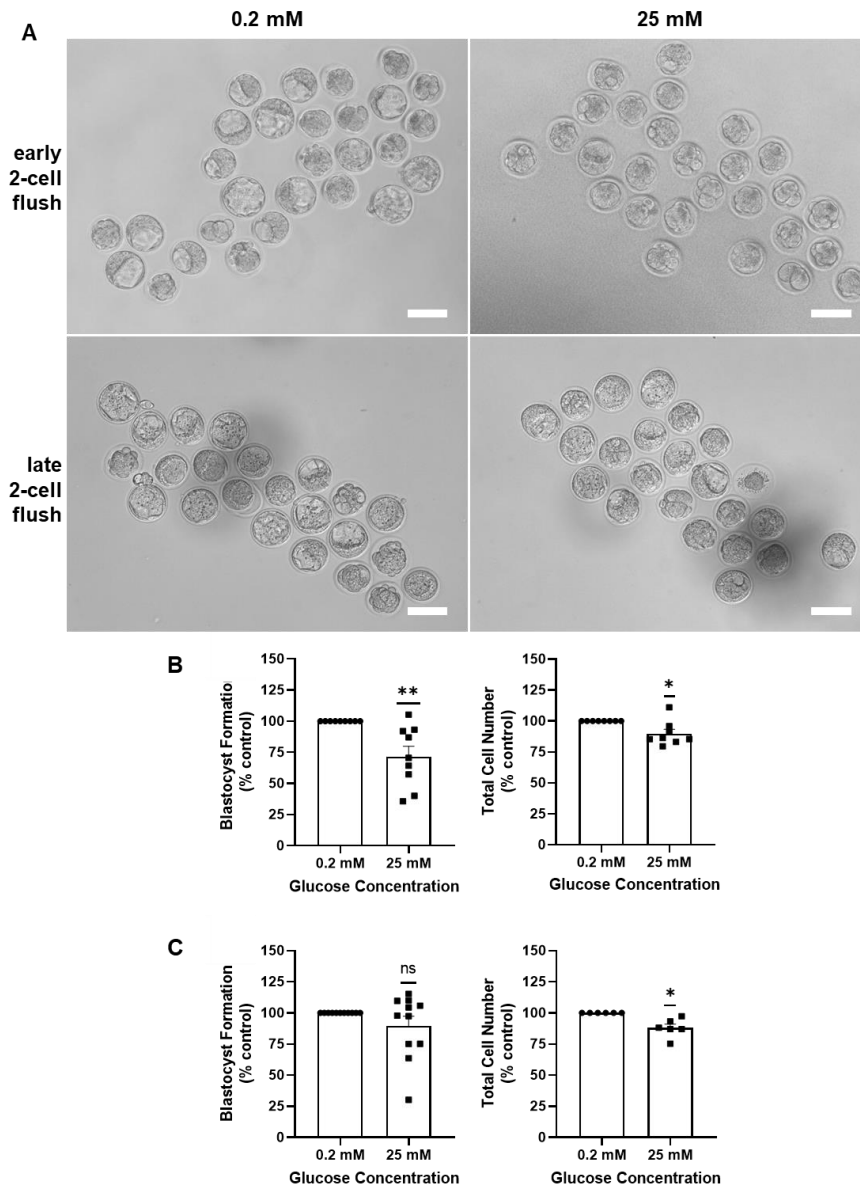


Figure 11. Blastocyst formation and total cell number after high glucose exposure to early and late 2-cell embryos.

Representative images (A) show early (36 hpi) and late (48 hpi) 2-cell embryos cultured in 0.2 mM (control) or 25 mM glucose until the blastocyst stage (96 hpi; E3.5). Scale bars represent 100 μm. Data shows average (+SEM) values for (B) percent blastocyst formation (N=9) and total cell number (N=8) for early 2-cell flushed embryos, and (C) percent blastocyst formation (N=11) and total cell number (N=6) for late 2-cell flushed embryos. Each experimental replicate consisted of a minimum of 20 embryos/treatment. Statistics were calculated via a one-sample t-test, where p<0.033*, p<0.002**, <0.001***. Created with the QuickFigures FIJI plugin

3.1.4 Effects of high glucose treatment beginning at 36 hpi on blastomere proliferation

An assessment of cell proliferation levels was also performed by measuring cells expressing Ki-67, a nuclear nonhistone protein that is universally expressed among proliferating cells during G1, S, G2, and mitosis, but absent in the G0 resting phase of quiescent cells (Graefe et al., 2019). No significant difference ($p=0.7849$) in the percent proliferating cells in blastocysts between control and hyperglycemic treatment groups for embryos flushed at the early 2-cell stage was observed (**Figure 12**).

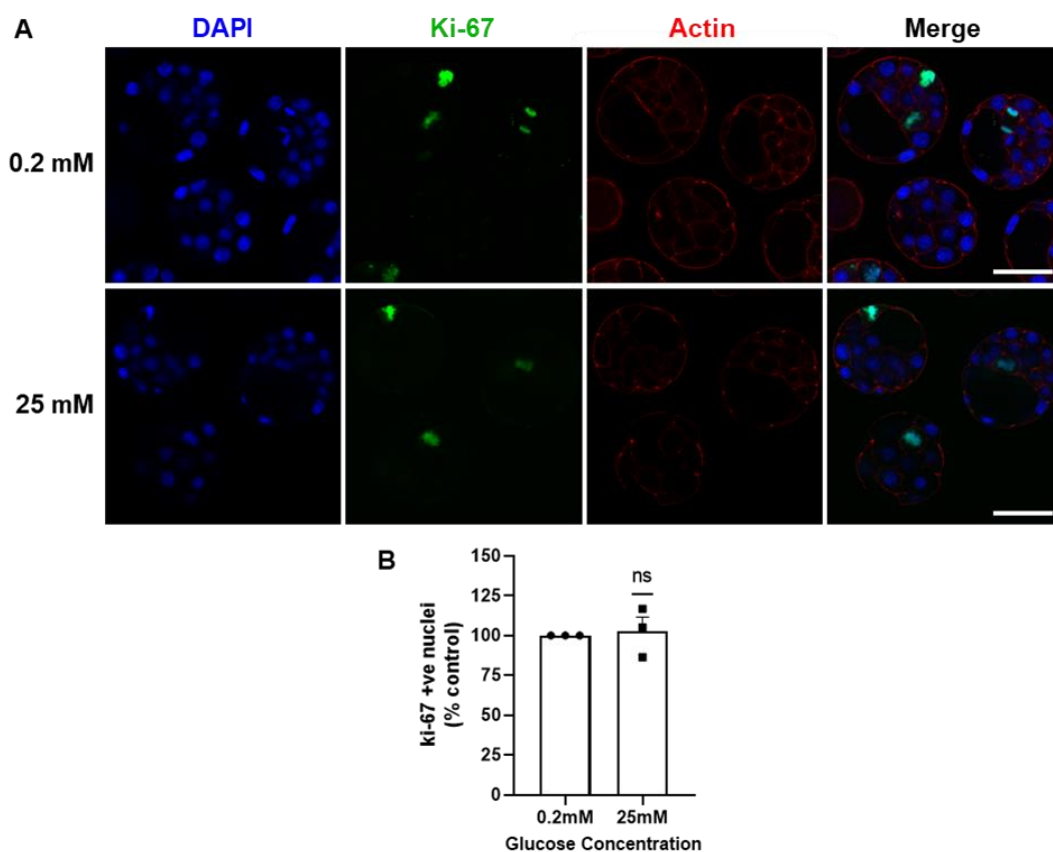


Figure 12. Ki-67 positive nuclei in blastocysts exposed to high glucose at the early 2-cell stage.

Representative images show (A) Ki-67 immunostaining in early (36 hpi) 2-cell embryos flushed and cultured in 0.2mM (control) and 25mM of glucose until blastocyst stage (96 hpi; E3.5). The scale bar represents 50 μ M. (B) Data shows average (+SEM) values for percent control levels of Ki-67-positive nuclei per embryo ($N=3$ replicates with a minimum of 15 embryos/group). Statistics were analyzed via a one-sample t-test, where $p<0.033^*$, $p<0.002^{**}$, $<0.001^{***}$.

3.2 Effects of high glucose on apoptosis and autophagy

3.2.1 Effects of high glucose treatment on preimplantation embryo apoptosis

To investigate apoptosis, experiments comparing high (25 mM) glucose exposure to early (36 hpi) and late (48 hpi) 2-cell embryos were performed. Cell death was analyzed via terminal deoxynucleotidyl transferase dUTP nick end labeling (TUNEL) quantification. The TUNEL assay detects apoptotic cells through sensitive labeling of strand breaks in fragmented DNA, which is a hall mark of apoptosis. The results indicate there was no significant changes in the number of TUNEL-positive nuclei between treatments in either the early or late 2-cell high glucose onset ($p=0.9591$ and $p=0.8250$) respectively (**Figure 13**).

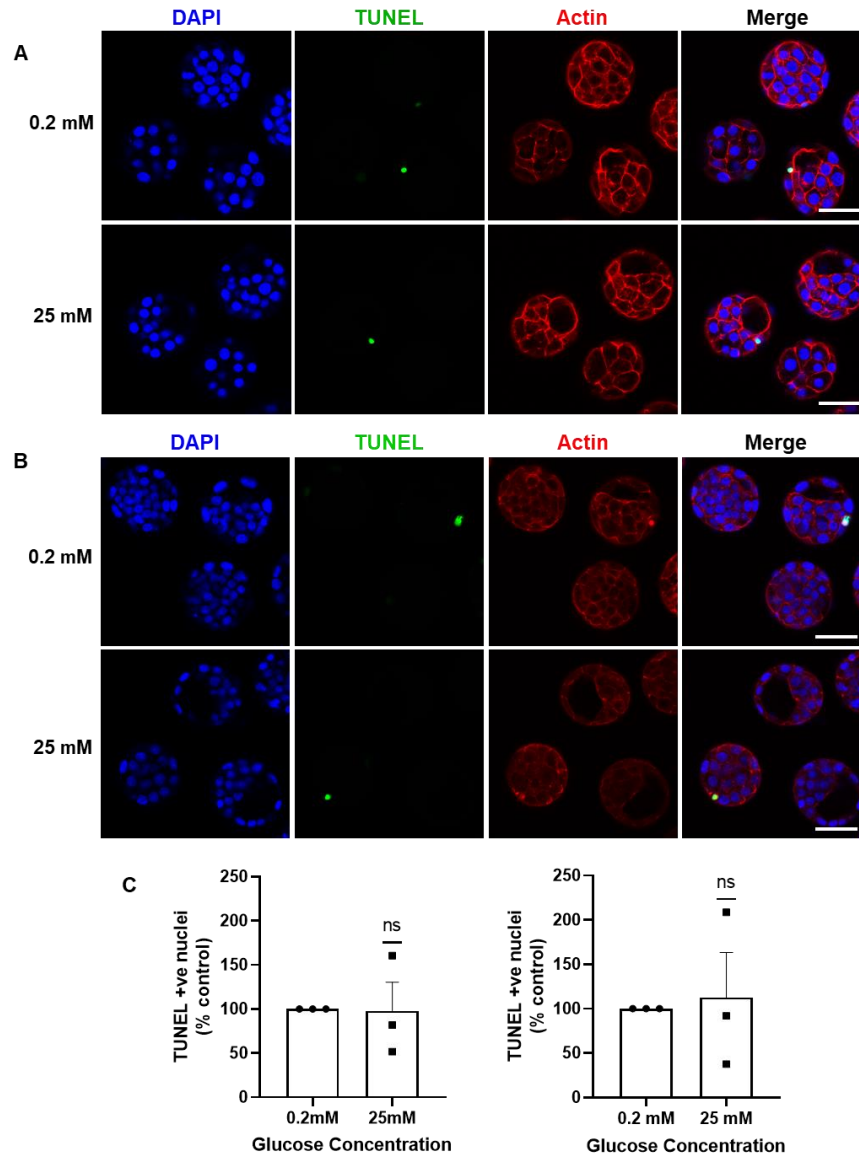


Figure 13. TUNEL-positive nuclei in blastocysts exposed to high glucose at the early 2-cell stage.

Representative images show TUNEL staining in (A) early (36 hpi) 2-cell and (B) late (48 hpi) 2-cell embryos flushed and cultured in 0.2 mM (control) and 25 mM of glucose until blastocyst stage (96 hpi; E3.5). Data shows average (+SEM) values for percent control levels of TUNEL-positive nuclei per blastocyst in (C) early 2-cell flush and (D) late 2-cells flush. N=3 replicates with a minimum of $n \geq 20$ embryos/group). Statistics were analyzed via a one-sample t-test, where $p < 0.033^*$, $p < 0.002^{**}$, $< 0.001^{***}$. The scale bars represent 50 μm . Created with the QuickFigures FIJI plugin.

3.2.2 Effects of high glucose treatment on LC3-II puncta

To assess the effects of high glucose on autophagy, I first examined the frequency of LC3-II fluorescent puncta in embryos flushed at early (36 hpi) and late (48 hpi) 2-cell stages and treated with control (0.2 mM) vs high (25 mM) glucose. The LC3I/II puncta analysis is an important marker in the detection and quantification of punctate structures that represent autophagosomes (Mizushima et al., 2010). I detected a significant ($p < 0.05$) increase in LC3 puncta numbers in embryos flushed at the earlier (36 hpi) 2-cell stage ($p = 0.0462$), while embryos exposed to glucose in the late (48 hpi) 2-cell stage displayed a non-significant ($p = 0.0738$), albeit apparent increase in LC3 puncta counts (**Figure 14**). The images show representative post-processing LC3-II puncta. Raw images can be observed in Supplementary Figure 1 (Appendix B).

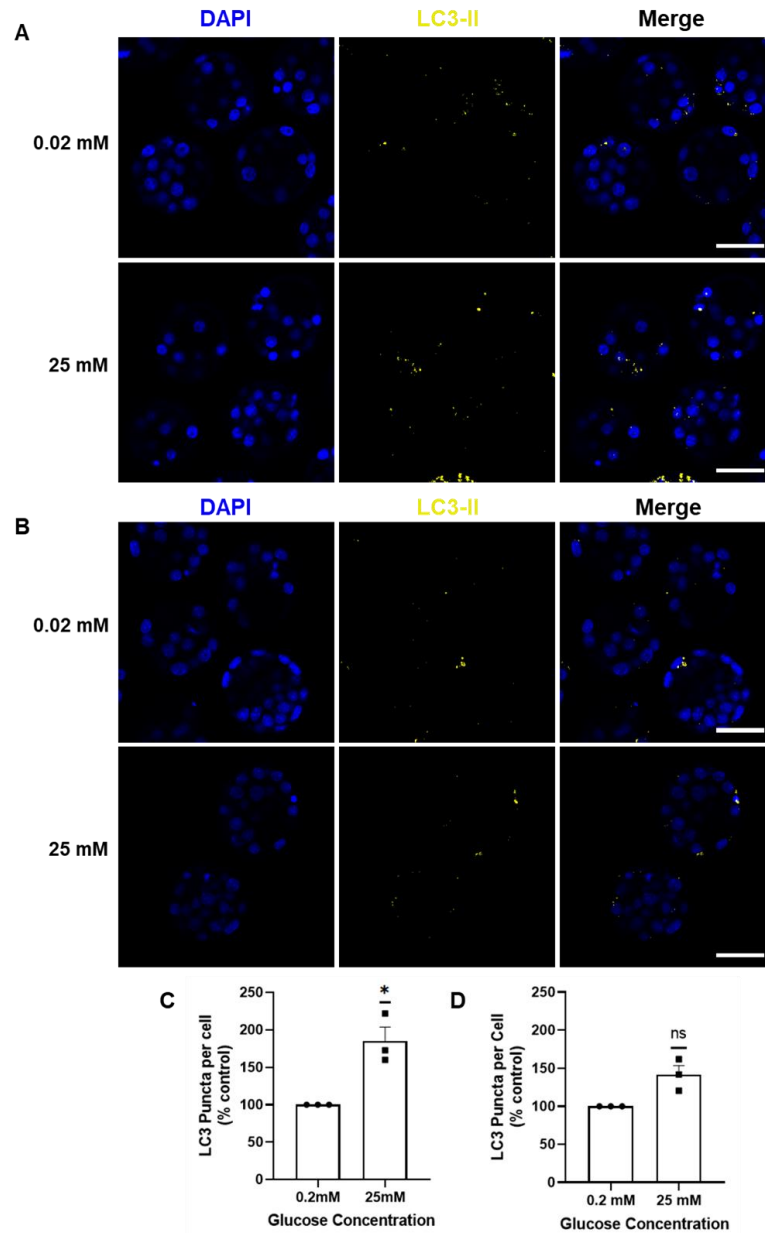


Figure 14. LC3I-II puncta per cell in embryos exposed to high glucose at the early and late 2-cell stage.

Representative images show LC3-II puncta in (A) early (36 hpi) 2-cell and (B) late (48 hpi) 2-cell embryos flushed and cultured in 0.2 mM (control) and 25 mM of glucose until blastocyst stage (96 hpi; E3.5). Data shows average (+SEM) values for percent control levels of average LC3-II puncta per cell in (C) early 2-cell flush (and (D) late 2-cells flush. N=3 replicates with a minimum of 20 embryos/group). Statistics were analyzed via a one-sample t-test, where $p < 0.033^*$, $p < 0.002^{**}$, $< 0.001^{***}$. The scale bars represent 50 μm . Image assembled with the QuickFigures FIJI plugin.

3.2.3 Determination of the onset timing of increased LC3-II puncta after 36 hpi glucose treatment

Next a time series experiment was conducted to investigate LC3-II puncta levels in early (36 hpi) flushed 2-cell embryos to determine the onset timing of increased LC3 puncta induction by high glucose culture. While there were no significant changes in the number of autophagosomes after glucose exposure from the early (36 hpi) 2-cell stage until the late (48 hpi) 2-cell stage (48hpi; $p=0.9270$), the 4-cell stage (60 hpi; $p=0.7167$), the 8-cell stage (72 hpi; $p=0.1414$), and the morula stage (84 hpi, $p=0.9118$), there was a significant increase in LC3 puncta counts per cell observed at the blastocyst stage ($p=0.0462$) (**Figure 15**).

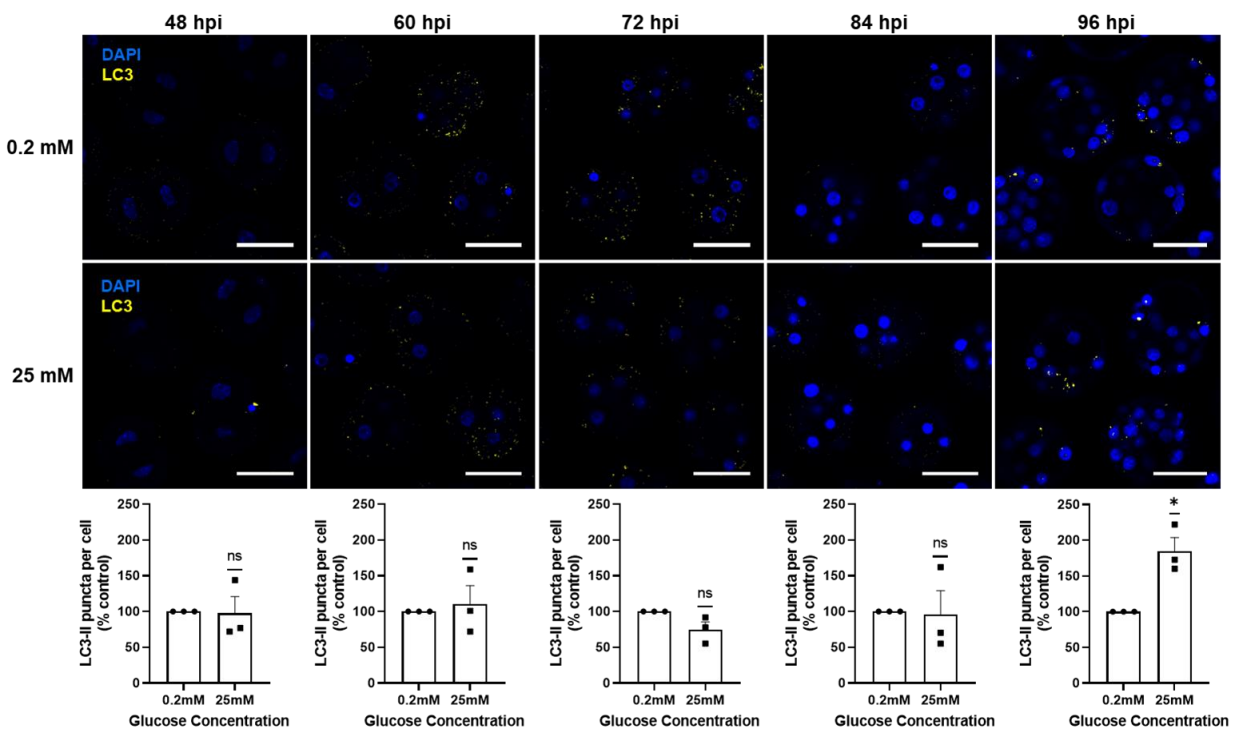


Figure 15. Developmental series of LC3-II puncta in embryos cultured in high glucose.

Representative images (A) show a developmental series of LC3-II puncta cultured from the early 2-cell stage (36 hpi) to 48 hpi, 60 hpi, 72 hpi, 84 hpi, and 96 hpi in 0.2 mM (control) and 25 mM of glucose. Data shows average (+SEM) values for percent control levels of LC3-II puncta per cell at each time point. Each time point contained 3 replicates ($n=3$) with a minimum of 20 embryos/group. Statistics were analyzed via a one-sample t-test, where $p<0.033^*$, $p<0.002^{**}$, $<0.001^{***}$. The scale bars represent 50 μm . Panels created with the QuickFigures FIJI plugin.

3.2.4 Effects of high glucose treatment on p62 immunofluorescence

An additional common marker in autophagic analysis is the protein p62. Also known as SQSTM-1 or sequestosome-1, p62 is an autophagosome cargo protein that selectively targets ubiquitinated substrates and matches them with LC3 in the autophagosome (Runwal et al., 2019). Because p62 is degraded by lysosomes along with the cellular substrates, decreased levels of p62 indicate increased functional autophagy, while accumulation of p62 occurs in autophagy deprived cells (X. C. Lee et al., 2021). My results showed a no significant ($p=0.2171$) difference in p62 fluorescence levels between the control and the high glucose treated embryos (**Figure 16**).

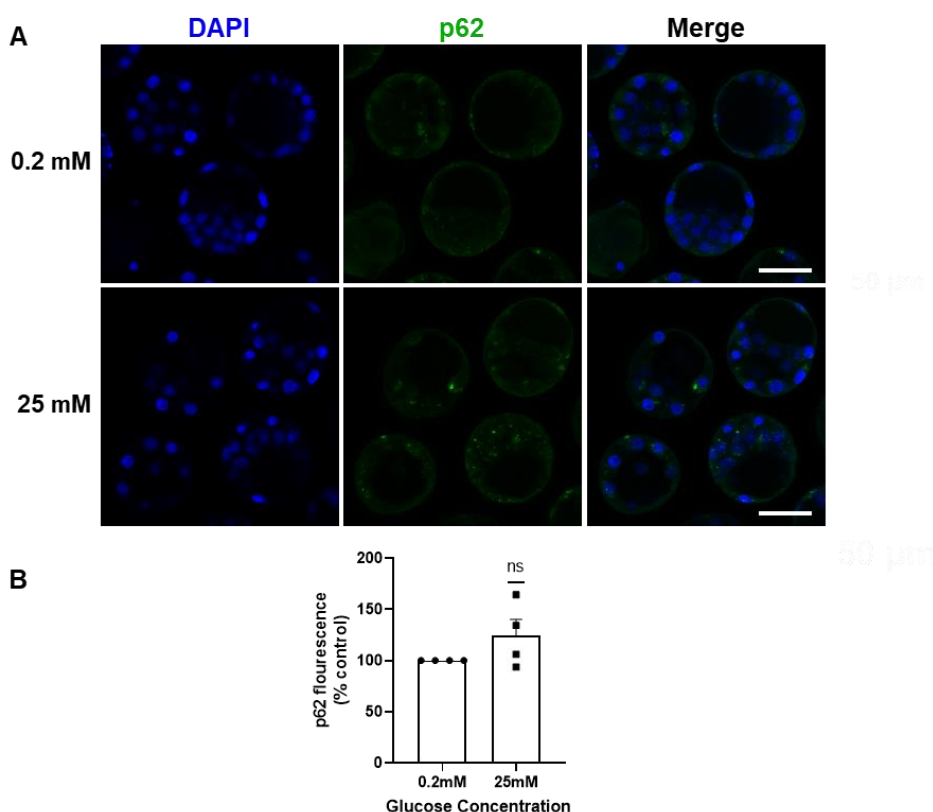


Figure 16: p62 fluorescence in embryos exposed to high glucose at the early 2-cell stage.

Representative images (A) show p62 fluorescence in early (36 hpi) 2-cell embryos flushed and cultured in 0.2 mM (control) and 25 mM of glucose until blastocyst stage (96 hpi; E3.5). Data (B) shows average (+SEM) values for percent control levels of average p62 fluorescence intensity per cell. 3 replicates ($n=3$) were performed with a minimum of 20 embryos/group. Statistics were analyzed via a one-sample t-test, where $p<0.033^*$, $p<0.002^{**}$, $<0.001^{***}$. The scale bars represent 50 μ m. Panels created with the QuickFigures FIJI plugin.

3.2.5 Effects of high glucose treatment on autophagosome formation during preimplantation development

The maturation of the autophagosome requires its fusion with lysosomes. This fusion is commonly examined to assess whether impaired or functional autophagy is occurring in the cells of interest. To test this fusion, I quantified the percentage of LC3-II puncta that were molecularly associated with lysosomes in blastocysts that had been cultured in 0.2 mM and 25 mM glucose from the early 2-cell stage (36 hpi). To do this, I measured the percentage of LC3-II puncta that were colocalized with LysoTracker Red puncta (a Lysosome stain) using the Colocalization tool in Imaris and the particle counter tool in ImageJ. My results showed a significant increase in colocalization of LC3-II puncta with LysoTracker Red ($p=0.04574$), implicating that autophagosomes were associated with lysosomes to mediate increased autophagy (**Figure 17**).

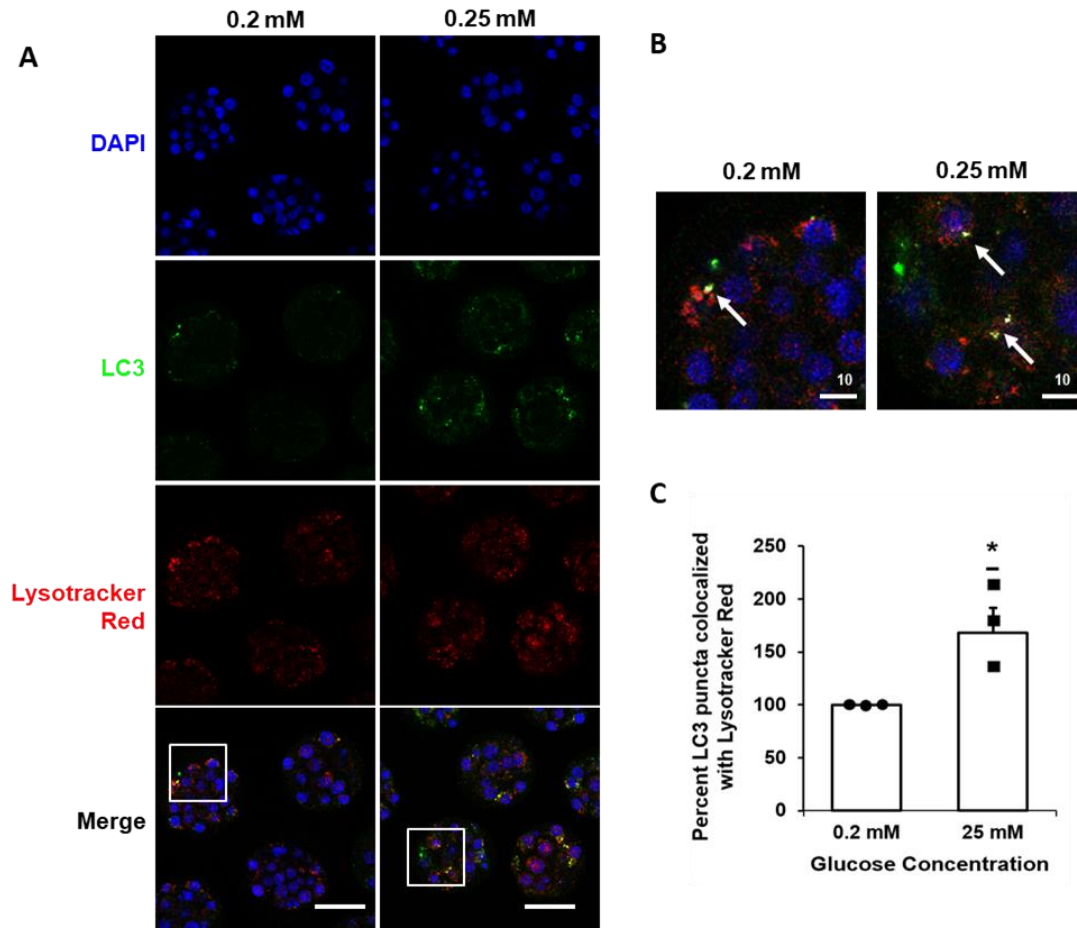


Figure 17: Colocalization of LC3-II puncta with Lysotracker Red in embryos treated with high glucose at the early 2-cell stage.

Representative images (A) show LC3 and Lysotracker Red fluorescence in early (36 hpi) 2-cell embryos flushed and cultured in 0.2 mM (control) and 25 mM of glucose until blastocyst stage (96 hpi; E3.5). The scale bars represent 50 μ m. Enlarged panels (B) show arrows pointing to overlapping LC3 and Lysotracker puncta to represent colocalization. The scale bars represent 10 μ m. Data shows (+SEM) values for percent LC3 puncta colocalized with Lysotracker Red, relative to control. Three replicates (n=3) were performed with a minimum of 20 embryos/group. Statistics were analyzed in Microsoft Excel via a students t-test, where $p < 0.05$. Panels were created with the QuickFigures FIJI plugin.

3.2.6 Effects of high glucose treatment on GLUT1 and GLUT3 mRNA transcript abundance

Glucose transporters function to carry glucose across a cell membrane. GLUT1 and GLUT3 are the most significant during mouse preimplantation embryonic development. I investigated the effects of high glucose treatment on relative mRNA levels of these glucose transporters by qPCR applied to early 2-cell embryos exposed to 0.2 mM and 25 mM glucose levels. The embryos were grouped based on development, into “blastocysts” “delayed (morulae)” embryos. The results indicate no significant differences in GLUT1 transporter relative mRNA levels across both the groups and treatments ($p>0.05$), however there was significantly more GLUT3 expression in the blastocysts than in the delayed embryos that were treated with high glucose.

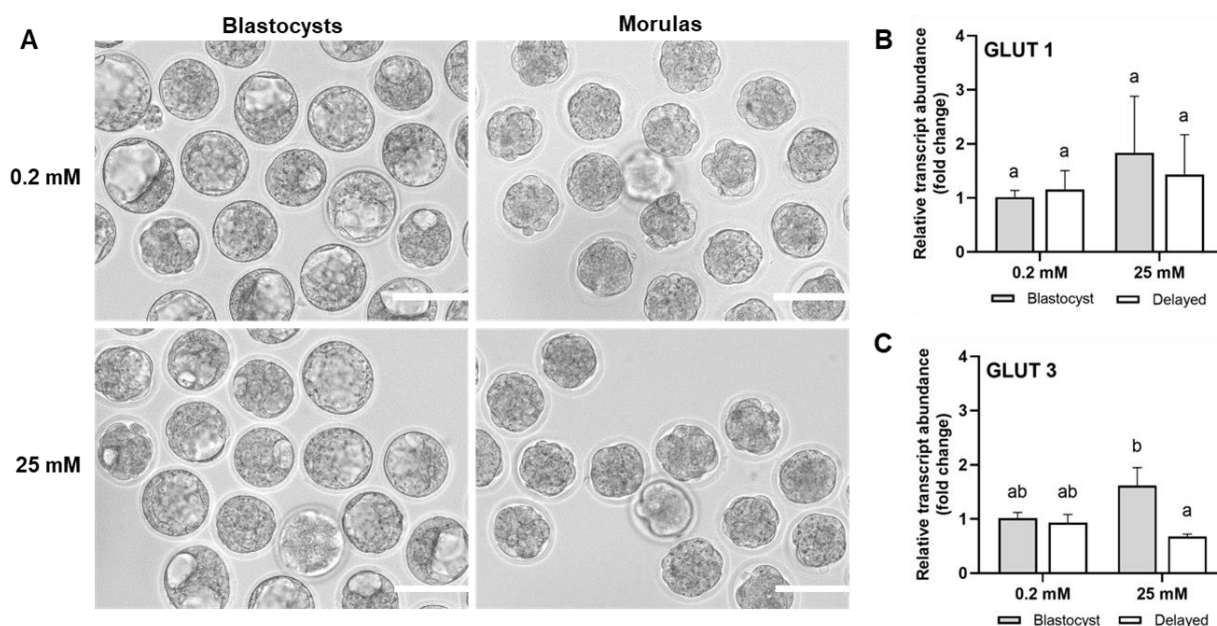


Figure 18. Relative mRNA expression of GLUT1 and GLUT3 in blastocyst, morulae (delayed) and arrested embryos.

Representative images (A) show embryos cultured from the early (26 hpi) 2-cell stage to blastocyst stage (96 hpi; E3.5) in 0.2 mM (control) and 25 mM glucose. Embryos are grouped by developmental progression into blastocyst, delayed (morulae), and arrested (not shown). Data (B) shows average (+SEM) values for GLUT1 and GLUT3 mRNA expression relative to control glucose blastocysts. Each group contains 3 replicates ($n=3$). Statistics were analyzed via a standard 2-way ANOVA where $p<0.05$ represents significance. The scale bars represent 100 μm . Panels created with the QuickFigures FIJI plugin.

Chapter 4

4 Discussion

Few studies exist investigating the effects of high glucose on autophagy and apoptosis in preimplantation embryos. Studies that do exist often involve extremely high non-physiological glucose concentrations and many key studies were published nearly 20 years ago. I developed a research mouse model using concentrations of glucose exposure comparable to murine diabetic physiology (25 mM) and investigated the effects on preimplantation development after exposure at the early (36 hpi) and late (48 hpi) 2-cell stage using CD1 mouse embryos cultured in vitro. The goal of this study was to determine if elevated glucose exposure affects embryonic developmental progression, regulation of programmed cell death such as apoptosis and autophagy, and if a change in the timing of glucose exposure onset between the early and late 2-cell stage incurs a differential response at the blastocyst stage. I hypothesized that high glucose exposure would impair embryonic development to the blastocyst stage, induce both apoptosis and autophagy, and that the timing of hyperglycemic insult would have an influential impact in their induction. My results indicated that glucose exposure at 48 hpi up to 25 mM does not result in a preimplantation impairment of development to the blastocyst stage but may decrease total cell number and induce cell survival mechanisms allowing the embryo to proceed to the implantation stage. However, initiating high glucose treatment at the early 2-cell stage (36 hpi) resulted in significant effects to blastocyst development and cell number along with significant increases in LC3-II puncta, LC3-lysosome colocalization, and GLUT3 relative mRNA levels. This is the first study that has assessed glucose level effects on preimplantation autophagy. While the outcome measures were restricted to effects to preimplantation development, it is likely that longer-term consequences of exposure to high glucose during preimplantation development would fully manifest themselves in later stages of development and pregnancy.

4.1 Effects of high glucose on preimplantation development

My initial experiments were a glucose dose response series ranging from control levels (0.2 mM) to 5 mM, 15 mM, and 25mM of D-glucose, including an osmolarity control of 25 mM L-glucose. After flushing and treating embryos at conventionally standard times (48 hpi) and culturing until embryonic day E3.5 (blastocyst cavitation stage) and E4.5 (zona hatching stage), I consistently observed no significant differences in blastocyst formation or altered zona hatching frequencies. This result was unexpected, as previous studies indicate that glucose exposure impaired blastocyst development both at levels of approximately 25mM and approximately 55 mM (Diamond et al., 1990, 1991; Pantaleon et al., 2009; Shen et al., 2009). Nonetheless, more recent studies also focusing on more relevant glucose concentrations have reported no changes to blastocyst formation at similar glucose exposures (Bermejo-Alvarez et al., 2012; Fraser et al., 2007). Interestingly, the study by Fraser et al., (2007) showed negative effects to blastocyst formation only when embryos were cultured in a “split” glucose exposure that alternated from “high (25.56 mM)”, to “low (5.56 mM) and back to “high” concentrations, suggesting there could be more factors at play than simply the concentration of glucose in the surrounding milieu, and that abrupt shifts in glucose concentration exposure may exceed the ability of early embryo adaptation mechanisms to glucose fluctuations sufficiently to impair early development.

As numerous recent studies suggest that a culture atmosphere of 20% oxygen is more stressful to preimplantation embryos than the physiologically relevant hypoxic uterine O₂ levels (approximately 5% oxygen) present during the first few days of embryonic development (Herbemont et al., 2021; Kasterstein et al., 2013), I co-cultured embryos in 20% O₂ combined with 25 mM glucose to attempt to unmask glucose effects. Contrary to my expectations, this also did not result in any significant decline in blastocyst formation or cell number. The level of oxygen in embryonic exposure ties in with its metabolism and is thought to impact oxidative phosphorylation activity and / or bring about the induction of oxidative stress to the embryo, which, as pointed out by Herbemont et al. (2021), is detrimental to the early embryo. As a history of varied significance of the benefits of hypoxic oxygen concentrations at this stage points toward an effect in the quality of blastocyst scores as an alternative finding to the actual

prevalence of blastocyst formation (Dumoulin et al., 1995; Kea et al., 2007), this may be one reason contributing to the results I observed. On another note, it has also been reported that high glucose stimulates O₂ consumption in the preimplantation embryo, depleting O₂ in the already hypoxic environment and leading to the production of ROS, and that increasing the environmental oxygen alleviated these effects (R. Li et al., 2005). If this was the case in my experiment, my combined treatment of high glucose and high O₂ might have alleviated the effects of high glucose by consuming glucose at a higher-than-normal rate which would have masked the effects, rather than revealing them. While my result was unexpected, it shows that mouse preimplantation embryos have remarkable adaptive capacity when confronted with extreme culture conditions. Clearly, they can resist the combined effects of 25 mM glucose and 20% O₂ culture with no significant changes in blastocyst formation.

In further attempts to unmask glucose effects, I next investigated the effects of shifting the treatment start time to the early 2-cell stage (36 hpi) and comparing this with the embryos flushed at the late 2-cell stage (48 hpi). This change resulted in a significant decrease in blastocyst formation by more than 25% of control levels in the early flushed 2-cells. During this time in the murine model, the embryonic genome is activated via a process known as zygotic genome activation (ZGA) (Clift & Schuh, 2013; Jing Qiu et al., 2003). ZGA is accompanied by a surge in the generation of important transcription factors and many other genes required to support early embryo development (Clift & Schuh, 2013). Preimplantation embryos are especially vulnerable to conditions that trigger oxidative stress, resulting in increased embryonic fragmentation and a reduced cleavage rate if they are not capable of producing certain antioxidants such as glutathione until beyond the 2-cell stage (Gardiner & Reed, 1995; H. W. Yang et al., 1998). These findings suggest that important changes occur during the 2-cell stage which impact its ability to resist high glucose levels, or that the extra 12 hours of glucose stress before the embryo can produce its own antioxidant response may be contributing to a significant decrease in blastocyst formation.

The characterization of this phenomenon during preimplantation embryo development is one of the most important and unique findings from my study. It highlights the likelihood that the 2-cell

stage is one of the most vulnerable phases of preimplantation development. This result certainly strengthens the pervasive concept that has emerged over time from many studies applied to 2 - cell stage mouse embryos, which is that early cleavage embryos cannot properly use glucose as a primary substrate and that if it is present in significant levels, it will greatly reduce development on to the blastocyst stage.

While the lack of blastocyst formation is a concrete indicator of disrupted embryonic progression, the ability to form a blastocyst and hatch from the zona is not in itself a comprehensive picture of embryonic health, as altered transcriptional, proliferative, metabolic, and genetic patterns may still occur at a cellular level. Therefore, I also measured the average total cell number of treated blastocysts and found it to significantly decrease by approximately 15% in both early and late 2-cell flushed embryos. Decreases in total cell number are a commonly reported outcome from high glucose embryo culture, thus my results align with much of the literature mentioned previously for both 25 mM and higher concentrations of glucose exposure. Altered ratios of the ICM and TE cells are also a commonly reported outcome measure in preimplantation embryos exposed to high glucose, seen in mice, rabbits and rats (Chi et al., 2020; Pampfer et al., 1990; Shen et al., 2009; Via y Rada et al., 2022).

As for all cellular systems, cell number in preimplantation embryos is controlled by the net balance of cell proliferation and cell death mechanisms. For these reasons I proceeded with investigating effects of high glucose on cell proliferation (Ki-67) and on apoptosis (TUNEL). Ki-67 is a nuclear protein that is universally expressed among proliferating cells (cell cycle phase G1, S, G2, and mitosis) and absent in quiescent cells (G0 resting phase) (Graefe et al., 2019). After culturing embryos from the early 2-cell stage in 25 mM glucose to the blastocyst stage, I did not find any significant changes in blastocyst Ki-67 staining. This suggests that high glucose is not significantly altering cell cycle progression. This result is supported by (Bermejo-Alvarez et al., 2012), who cultured embryos at similar glucose levels of 28 mM and did not observe altered proliferation. Other studies, however, did report delayed proliferation in mice embryos exposed to 27 mM and 25.56 mM of glucose (Fraser et al., 2007; Pantaleon et al., 2009). In rabbit embryos treated with 15mM glucose, embryonic cells were segregated before analysis,

with results showing that ICM cell number was decreased, while TE cell number was increased after exposure to high glucose (Via y Rada et al., 2022).

In summary, these results suggest that CD1 2-cell embryos treated at 48hrs post-hCG can overcome moderate glucose induced stress to maintain a normal pattern of preimplantation development. They also demonstrate that the onset of glucose treatment time plays a critical role in the capacity for stress resistance in embryos during the preimplantation period. While very few studies have focused on events transpiring between the early and late 2-cell stages of preimplantation development, the effects of maternal diabetes during the preconception (oocyte and fertilization) versus gestational stages (2-cell to blastocyst and implantation), have shown (using reciprocal embryo transfer techniques) that the time of exposure to glucose induced metabolic changes represents a critical developmental window during which the embryo is highly sensitive to maternal glucose levels (Tsai et al., 2020). Interestingly, studies show that diabetic embryopathy (fetal and blastocyst measures) can originate from both oogenetic (Chang et al., 2005; Wyman et al., 2008) and post-fertilization stages (Otani et al., 1991; Tsai et al., 2020). T.

4.2 Effects of high glucose on apoptosis

After investigating the embryonic developmental responses to 25 mM glucose exposure, I focused on the induction of apoptosis and autophagy. I found that treating early and late 2-cell embryos with 25 mM of glucose until the blastocyst stage (E3.5; 96 hpi) resulted in no significant changes to TUNEL staining, indicating no difference in DNA fragmentation between these groups. This result was unexpected, and contrasts with many studies in the literature which report increased apoptosis at various concentrations of high glucose exposure (M. Chi et al., 2000; Keim et al., 2001; Leunda-Casi et al., 2002; Moley, Chi, Knudson, et al., 1998; Shen et al., 2009). While multiple studies have reported a significant increase in apoptosis as measured by TUNEL staining, many of these studies employed glucose levels much higher than 25mM (M. Chi et al., 2000; Keim et al., 2001; Moley, Chi, & Mueckler, 1998), which is likely the major defining factor influencing this result. Some studies have found only apoptosis in the ICM or TE

cell types. As I did not segregate these cell types before assessing apoptosis, it is possible that differential effects of high glucose on TE or ICM may have occurred. It is important for future studies to conduct a cell lineage specific analysis of the effects of 25 mM glucose exposure on apoptosis. However, a study performed by Fraser et al (2007) showed similar results to my own after treating embryos at 25.56 mM of glucose. Interestingly, Fraser reported no significant increase in apoptotic cells, except for in groups where a split culture technique was used. Embryos were transferred between control and high glucose exposures every 24 hours until the late blastocyst stage. This indicates that fluctuating glucose concentrations may have a worse effect than a constant hyperglucose environment.

Hyperglycemic induced apoptosis in preimplantation embryos has mainly been reported to act through intrinsic mechanisms. However, the exact mechanism for glucotoxicity is currently unknown. Some intrinsic methods reported are oxidative stress-induced mitochondrial dysfunction and activation of the Bax, Bak and Bcl-2 pathways, including the involvement of the DNA damage sensor p53 for Bax upregulation (M. Chi et al., 2000; Keim et al., 2001; Peña-Blanco & García-Sáez, 2018) and activation of the hexosamine pathway, resulting in GSH depletion, oxidative stress, and mitochondrial Cyt C release (Horal et al., 2004). One study hypothesized that a reported decrease in glucose transporters GLUT1, GLUT2 and GLUT3 expression after high glucose exposure (Moley, Chi, & Mueckler, 1998) may lead to insufficient embryonic levels of glucose, causing metabolic deficiencies, mitochondrial dysregulation, and intrinsic cell death (Leunda-Casi et al., 2002). Other studies implicated the role of the stress-responsive JNK/MAPK signaling pathways (Lin et al., 2000) and hypoxic inducible factor-1a (HIF-1a) stabilization of p53 (Carmeliet et al., 1998; M. Chi et al., 2000).

Finally, while TUNEL analysis is a standard and widely accepted technique of measuring apoptosis, a recent study reported on the efficient efferocytosis (phagocytosis and removal of DNA fragments and apoptotic blebbing cells) by neighboring blastomeres in the embryo (Pisko et al., 2021). This suggests that DNA fragments are being removed faster than they can be detected. Thus, to obtain a more comprehensive assessment of the apoptotic fingerprint within the embryonic environment, a secondary analysis of apoptosis is desired. Apoptotic intrinsic and

extrinsic signaling pathways differ in origin but converge at the non-reversible activation of executioner caspase proteins: caspase-3, -7, and -9 (Brentnall et al., 2013). In my research, I attempted to quantify cleaved caspase-3 through immunofluorescent techniques. While my antibody staining was inconsistent and not fit for analysis, I believe that future studies of embryonic response to glucose should include a proteolytic analysis of executioner caspase proteins.

4.3 Effects of high glucose on autophagy

My study also uniquely investigated possible interactions between high glucose exposure and autophagy during mouse preimplantation development. While apoptosis is a key mechanism of cell death, autophagy is more frequently a critical mechanism for survival and normal development in embryos during cellular stress. It is activated immediately after fertilization and throughout the embryonic stages (Lee et al., 2011; Z. C. L. Leung et al., 2022). Autophagy allows for the progression of the preimplantation embryo past the two-cell stage by its fundamental ability to break down and provide building blocks for anabolic mechanisms, critical for new protein synthesis and maternal protein breakdown during zygotic genome activation (ZGA) (Lee et al., 2011). Autophagy is also necessary for responding to cellular damage and it provides the early embryo with an ability to resist environmental stressors.

A few studies have detected links between high glucose and autophagy in preimplantation mouse embryos (Adastra et al., 2011; Tsukamoto et al., 2008), however little is known on this matter. The detection and quantification of LC3 puncta is a useful measure of potential autophagic upregulation, as cleavage and lipidation of cytosolic LC3 into LC3-II creates aggregates that represent autophagosomes (Mizushima et al., 2010). However, complete autophagic flux requires the removal and degradation of these autophagosomes, and additional analyses are required. One method is the measure of LC3 puncta:lysosome colocalization via a LysoTracker Red stain, which represents the association (and fusion) of lysosomes with autophagosomes into an autolysosome. This indicates that the autophagosome's cargo is likely degrading. During

impaired autophagy, LC3 puncta aggregates will accumulate in the absence of colocalization and resultant lack of subsequent removal of cellular debris.

My results indicate that LC3 puncta counts increased by ~80% of control values in embryos flushed at the early 2-cell stage, while embryos exposed to 25 mM glucose in the late 2-cell stage showed a non-significant, but apparent trend of ~40% increase in LC3 puncta. Other than one other paper (Adastra et al., 2011), this is one of the first known reports of high glucose effects on autophagy during mouse preimplantation development. The differential significance between the LC3 induction in the early and late-flushed embryos is intriguing, supporting the concept that a 12-hour period exists between the early and late 2-cell embryo where sensitivity to glucose concentrations is present, rendering them less able to resist effects of the hyperglycemic environment than they otherwise would be. There could be multiple reasons for why this may occur. However, since zygotic genome activation occurs primarily during the 2-cell stage in mouse embryos (Jing Qiu et al., 2003), early 2-cell embryos may not have the adaptive ability to induce a response to cellular stress with transcriptional and translational regulation. This would result in higher levels of stress at the cleavage stage which could induce survival mechanisms including autophagy later in development.

In response to this, I performed a time course analysis examining the timing of the onset of elevated LC3 puncta levels (autophagic responses) to hyper glucose by performing a developmental time course series where I flushed the embryos at the early 2-cell stage and harvested 20 embryos every 12 hours until 84 hours post fertilization for LC3 puncta analysis. I observed no significant change in LC3 puncta levels between treated and control embryos until the blastocyst cavitation stage (E3.5; 96hpi). This result suggests the following: While it is clear autophagy is required to maintain preimplantation development from the 1-cell to blastocyst stages, studies to date have not determined how levels of autophagy fluctuate in response to various stressors throughout preimplantation development. What is most intriguing from these outcomes is that LC3 puncta levels were not impacted significantly until the blastocyst stage. This suggests that the high glucose effect, while being initiated at the early 2-cell stage (36hpi), does not have an immediate impact on development and, in fact, components of the response do

not reveal themselves until up to 2 days later following initial exposure occurs, at the blastocyst stage. This outcome reveals facets of both embryo metabolism and autophagy induction during preimplantation development.

P62 is a secondary marker of autophagy to LC3, though it has a different function. Upregulated by the conserved autophagy and lysosomal regulator transcription factor EB (TFEB) (Settembre et al., 2011) through nutrient sensor mTORC1 modulation (Martina et al., 2012) as well as the oxidative stress transcription factor Nrf2 (Jain et al., 2010), it plays a role in sequestering ubiquitinated cellular cargo and recruiting them to LC3 in the maturing autophagosome (X. C. Lee et al., 2021). Since p62 is degraded alongside the lysosomal contents, a large buildup of p62 indicates autophagic impairment. I did not observe a significant change in p62 from control levels. This could be indicating successful degradation of the autophagosome, however, a decrease in p62 is frequently observed alongside highly active autophagic flux (Mizushima et al., 2010). Additionally, another LC3 interactor, NBR1 (neighbor of the BRCA gene 1), functions similarly to p62, and can mediate autophagy in p62-inhibited systems (Kirkin et al., 2009).

With data supporting evidence for an upregulation in autophagy after hyperglycemic exposure, I measured colocalization of LC3puncta with Lysotracker Red (a lysosomal stain) to ensure that increased LC3 puncta was not simply due to autophagic failure and a buildup of undegraded autophagosomes. My results showed an increased by approximately 70% of control levels of the association of LC3 puncta with lysosomes (**Figure 17**). In combination with previously measured increases in LC3 puncta, this strongly supports the formation and subsequent degradation of autophagosomes, likely meaning there is increased autophagy after high glucose culture from the early 2-cell stage to the blastocyst stage.

Taken together, my study shows that a 25 mM concentration of glucose exposure from the early 2-cell stage stimulates an increase in autophagosome formation and degradation, with no increase in apoptosis, at the blastocyst stage. These effects are not significantly seen in embryos flushed from the late 2-cell stage, signifying that the 12 hour window between the early and late stages remains an important time where the embryo is sensitive to stress induced by the higher levels of glucose.

4.4 Glucose transporter roles in the embryonic hyperglycemic response

To analyze how glucose transport may play a role in the embryonic response to high glucose, I examined the impact of high glucose on relative mRNA levels of glucose transporters between blastocysts versus delayed embryos by the 96 hpi (blastocyst stage) time point. The embryos were also exposed to 0.2 mM (control) and 25 mM (high) glucose levels. GLUT1 is expressed in all preimplantation stages of the mouse and is the primary transporter of glucose until the expression of GLUT3 at the compaction stage (Pantaleon et al., 1997). It allows for glucose metabolism through the HBP and PPP pathways to facilitate ICM versus TE cell differentiation (Chi et al., 2020). Embryonic glucose sensing through the HBP pathway is critical for the activation of GLUT3, the major glucose transporter in the blastocyst (Pantaleon et al., 2008). GLUT3, after its expression during the morula stage, becomes the major glucose transporter facilitating the surge in embryonic influx of glucose after cavitation (Pantaleon et al., 2008). My results showed that there were no significant changes in the levels of the GLUT1 transporter between glucose concentrations or between embryonic developmental groups, while GLUT3 expression was significantly increased in blastocysts cultured under high glucose compared to delayed embryos of the same treatment. The significantly increased expression of GLUT3 compared to GLUT1 between the blastocyst and developmentally delayed embryos was unexpected, as previous studies by Kelle Moley's group showed decreases in GLUT1 and GLUT3 upon preimplantation embryonic exposure to high glucose both in vivo and in vitro (M. Chi et al., 2002; Moley, Chi, Knudson, et al., 1998). Additionally, in cancer cells (Marín-Hernández et al., 2014) and in neuronal rat cells (Nagamatsu et al., 1994), GLUT1 and GLUT3 expression is upregulated under glucose deprivation. This outcome supports the time course assessment of LC3 puncta accumulation that I observed to occur at the blastocyst stage following exposure to high glucose from the 36 hpi onward. Based on my findings I would propose that high glucose treatment beginning at 36 hpi results in enhanced GLUT3 expression which may enhance glucose uptake, triggering enhanced autophagy as revealed by elevated LC3 puncta.

This possible interaction of glucose levels and autophagy activation during preimplantation development is a major novel discovery of my studies.

In summary, the collective understanding of mouse preimplantation embryo metabolism formulated from many studies over the years has established that the early cleavage stage embryo has limited ability to uptake or utilize glucose for metabolism until late compaction/morula and cavitation stages are reached. Since the embryos in my study were cultured continuously in the presence of a fixed glucose concentration, I would propose that high glucose exposure could enact its impact on development at different time points and in different manners. As previously discussed, there is a differential 2-cell impact based on the timing of exposure. The time course experiment suggests that minimal consequences to the embryo occur until the blastocyst stage is reached. This is exciting as the blastocyst stage is a time when glucose transport is enhanced due to increased GLUT 3 expression and a shift in metabolism from employing pyruvate as the primary early embryonic energy substrate to glucose becoming the primary energy substrate. It would seem reasonable to propose, therefore, that it is not until the blastocyst stage when high glucose levels are likely to exert a major influence on preimplantation embryo autophagy, and the enhanced blastocyst levels of LC3-II puncta observed in my study certainly support this conclusion.

4.5 Limitations

The metabolic and supra-physical characteristics seen in metabolic diseases, such as diabetes, often involve more than one affecting insult. Thus, an in vitro model using only high levels of glucose does not consider other factors often heavily associated with diabetes such as increased BMI, fatty acid levels, and insulin changes. Alterations in fatty acids have been shown recently in our lab to negatively affect preimplantation embryo development (Z. C. L. Leung et al., 2022; Yousif et al., 2020). Thus in the diabetic mouse, there are more factors that could be contributing to alterations in preimplantation embryonic development other than high levels of glucose. Embryos express insulin responsive GLUT4 and GLUT8 from the 8-cell and blastocyst stage in both mice and rabbits (Carayannopoulos et al., 2000a, 2000b; Tonack et al., 2004). In addition,

embryos in diabetic patients are certain to be affected differently than in vitro treated early embryos, due, for example, to insulin treatment taken by diabetic patients.

As with any study, one must consider forms of limitations to my experimental design, results, and analysis. In my experimental design, a more robust study would have compared the results I gathered to in-vivo results of embryos derived from diabetic maternal mice, looking at developmental competence as far as the implantation stage. In my case this was not possible as an AUP for diabetic mice models was not currently in order in my lab, and I was the first in my lab to focus on hyperglycemic studies. If future studies were to continue with this project, it would be beneficial to consider these options. Additionally, I think it would be beneficial to add an extra group of ultra-high glucose exposure to use as a comparison with older studies that use similar concentrations, and as an internal positive control to compare with the 25 mM glucose. As autophagy is a complex process, my study would benefit from a more robust analysis of autophagy. The measurement of autophagic flux, combining chloroquine with hyperglycemic studies, and immunofluorescence analyses of some of the ATG specified proteins is warranted. Finally, it would be useful to investigate a deeper mechanistic control of autophagy, such as examining affects to JNK/SAPK signaling, p66shc, or other stress responsive signaling mechanisms known to be important mediators of oxidative stress, apoptosis, and autophagy (Moruno et al., 2012; Soliman et al., 2014).

Technical Limitations: Confocal z-stack imaging of the embryos was only at every 6 uM. Ideally a distance of 2-3 uM would be better for resolution of all the LC3 puncta. However, this would result in extremely long imaging time, exposing the samples to a significantly higher degree of laser light. Additionally, it would create extremely large images with up to 40 z slices per embryo, which are difficult to store, transfer, and handle in a program. Additionally, there were challenges to switching to the new confocal in the Robarts facility. Even after troubleshooting with imaging facility technicians, I found the new microscope produced clear focused images near the bottom of the embryo, but blurry images at z slices near the top of the embryo, rendering some images unusable. Many confocal imaging investigators still use the conventional mounting methods with glass slides and cover slips, as slight compression of the embryo without bursting

them might help with the image resolution and focus. This is a more intensive staining process with higher rates of sample loss and there are pros and cons to both methods – however it is something to consider in future investigations.

5 Conclusion and future directions

My study has uncovered two very novel aspects of glucose-based influences on mouse preimplantation development. The first is that there is a 12 hr developmental window at the 2-cell stage in which mouse early embryos are vulnerable to high diabetic physiological levels of glucose, resulting in reduced blastocyst formation and cell number. Secondly, this early exposure to high glucose induces key components of the autophagy pathway including increased LC3-II puncta and autophagosome formation. This may occur as an attempt to offset metabolic consequences downstream from higher glucose level exposure. Finally, an increase in GLUT3 mRNA levels is part of the early mouse embryo response to elevated glucose and may provide a mechanism for increased glucose uptake.

In particular, I would suggest 3 main future directions for studies in this area of research. Future studies should focus on mechanistic and regulatory mechanisms activated, not just developmental parameters. Future studies should try to elucidate still unsolved questions regarding how glucose originally induces oxidative stress in the embryo. Future studies should investigate the interplay between autophagy and apoptosis more comprehensively as their synergy will impact greatly on the health and viability of embryos and fetuses derived from diabetic patients.

References

- Adastra, K. L., Chi, M. M., Riley, J. K., & Moley, K. H. (2011). A differential autophagic response to hyperglycemia in the developing murine embryo. *Reproduction*, *141*, 607–615. <https://doi.org/10.1530/REP-10-0265>
- Aghayan, M., Rao, L. V., Smith, R. M., Jarret, L., Charron, M. J., Thorens, B., & Heyner, S. (1992). Developmental expression and cellular localization of glucose transporter molecules during mouse preimplantation development. *Development*, *115*(1), 305–312. <https://doi.org/10.1242/DEV.115.1.305>
- Agulhon, C., Rostaing, P., Ravassard, P., Sagné, C., Triller, A., & Giros, B. (2003). Lysosomal amino acid transporter LYAAT-1 in the rat central nervous system: an in situ hybridization and immunohistochemical study. *The Journal of Comparative Neurology*, *462*(1), 71–89. <https://doi.org/10.1002/CNE.10712>
- Aiken, C. E. M., Swoboda, P. P. L., Skepper, J. N., & Johnson, M. H. (2004). The direct measurement of embryogenic volume and nucleo-cytoplasmic ratio during mouse pre-implantation development. *Reproduction*, *128*(5), 527–535. <https://doi.org/10.1530/REP.1.00281>
- Akar, Y., Ahmad, N., & Khalid, M. (2019). The effect of cadmium on the bovine in vitro oocyte maturation and early embryo development. *Https://Doi.Org/10.1016/j.Ijvsm.2018.03.001*, *6*, S73–S77. <https://doi.org/10.1016/J.IJVSM.2018.03.001>
- Akella, N. M., Ciraku, L., & Reginato, M. J. (2019). Fueling the fire: emerging role of the hexosamine biosynthetic pathway in cancer. *BMC Biology* *2019 17:1*, *17*(1), 1–14. <https://doi.org/10.1186/S12915-019-0671-3>
- Amaral, J. D., Xavier, J. M., Steer, C. J., & Rodrigues, C. M. (2010). The role of p53 in apoptosis. *Discovery Medicine*, *9*(45), 145–152.

- Amstad, P. A., Yu, G., Johnson, G. L., Lee, B. W., Dhawan, S., & Phelps, D. J. (2001). Detection of caspase activation in situ by fluorochrome-labeled caspase inhibitors. *BioTechniques*, 31(3), 608–610, 612, 614, passim. <https://doi.org/10.2144/01313pf01>
- Axe, E. L., Walker, S. A., Manifava, M., Chandra, P., Roderick, H. L., Habermann, A., Griffiths, G., & Ktistakis, N. T. (2008). Autophagosome formation from membrane compartments enriched in phosphatidylinositol 3-phosphate and dynamically connected to the endoplasmic reticulum. *The Journal of Cell Biology*, 182(4), 685–701. <https://doi.org/10.1083/jcb.200803137>
- Bermejo-Alvarez, P., Roberts, R. M., & Rosenfeld, C. S. (2012). Effect of Glucose Concentration During in Vitro Culture of Mouse Embryos on Development to Blastocyst, Success of Embryo Transfer and Litter Sex Ratio. *Molecular Reproduction and Development*, 79(5), 329–336. <https://doi.org/10.1002/mrd.22028>
- Bernard, A., Jin, M., Xu, Z., & Klionsky, D. J. (2015). A large-scale analysis of autophagy-related gene expression identifies new regulators of autophagy. *Autophagy*, 11(11), 2114–2122. <https://doi.org/10.1080/15548627.2015.1099796>
- Bossen, C., Ingold, K., Tardivel, A., Bodmer, J.-L., Gaide, O., Hertig, S., Ambrose, C., Tschopp, J., & Schneider, P. (2006). Interactions of Tumor Necrosis Factor (TNF) and TNF Receptor Family Members in the Mouse and Human. *Journal of Biological Chemistry*, 281(20), 13964–13971. <https://doi.org/10.1074/jbc.M601553200>
- Brill, A., Torchinsky, A., Carp, H., & Toder, V. (1999). The Role of Apoptosis in Normal and Abnormal Embryonic Development. In *Journal of Assisted Reproduction and Genetics* (Vol. 16, Issue 10).
- Brison, D. R. (2000). Apoptosis in mammalian preimplantation embryos: regulation by survival factors. *Human Fertility (Cambridge, England)*, 3(1), 36–47. <https://doi.org/10.1080/1464727002000198671>

- Brownlee, M. (2005). The Pathobiology of Diabetic Complications A Unifying Mechanism. *Diabetes*, 54. <http://diabetesjournals.org/diabetes/article-pdf/54/6/1615/381945/zdb00605001615.pdf>
- Butkinaree, C., Park, K., & Hart, G. W. (2010). O-linked beta-N-acetylglucosamine (O-GlcNAc): Extensive crosstalk with phosphorylation to regulate signaling and transcription in response to nutrients and stress. *Biochimica et Biophysica Acta*, 1800(2), 96–106. <https://doi.org/10.1016/J.BBAGEN.2009.07.018>
- Cagnone, G. L. M., Dufort, I., Vigneault, C., & Sirard, M. A. (2012). Differential gene expression profile in bovine blastocysts resulting from hyperglycemia exposure during early cleavage stages. *Biology of Reproduction*, 86(2), 1–12. <https://doi.org/10.1095/BIOLREPROD.111.094391/2530691>
- Canadian Diabetes Association. (n.d.). *Gestational diabetes - Diabetes Canada*. Retrieved April 11, 2023, from <https://www.diabetes.ca/about-diabetes/gestational>
- Carayannopoulos, M. O., Chi, M. M. Y., Cui, Y., Pingsterhaus, J. M., McKnight, R. A., Mueckler, M., Devaskar, S. U., & Moley, K. H. (2000a). GLUT8 is a glucose transporter responsible for insulin-stimulated glucose uptake in the blastocyst. *Proceedings of the National Academy of Sciences of the United States of America*, 97(13), 7313–7318. <https://doi.org/10.1073/PNAS.97.13.7313>
- Carayannopoulos, M. O., Chi, M. M. Y., Cui, Y., Pingsterhaus, J. M., McKnight, R. A., Mueckler, M., Devaskar, S. U., & Moley, K. H. (2000b). GLUT8 is a glucose transporter responsible for insulin-stimulated glucose uptake in the blastocyst. *Proceedings of the National Academy of Sciences of the United States of America*, 97(13), 7313–7318. <https://doi.org/10.1073/PNAS.97.13.7313>
- Cardone, M. H., Salvesen, G. S., Widmann, C., Johnson, G., & Frisch, S. M. (1997). The regulation of anoikis: MEKK-1 activation requires cleavage by caspases. *Cell*, 90(2), 315–323. [https://doi.org/10.1016/s0092-8674\(00\)80339-6](https://doi.org/10.1016/s0092-8674(00)80339-6)

- Carmeliet, P., Dor, Y., Herber, J. M., Fukumura, D., Brusselmans, K., Dewerchin, M., Neeman, M., Bono, F., Abramovitch, R., Maxwell, P., Koch, C. J., Ratcliffe, P., Moons, L., Jain, R. K., Collen, D., & Keshet, E. (1998). Role of HIF-1 α in hypoxia-mediated apoptosis, cell proliferation and tumour angiogenesis. *Nature* 1998 394:6692, 394(6692), 485–490. <https://doi.org/10.1038/28867>
- Castori, M. (2013). Diabetic Embryopathy: A Developmental Perspective from Fertilization to Adulthood. *Molecular Syndromology*, 4(1–2), 74. <https://doi.org/10.1159/000345205>
- Chang, A. S., Dale, A. N., & Moley, K. H. (2005). Maternal Diabetes Adversely Affects Preovulatory Oocyte Maturation, Development, and Granulosa Cell Apoptosis. *Endocrinology*, 146(5), 2445–2453. <https://doi.org/10.1210/EN.2004-1472>
- Chatot, C. L., Lewis-Williams, J., Torres, I., & Ziomek, C. A. (1994). One-minute exposure of 4-cell mouse embryos to glucose overcomes morula block in CZB medium. *Molecular Reproduction and Development*, 37(4), 407–412. <https://doi.org/10.1002/MRD.1080370407>
- Chaveroux, C., Sarcinelli, C., Barbet, V., Belfeki, S., Barthelaix, A., Ferraro-Peyret, C., Lebecque, S., Renno, T., Bruhat, A., Fafournoux, P., & Manié, S. N. (2016). Nutrient shortage triggers the hexosamine biosynthetic pathway via the GCN2-ATF4 signalling pathway. *Scientific Reports* 2016 6:1, 6(1), 1–10. <https://doi.org/10.1038/srep27278>
- Chazaud, C., Yamanaka, Y., Pawson, T., & Rossant, J. (2006). Early Lineage Segregation between Epiblast and Primitive Endoderm in Mouse Blastocysts through the Grb2-MAPK Pathway. *Developmental Cell*, 10, 615–624. <https://doi.org/10.1016/j.devcel.2006.02.020>
- Chi, F., Sharpley, M. S., Nagaraj, R., Roy, S. sen, & Banerjee, U. (2020). Glycolysis Independent Glucose Metabolism Distinguishes TE from ICM Fate During Mammalian Embryogenesis. *Developmental Cell*, 53(1), 9. <https://doi.org/10.1016/J.DEVCEL.2020.02.015>
- Chi, M., Hoehn, A., & Moley, K. H. (2002). Metabolic changes in the glucose-induced apoptotic blastocyst suggest alterations in mitochondrial physiology. *American Journal of Physiology*

- *Endocrinology and Metabolism*, 283(2 46-2), 226–232.

<https://doi.org/10.1152/AJPENDO.00046.2002/ASSET/IMAGES/LARGE/H10820919002>.
JPEG

Chi, M., Pingsterhaus, J., Carayannopoulos, M., & Moley, K. H. (2000). *Decreased Glucose Transporter Expression Triggers BAX-dependent Apoptosis in the Murine Blastocyst**.
<https://doi.org/10.1074/jbc.M005508200>

Chi, Sharpley, M. S., Nagaraj, R., Roy, S. Sen, & Banerjee, U. (2020). Glycolysis-Independent Glucose Metabolism Distinguishes TE from ICM Fate during Mammalian Embryogenesis. *Developmental Cell*, 53(1), 9-26.e4. <https://doi.org/10.1016/J.DEVCEL.2020.02.015>

Chowdhury, S., Otomo, C., Leitner, A., Ohashi, K., Aebersold, R., Lander, G. C., & Otomo, T. (2018). Insights into autophagosome biogenesis from structural and biochemical analyses of the ATG2A-WIPI4 complex. *Proceedings of the National Academy of Sciences of the United States of America*, 115(42), E9792–E9801.
https://doi.org/10.1073/PNAS.1811874115/SUPPL_FILE/PNAS.1811874115.SM01.GIF

Clift, D., & Schuh, M. (2013). Restarting life: fertilization and the transition from meiosis to mitosis. *Nature Reviews Molecular Cell Biology* 2013 14:9, 14(9), 549–562.
<https://doi.org/10.1038/nrm3643>

Cockburn, K., & Rossant, J. (2010). Making the blastocyst: lessons from the mouse. *The Journal of Clinical Investigation*, 120(4), 995–1003. <https://doi.org/10.1172/JCI41229>

Coles, C. (1994). Critical Periods for Prenatal Alcohol Exposure: Evidence From Animal and Human Studies. *Alcohol Health and Research World*, 18(1), 22.
[/pmc/articles/PMC6876479/](https://pubmed.ncbi.nlm.nih.gov/6876479/)

Danielle Fontaine. (2019). *5 Common Questions for Diabetic Models*. 5 Common Questions for Diabetic Models. <https://www.jax.org/news-and-insights/jax-blog/2019/september/5-common-questions-for-diabetic-models>

- D'arcy, M. S. (2019). Cell death: a review of the major forms of apoptosis, necrosis and autophagy. *Cell Biology International*, 43. <https://doi.org/10.1002/cbin.11137>
- De La Fuente, R. (2006). Chromatin modifications in the germinal vesicle (GV) of mammalian oocytes. *Developmental Biology*, 292(1), 1–12. <https://doi.org/10.1016/J.YDBIO.2006.01.008>
- Dean, M. (2019). Glycogen in the uterus and fallopian tubes is an important source of glucose during early pregnancy. *Biology of Reproduction*, 101(2), 297–305. <https://doi.org/10.1093/BIOLRE/IOZ102>
- Denzel, M. S., & Antebi, A. (2015). Hexosamine pathway and (ER) protein quality control. *Current Opinion in Cell Biology*, 33, 14–18. <https://doi.org/10.1016/J.CEB.2014.10.001>
- Di Bartolomeo, S., Corazzari, M., Nazio, F., Oliverio, S., Lisi, G., Antonioli, M., Pagliarini, V., Matteoni, S., Fuoco, C., Giunta, L., D'Amelio, M., Nardacci, R., Romagnoli, A., Piacentini, M., Cecconi, F., & Fimia, G. M. (2010). The dynamic interaction of AMBRA1 with the dynein motor complex regulates mammalian autophagy. *The Journal of Cell Biology*, 191(1), 155–168. <https://doi.org/10.1083/jcb.201002100>
- Diamond, M. P., Harbert-Moley, K., Logan, J., Pellicer, A., Lavy, G., Vaughn, W. K., & DeCherney, A. H. (1990). Manifestation of diabetes mellitus on mouse follicular and pre-embryo development: Effect of hyperglycemia per se. *Metabolism - Clinical and Experimental*, 39(3), 220–224. [https://doi.org/10.1016/0026-0495\(90\)90039-F](https://doi.org/10.1016/0026-0495(90)90039-F)
- Diamond, M. P., Pettway, Z. Y., Logan, J., Moley, K., Vaughn, W., & DeCherney, A. H. (1991). Dose-response effects of glucose, insulin, and glucagon on mouse pre-embryo development. *Metabolism - Clinical and Experimental*, 40(6), 566–570. [https://doi.org/10.1016/0026-0495\(91\)90045-X](https://doi.org/10.1016/0026-0495(91)90045-X)
- Dikic, I., & Elazar, Z. (2018). Mechanism and medical implications of mammalian autophagy. *Nature Reviews Molecular Cell Biology*, 19(6), 349–364. <https://doi.org/10.1038/s41580-018-0003-4>

- Ding, X., Jiang, X., Tian, R., Zhao, P., Li, L., Wang, X., Chen, S., Zhu, Y., Mei, M., Bao, S., Liu, W., Tang, Z., & Sun, Q. (2019). RAB2 regulates the formation of autophagosome and autolysosome in mammalian cells. *Autophagy*, *15*(10), 1774–1786.
<https://doi.org/10.1080/15548627.2019.1596478>
- Ducibella, T., Albertini, D. F., Anderson, E., & Biggers, J. D. (1975). The preimplantation mammalian embryo: Characterization of intercellular junctions and their appearance during development. *Developmental Biology*, *45*(2), 231–250. [https://doi.org/10.1016/0012-1606\(75\)90063-9](https://doi.org/10.1016/0012-1606(75)90063-9)
- Dumollard, R., Duchen, M., & Carroll, J. (2007). The role of mitochondrial function in the oocyte and embryo. *Current Topics in Developmental Biology*, *77*, 21–49.
[https://doi.org/10.1016/S0070-2153\(06\)77002-8](https://doi.org/10.1016/S0070-2153(06)77002-8)
- Dumoulin, J. C. M., Vanvuchelen, R. C. M., Land, J. A., Pieters, M. H. E. C., Geraedts, J. P. M., & Evers, J. L. H. (1995). Effect of oxygen concentration on in vitro fertilization and embryo culture in the human and the mouse. *Fertility and Sterility*, *63*(1), 115–119.
[https://doi.org/10.1016/S0015-0282\(16\)57305-1](https://doi.org/10.1016/S0015-0282(16)57305-1)
- Dutta, S. (2015). Human teratogens and their effects: a critical evaluation. *International Journal of Information Research and Review*, *2*(03), 525–536. <http://www.chw.org/>
- Elmore, S. (2007). Apoptosis: A Review of Programmed Cell Death. *Toxicologic Pathology*, *35*(4), 495. <https://doi.org/10.1080/01926230701320337>
- Eriksson, U. J., Brolin, S. E., & Naeser, P. (1989). Influence of sorbitol accumulation on growth and development of embryos cultured in elevated levels of glucose and fructose. *Diabetes Research (Edinburgh, Scotland)*, *11*(1), 27–32.
- Evers, I. M., De Valk, H. W., & Visser, G. H. A. (2004). Risk of complications of pregnancy in women with type 1 diabetes: nationwide prospective study in the Netherlands. *BMJ*, *328*(7445), 915. <https://doi.org/10.1136/BMJ.38043.583160.EE>

- Fabro, S., McLachlan, J. A., & Dames, N. M. (1984). Chemical exposure of embryos during the preimplantation stages of pregnancy: mortality rate and intrauterine development. *American Journal of Obstetrics and Gynecology*, 148(7), 929–938. [https://doi.org/10.1016/0002-9378\(84\)90535-0](https://doi.org/10.1016/0002-9378(84)90535-0)
- Fraser, R. B., Waite, S. L., Wood, K. A., & Martin, K. L. (2007). Impact of hyperglycemia on early embryo development and embryopathy: In vitro experiments using a mouse model. *Human Reproduction*, 22(12), 3059–3068. <https://doi.org/10.1093/humrep/dem318>
- Fu, J., Tay, S. S. W., Ling, E. A., & Dheen, S. T. (2007). Aldose reductase is implicated in high glucose-induced oxidative stress in mouse embryonic neural stem cells. *Journal of Neurochemistry*, 103(4), 1654–1665. <https://doi.org/10.1111/j.1471-4159.2007.04880.x>
- Fujita, N., Itoh, T., Omori, H., Fukuda, M., Noda, T., & Yoshimori, T. (2008). The Atg16L complex specifies the site of LC3 lipidation for membrane biogenesis in autophagy. *Molecular Biology of the Cell*, 19(5), 2092–2100. <https://doi.org/10.1091/MBE07-12-1257>
- Ganesan, D., & Cai, Q. (2021). Understanding amphisomes. *The Biochemical Journal*, 478(10), 1959. <https://doi.org/10.1042/BCJ20200917>
- Gardiner, C. S., & Reed, D. J. (1995). Synthesis of glutathione in the preimplantation mouse embryo. *Archives of Biochemistry and Biophysics*, 318(1), 30–36. <https://doi.org/10.1006/ABBI.1995.1200>
- Gardner, D. K. (2015). Lactate production by the mammalian blastocyst: Manipulating the microenvironment for uterine implantation and invasion? *Bioessays*, 37(4), 364. <https://doi.org/10.1002/BIES.201400155>
- Gardner, D. K., & Leese, H. J. (1987). Assessment of embryo viability prior to transfer by the noninvasive measurement of glucose uptake. *The Journal of Experimental Zoology*, 242(1), 103–105. <https://doi.org/10.1002/JEZ.1402420115>

- Gardner, D. K., & Leese, H. J. (1990). Concentrations of nutrients in mouse oviduct fluid and their effects on embryo development and metabolism Concentrations of nutrients in mouse oviduct fluid and their effects on embryo development and metabolism in vitro. *Journal of Reproduction and Fertility*, 88, 361–368. <https://doi.org/10.1530/jrf.0.0880361>
- Ge, T., Yang, J., Zhou, S., Wang, Y., Li, Y., & Tong, X. (2020). The Role of the Pentose Phosphate Pathway in Diabetes and Cancer. *Frontiers in Endocrinology*, 11, 365. <https://doi.org/10.3389/FENDO.2020.00365/BIBTEX>
- Goldar, S., Khaniani, M. S., Derakhshan, S. M., & Baradaran, B. (2015). Molecular Mechanisms of Apoptosis and its Role in Cancer Development and Treatment. *Asian Pacific Journal of Cancer Prevention*, 16, 2129–2144. <https://koreascience.kr/article/JAKO201528551641815.pdf>
- Goldbeter, A., Bessonnard, S., De Mot, L., Gonze, D., Barriol, M., Dennis, C., Ve Dupont, G., & Chazaud, C. (2014). *Gata6, Nanog and Erk signaling control cell fate in the inner cell mass through a tristable regulatory network*. <https://doi.org/10.1242/dev.109678>
- Gott, A. L., Hardy, K., Winston, R. M. L., & Leese, H. J. (1990). Non-invasive measurement of pyruvate and glucose uptake and lactate production by single human preimplantation embryos. *Human Reproduction*, 5(1), 104–108.
- Graefe, C., Eichhorn, L., Wurst, P., Kleiner, J., Heine, A., Panetas, I., Abdulla, Z., Hoeft, A., Frede, S., Kurts, C., Endl, E., & Weisheit, C. K. (2019). Optimized Ki-67 staining in murine cells: a tool to determine cell proliferation. *Molecular Biology Reports*, 46(4), 4631–4643. <https://doi.org/10.1007/S11033-019-04851-2>
- Grasso, D., Renna, F. J., & Vaccaro, M. I. (2018). Initial Steps in Mammalian Autophagosome Biogenesis. *Frontiers in Cell and Developmental Biology*, 6. <https://doi.org/10.3389/fcell.2018.00146>

- Gudmundsson, S. R., Kallio, K. A., Vihinen, H., Jokitalo, E., Ktistakis, N., & Eskelinen, E. L. (2022). Morphology of Phagophore Precursors by Correlative Light-Electron Microscopy. *Cells*, 11(19), 3080. <https://doi.org/10.3390/CELLS11193080/S1>
- Han, B. G., Hao, C. M., Tchekneva, E. E., Wang, Y. Y., Chieh, A. L., Ebrahim, B., Harris, R. C., Kern, T. S., Wasserman, D. H., Breyer, M. D., & Qi, Z. (2008). Markers of glycemic control in the mouse: Comparisons of 6-h-and overnight-fasted blood glucoses to Hb A1c. *American Journal of Physiology - Endocrinology and Metabolism*, 295(4), 981–986. <https://doi.org/10.1152/AJPENDO.90283.2008/ASSET/IMAGES/LARGE/ZH10100854360004.JPEG>
- Hansen, T. E., & Johansen, T. (2011). Following autophagy step by step. *BMC Biology*, 9(39). <https://doi.org/10.1186/1741-7007-9-39>
- Hardie, D. G., Ross, F. A., & Hawley, S. A. (2012). AMPK: a nutrient and energy sensor that maintains energy homeostasis. *Nature Reviews Molecular Cell Biology* 2012 13:4, 13(4), 251–262. <https://doi.org/10.1038/nrm3311>
- Hardy, M. L. M., Day, M. L., Morris, M. B., Van Winkle, L. J., & Ryznar, R. J. (2021). Redox Regulation and Oxidative Stress in Mammalian Oocytes and Embryos Developed In Vivo and In Vitro. *International Journal of Environmental Research and Public Health* 2021, Vol. 18, Page 11374, 18(21), 11374. <https://doi.org/10.3390/IJERPH182111374>
- Harris, S. E., Gopichandran, N., Picton, H. M., Leese, H. J., & Orsi, N. M. (2005). Nutrient concentrations in murine follicular fluid and the female reproductive tract. *Theriogenology*, 64(4), 992–1006. <https://doi.org/10.1016/J.THERIOGENOLOGY.2005.01.004>
- Hawthorne, G., Robson, S., Ryall, E. A., Sen, D., Roberts, S. H., & Ward Platt, M. P. (1997). Prospective population based survey of outcome of pregnancy in diabetic women: Results of the Northern Diabetic Pregnancy Audit, 1994. *British Medical Journal*, 315(7103). <https://doi.org/10.1136/bmj.315.7103.279>

- He, C., Song, H., Yorimitsu, T., Monastyrska, I., Yen, W. L., Legakis, J. E., & Klionsky, D. J. (2006). Recruitment of Atg9 to the preautophagosomal structure by Atg11 is essential for selective autophagy in budding yeast. *The Journal of Cell Biology*, 175(6), 925–935. <https://doi.org/10.1083/JCB.200606084>
- Hilverling, A., Szegő, E. M., Dinter, E., Cozma, D., Saridaki, T., & Falkenburger, B. H. (2022). Maturing Autophagosomes are Transported Towards the Cell Periphery. *Cellular and Molecular Neurobiology*, 42(1), 155–171. <https://doi.org/10.1007/s10571-021-01116-0>
- Hirate, Y., Hirahara, S., Inoue, K. I., Suzuki, A., Alarcon, V. B., Akimoto, K., Hirai, T., Hara, T., Adachi, M., Chida, K., Ohno, S., Marikawa, Y., Nakao, K., Shimono, A., & Sasaki, H. (2013). Polarity-Dependent Distribution of Angiomotin Localizes Hippo Signaling in Preimplantation Embryos. *Current Biology*, 23(13), 1181–1194. <https://doi.org/10.1016/J.CUB.2013.05.014>
- Hogan, A., Heyner, S., Charron, M. J., Copeland, N. G., Gilbert, D. J., Jenkins Thorens, N. A. B., & Schultz, G. A. (1991). Glucose transporter gene expression in early mouse embryos. *Development (Cambridge, England)*, 113(1), 363–372. <https://doi.org/10.1242/DEV.113.1.363>
- Horal, M., Zhang, Z., Stanton, R., Virkamäki, A., & Loeken, M. R. (2004). Activation of the hexosamine pathway causes oxidative stress and abnormal embryo gene expression: Involvement in diabetic teratogenesis. *Birth Defects Research Part A - Clinical and Molecular Teratology*, 70(8), 519–527. <https://doi.org/10.1002/BDRA.20056>
- Hosokawa, N., Hara, T., Kaizuka, T., Kishi, C., Takamura, A., Miura, Y., Iemura, S.-I., Natsume, T., Takehana, K., Yamada, N., Guan, J.-L., Oshiro, N., Mizushima, N., & Schmid, S. L. (1981). Nutrient-dependent mTORC1 Association with the ULK1-Atg13-FIP200 Complex Required for Autophagy. *Molecular Biology of the Cell*, 20. <https://doi.org/10.1091/mbc.E08>

- Hugentobler, S. A., Humpherson, P. G., Leese, H. J., Sreenan, J. M., & Morris, D. G. (2008). Energy substrates in bovine oviduct and uterine fluid and blood plasma during the oestrous cycle. *Molecular Reproduction and Development*, 75(3), 496–503.
<https://doi.org/10.1002/MRD.20760>
- Jacobson, M. D., Weil, M., & Raff, M. C. (1997). Programmed cell death in animal development. *Cell*, 88(3), 347–354. [https://doi.org/10.1016/s0092-8674\(00\)81873-5](https://doi.org/10.1016/s0092-8674(00)81873-5)
- Jain, A., Lamark, T., Sjøttem, E., Larsen, K. B., Awuh, J. A., Øvervatn, A., McMahon, M., Hayes, J. D., & Johansen, T. (2010). p62/SQSTM1 is a target gene for transcription factor NRF2 and creates a positive feedback loop by inducing antioxidant response element-driven gene transcription. *Journal of Biological Chemistry*, 285(29), 22576–22591.
<https://doi.org/10.1074/jbc.M110.118976>
- Javed, M. H., & Wright, R. W. (1991). Determination of pentose phosphate and Embden-Meyerhof pathway activities in bovine embryos. *Theriogenology*, 35(5), 1029–1037.
[https://doi.org/10.1016/0093-691X\(91\)90312-2](https://doi.org/10.1016/0093-691X(91)90312-2)
- Jing Qiu, J., Wen Zhang, W., Wu, Z. L., Hong Wang, Y., Qian, M., & Ping, Y. L. (2003). Delay of ZGA initiation occurred in 2-cell blocked mouse embryos. *Cell Research*, 13(3), 179–185. <http://www.cell-research.com>
- Kaiser, N., Sasson, S., Feener, E. P., Boukobza-Vardi, N., Higashi, S., Moller, D. E., Davidheiser, S., Przybylski, R. J., & King, G. L. (1993). Differential Regulation of Glucose Transport and Transporters by Glucose in Vascular Endothelial and Smooth Muscle Cells. *Diabetes*, 42, 80–89.
- Kawamura, K., Kawamura, N., Kumagai, J., Fukuda, J., & Tanaka, T. (2007). Tumor Necrosis Factor Regulation of Apoptosis in Mouse Preimplantation Embryos and Its Antagonism by Transforming Growth Factor Alpha/Phosphatidylinositol 3-Kinase Signaling System. *Biology of Reproduction*, 76(4), 611–618.
<https://doi.org/10.1095/BIOLREPROD.106.058008>

- Kea, B., Gebhardt, J., Watt, J., Westphal, L. M., Lathi, R. B., Milki, A. A., & Behr, B. (2007). Effect of reduced oxygen concentrations on the outcome of in vitro fertilization. *Fertility and Sterility*, 87(1), 213–216. <https://doi.org/10.1016/J.FERTNSTERT.2006.05.066>
- Keim, A. L., Chi, M. M., & Moley, K. H. (2001). Hyperglycemia-Induced Apoptotic Cell Death in the Mouse Blastocyst Is Dependent on Expression of p53. *MOLECULAR REPRODUCTION AND DEVELOPMENT*, 60, 214–224.
- Kendrick, A. A., & Christensen, J. R. (2022). Bidirectional lysosome transport: a balancing act between ARL8 effectors. *Nature Communications* 2022 13:1, 13(1), 1–3. <https://doi.org/10.1038/s41467-022-32965-y>
- Kirkin, V., Lamark, T., Sou, Y. S., Bjørkøy, G., Nunn, J. L., Bruun, J. A., Shvets, E., McEwan, D. G., Clausen, T. H., Wild, P., Bilusic, I., Theurillat, J. P., Øvervatn, A., Ishii, T., Elazar, Z., Komatsu, M., Dikic, I., & Johansen, T. (2009). A Role for NBR1 in Autophagosomal Degradation of Ubiquitinated Substrates. *Molecular Cell*, 33(4), 505–516. <https://doi.org/10.1016/J.MOLCEL.2009.01.020>
- Korotkevich, E., Niwayama, R., Courtois, A., Friese, S., Berger, N., Buchholz, F., & Hiiragi, T. (2017). The Apical Domain Is Required and Sufficient for the First Lineage Segregation in the Mouse Embryo. *Developmental Cell*, 40(3), 235–247.e7. <https://doi.org/10.1016/J.DEVCEL.2017.01.006>
- Ktistakis, N. T., & Tooze, S. A. (2016). Digesting the Expanding Mechanisms of Autophagy. *Trends in Cell Biology*, 26(8), 624–635. <https://doi.org/10.1016/j.tcb.2016.03.006>
- Kyrylkova, K., Kyryachenko, S., Leid, M., & Kiousi, C. (2012). Detection of apoptosis by TUNEL assay. *Methods in Molecular Biology (Clifton, N.J.)*, 887, 41–47. https://doi.org/10.1007/978-1-61779-860-3_5
- Lamb, C. A., Yoshimori, T., & Tooze, S. A. (2013). The autophagosome: origins unknown, biogenesis complex. *Nature Reviews Molecular Cell Biology* 2013 14:12, 14(12), 759–774. <https://doi.org/10.1038/nrm3696>

- Lee, Hwang, K.-C., Sun, S.-C., Xu, Y.-N., & Kim, N.-H. (2011). Modulation of autophagy influences development and apoptosis in mouse embryos developing in vitro. *Molecular Reproduction and Development*, 78(7), 498–509. <https://doi.org/10.1002/mrd.21331>
- Lee, J. E., Oh, H. A., Song, H., Jun, J. H., Roh, C. R., Xie, H., Dey, S. K., & Lim, H. J. (2011). Autophagy Regulates Embryonic Survival During Delayed Implantation. *Endocrinology*, 152(5), 2067–2075. <https://doi.org/10.1210/EN.2010-1456>
- Lee, & Lee, J.-A. (2016). Role of the mammalian ATG8/LC3 family in autophagy: differential and compensatory roles in the spatiotemporal regulation of autophagy. *BMB Rep*, 49(8), 424–430. <https://doi.org/10.5483/BMBRep.2016.49.8.081>
- Lee, X. C., Werner, E., & Falasca, M. (2021). Molecular Mechanism of Autophagy and Its Regulation by Cannabinoids in Cancer. *Cancers 2021, Vol. 13, Page 1211*, 13(6), 1211. <https://doi.org/10.3390/CANCERS13061211>
- Leese, H. J., & Barton, A. M. (1984). Pyruvate and glucose uptake by mouse ova and preimplantation embryos. *J. Reprod. Fert.*, 72, 9–13.
- Legault, L. M., Doiron, K., Breton-Larrivée, M., Langford-Avelar, A., Lemieux, A., Caron, M., Jerome-Majewska, L. A., Sinnett, D., & McGraw, S. (2021). Pre-implantation alcohol exposure induces lasting sex-specific DNA methylation programming errors in the developing forebrain. *Clinical Epigenetics 2021 13:1*, 13(1), 1–20. <https://doi.org/10.1186/S13148-021-01151-0>
- Leidenfrost, S., Boelhauve, M., Reichenbach, M., Güngör, T., Reichenbach, H.-D., Sinowatz, F., Wolf, E., & Habermann, F. A. (2011). Cell Arrest and Cell Death in Mammalian Preimplantation Development: Lessons from the Bovine Model. *PLoS ONE*, 6(7), e22121. <https://doi.org/10.1371/journal.pone.0022121>
- Leonavicius, K., Royer, C., Preece, C., Davies, B., Biggins, J. S., & Srinivas, S. (2018). Mechanics of mouse blastocyst hatching revealed by a hydrogel-based microdeformation assay. *Proceedings of the National Academy of Sciences of the United States of America*,

115(41), 10375–10380.

https://doi.org/10.1073/PNAS.1719930115/SUPPL_FILE/PNAS.1719930115.SM04.AVI

Leunda-Casi, A., Genicot, G., Donnay, I., Pampfer, S., & Hertogh, R. De. (2002). Increased cell death in mouse blastocysts exposed to high D-glucose in vitro: implications of an oxidative stress and alterations in glucose metabolism. *Diabetologia*, 45(4), 571–579.

Leung, Z. (2021). Free fatty acid treatment alters autophagy during mouse preimplantation embryo development. *Electronic Thesis and Dissertation Repository*.
<https://ir.lib.uwo.ca/etd/8160>

Leung, Z. C. L., Rafea, B. A., Watson, A. J., & Betts, D. H. (2022). Free fatty acid treatment of mouse preimplantation embryos demonstrates contrasting effects of palmitic acid and oleic acid on autophagy. *American Journal of Physiology. Cell Physiology*, 322(5), C833–C848.
<https://doi.org/10.1152/AJPCELL.00414.2021>

Li, R., Chase, M., Jung, S. K., Smith, P. J. S., & Loeken, M. R. (2005). Hypoxic stress in diabetic pregnancy contributes to impaired embryo gene expression and defective development by inducing oxidative stress. *American Journal of Physiology - Endocrinology and Metabolism*, 289(4 52-4), 591–599.
<https://doi.org/10.1152/AJPENDO.00441.2004/ASSET/IMAGES/LARGE/ZH10100543050006.JPEG>

Li, & Winuthayanon, W. (2017). Oviduct: roles in fertilization and early embryo development. *Journal of Endocrinology*, 232(1), R1–R26. <https://doi.org/10.1530/JOE-16-0302>

Li, X., & Darzynkiewicz, Z. (2000). Cleavage of Poly(ADP-ribose) polymerase measured in situ in individual cells: relationship to DNA fragmentation and cell cycle position during apoptosis. *Experimental Cell Research*, 255(1), 125–132.
<https://doi.org/10.1006/excr.1999.4796>

Lin, Z., Weinberg, J. M., Malhotra, R., Merritt, S. E., Holzman, L. B., & Brosius, F. C. (2000). GLUT-1 reduces hypoxia-induced apoptosis and JNK pathway activation. *American*

Journal of Physiology - Endocrinology and Metabolism, 278(5 41-5).

<https://doi.org/10.1152/AJPENDO.2000.278.5.E958/ASSET/IMAGES/LARGE/AEND10525007X.JPEG>

Lloyd, J. B. (1996). Metabolite efflux and influx across the lysosome membrane. *Sub-Cellular Biochemistry*, 27, 361–386. https://doi.org/10.1007/978-1-4615-5833-0_11

Ludwig, L. M., Maxcy, K. L., & LaBelle, J. L. (2019). Flow Cytometry-Based Detection and Analysis of BCL-2 Family Proteins and Mitochondrial Outer Membrane Permeabilization (MOMP). *Methods in Molecular Biology (Clifton, N.J.)*, 1877, 77–91. https://doi.org/10.1007/978-1-4939-8861-7_5

Maître, J. L., Niwayama, R., Turlier, H., Nedelec, F., & Hiiragi, T. (2015). Pulsatile cell-autonomous contractility drives compaction in the mouse embryo. *Nature Cell Biology* 2014 17:7, 17(7), 849–855. <https://doi.org/10.1038/ncb3185>

Marshall, S., Bacote, V., & Traxinger, R. R. (1991). Discovery of a metabolic pathway mediating glucose-induced desensitization of the glucose transport system. Role of hexosamine biosynthesis in the induction of insulin resistance. *Journal of Biological Chemistry*, 266(8), 4706–4712. [https://doi.org/10.1016/S0021-9258\(19\)67706-9](https://doi.org/10.1016/S0021-9258(19)67706-9)

Martina, J. A., Chen, Y., Gucek, M., & Puertollano, R. (2012). MTORC1 functions as a transcriptional regulator of autophagy by preventing nuclear transport of TFEB. *Autophagy*, 8(6), 903–914. https://doi.org/10.4161/AUTO.19653/SUPPL_FILE/KAUP_A_10919653_SM0001.ZIP

Martinou, J.-C., & Youle, R. J. (2011). Mitochondria in Apoptosis: Bcl-2 Family Members and Mitochondrial Dynamics. *Developmental Cell*, 21(1), 92–101. <https://doi.org/10.1016/j.devcel.2011.06.017>

Matoba, K., Kotani, T., Tsutsumi, A., Tsuji, T., Mori, T., Noshiro, D., Sugita, Y., Nomura, N., Iwata, S., Ohsumi, Y., Fujimoto, T., Nakatogawa, H., Kikkawa, M., & Noda, N. N. (2020).

- Atg9 is a lipid scramblase that mediates autophagosomal membrane expansion. *Nature Structural & Molecular Biology*, 27(12). <https://doi.org/10.1038/S41594-020-00518-W>
- Matsui, T., Jiang, P., Nakano, S., Sakamaki, Y., Yamamoto, H., & Mizushima, N. (2018). Autophagosomal YKT6 is required for fusion with lysosomes independently of syntaxin 17. *Journal of Cell Biology*, 217(8), 2633–2645. <https://doi.org/10.1083/jcb.201712058>
- Matsumoto, H. (2017). Molecular and cellular events during blastocyst implantation in the receptive uterus: clues from mouse models. *The Journal of Reproduction and Development*, 63(5), 445. <https://doi.org/10.1262/JRD.2017-047>
- Mazo, G. (2021). QuickFigures: A toolkit and ImageJ PlugIn to quickly transform microscope images into scientific figures. *PLOS ONE*, 16(11), e0240280. <https://doi.org/10.1371/JOURNAL.PONE.0240280>
- McGrath, M. J., Eramo, M. J., Gurung, R., Sriratana, A., Gehrig, S. M., Lynch, G. S., Lourdes, S. R., Koentgen, F., Feeney, S. J., Lazarou, M., McLean, C. A., & Mitchell, C. A. (2021). Defective lysosome reformation during autophagy causes skeletal muscle disease. *The Journal of Clinical Investigation*, 131(1). <https://doi.org/10.1172/JCI135124>
- Meilhac, S. M., Adams, R. J., Morris, S. A., Danckaert, A., Le Garrec, J.-F., & Zernicka-Goetz, M. (2009). Active cell movements coupled to positional induction are involved in lineage segregation in the mouse blastocyst. *Developmental Biology*, 331(2), 210–221. <https://doi.org/10.1016/j.ydbio.2009.04.036>
- Mihajlovic, A. I., Thamodaran, V., & Bruce, A. W. (2015). The first two cell-fate decisions of preimplantation mouse embryo development are not functionally independent. *Scientific Reports* 2015 5:1, 5(1), 1–16. <https://doi.org/10.1038/srep15034>
- Mindell, J. A. (2012). Lysosomal Acidification Mechanisms*. *Annual Review of Physiology*, 74, 69–86. <https://doi.org/10.1146/ANNUREV-PHYSIOL-012110-142317>

- Mizushima, N., Yoshimori, T., & Levine, B. (2010). Methods in Mammalian Autophagy Research. *Cell*, 140(3), 313–326. <https://doi.org/10.1016/j.cell.2010.01.028>
- Moley, K. H., Chi, M. M., Manchester, J. K., McDougal, D. B., & Lowry, O. H. (1996). Alterations of intraembryonic metabolites in preimplantation mouse embryos exposed to elevated concentrations of glucose: a metabolic explanation for the developmental retardation seen in preimplantation embryos from diabetic animals. *Biology of Reproduction*, 54(6), 1209–1216. <https://doi.org/10.1095/biolreprod54.6.1209>
- Moley, K. H., Chi, M. M. Y., & Mueckler, M. M. (1998). Maternal hyperglycemia alters glucose transport and utilization in mouse preimplantation embryos. *American Journal of Physiology - Endocrinology and Metabolism*, 275(1 38-1). <https://doi.org/10.1152/AJPENDO.1998.275.1.E38>
- Moley, K. H., Chi, M.-Y., Knudson, C. M., Korsmeyer, S. J., & Mueckler, & M. M. (1998). Hyperglycemia induces apoptosis in pre-implantation embryos through cell death effector pathways. *NATURE MEDICINE* •, 4. <http://medicine.nature.com>
- Morris, S. A., Teo, R. T. Y., Li, H., Robson, P., Glover, D. M., Zernicka-Goetz, M., & Gurdon, J. B. (2010). *Origin and formation of the first two distinct cell types of the inner cell mass in the mouse embryo Successive Waves of Divisions Generate Inside Cells with Progressively Restricted Fate. We identified three waves of asymmetric divisions.* 107(14). <https://doi.org/10.1073/pnas.0915063107>
- Moruno, F., Pérez-Jiménez, E., & Knecht, E. (2012). Regulation of Autophagy by Glucose in Mammalian Cells. *Cells*, 1(3), 372. <https://doi.org/10.3390/CELLS1030372>
- Mukhopadhyay, S., Panda, P. K., Sinha, N., Das, D. N., & Bhutia, S. K. (2014). Autophagy and apoptosis: Where do they meet? *Apoptosis*, 19(4), 555–566. <https://doi.org/10.1007/s10495-014-0967-2>

- Negrato, C. A., Mattar, R., & Gomes, M. B. (2012). Adverse pregnancy outcomes in women with diabetes. *Diabetology and Metabolic Syndrome*, 4(1), 1–6.
<https://doi.org/10.1186/1758-5996-4-41/METRICS>
- Nicholson, D. W., & Thornberry, N. A. (1997). Caspases: killer proteases. *Trends in Biochemical Sciences*, 22(8), 299–306. [https://doi.org/10.1016/s0968-0004\(97\)01085-2](https://doi.org/10.1016/s0968-0004(97)01085-2)
- Nishioka, N., Inoue, K. ichi, Adachi, K., Kiyonari, H., Ota, M., Ralston, A., Yabuta, N., Hirahara, S., Stephenson, R. O., Ogonuki, N., Makita, R., Kurihara, H., Morin-Kensicki, E. M., Nojima, H., Rossant, J., Nakao, K., Niwa, H., & Sasaki, H. (2009). The Hippo Signaling Pathway Components Lats and Yap Pattern Tead4 Activity to Distinguish Mouse Trophoctoderm from Inner Cell Mass. *Developmental Cell*, 16(3), 398–410.
<https://doi.org/10.1016/J.DEVCEL.2009.02.003>
- Nishioka, N., Yamamoto, S., Kiyonari, H., Sato, H., Sawada, A., Ota, M., Nakao, K., & Sasaki, H. (2008). Tead4 is required for specification of trophoctoderm in pre-implantation mouse embryos. *Mechanisms of Development*, 125(3–4), 270–283.
<https://doi.org/10.1016/J.MOD.2007.11.002>
- Obeng, E. (2021). Apoptosis (programmed cell death) and its signals - A review. *Brazilian Journal of Biology*, 81(4), 1133–1143. <https://doi.org/10.1590/1519-6984.228437>
- O'Fallon, J. V., & Wright, R. W. (1986). Quantitative Determination of the Pentose Phosphate Pathway in Preimplantation Mouse Embryos. *Biology of Reproduction*, 34(1), 58–64.
<https://doi.org/10.1095/BIOLREPROD34.1.58>
- Ohnishi, Y., Huber, W., Tsumura, A., Kang, M., Xenopoulos, P., Kurimoto, K., Oleå, A. K., Araújo-Bravo, M. J., Saitou, M., Hadjantonakis, A. K., & Hiiragi, T. (2013). Cell-to-cell expression variability followed by signal reinforcement progressively segregates early mouse lineages. *Nature Cell Biology* 2013 16:1, 16(1), 27–37.
<https://doi.org/10.1038/ncb2881>

- Olivas, T. J., Wu, Y., Yu, S., Luan, L., Choi, P., Nag, S., Camilli, P. De, Gupta, K., & Melia, T. J. (2022). ATG9 vesicles comprise the seed membrane of mammalian autophagosomes. *BioRxiv*, 2022.08.16.504143. <https://doi.org/10.1101/2022.08.16.504143>
- Orietti, L. C., Rosa, V. S., Antonica, F., Kyprianou, C., Mansfield, W., Marques-Souza, H., Shahbazi, M. N., & Zernicka-Goetz, M. (2021). Embryo size regulates the timing and mechanism of pluripotent tissue morphogenesis. *Stem Cell Reports*, 16(5), 1182–1196. <https://doi.org/10.1016/j.stemcr.2020.09.004>
- Ornoy, A. (2007). Embryonic oxidative stress as a mechanism of teratogenesis with special emphasis on diabetic embryopathy. *Reproductive Toxicology*, 24(1), 31–41. <https://doi.org/10.1016/j.reprotox.2007.04.004>
- Orsi, A., Razi, M., Dooley, H. C., Robinson, D., Weston, A. E., Collinson, L. M., & Tooze, S. A. (2012). Dynamic and transient interactions of Atg9 with autophagosomes, but not membrane integration, are required for autophagy. *Molecular Biology of the Cell*, 23(10), 1860–1873. <https://doi.org/10.1091/MBC.E11-09-0746>
- Orth, K., Chinnaiyan, A. M., Garg, M., Froelich, C. J., & Dixit, V. M. (1996). The CED-3/ICE-like protease Mch2 is activated during apoptosis and cleaves the death substrate lamin A. *The Journal of Biological Chemistry*, 271(28), 16443–16446.
- Otani, H., Tanaka, O., Tatewaki, R., Naora, H., & Yoneyama, T. (1991). Diabetic environment and genetic predisposition as causes of congenital malformations in NOD mouse embryos. *Diabetes*, 40(10), 1245–1250. <https://doi.org/10.2337/diab.40.10.1245>
- Ozaki, T., & Nakagawara, A. (2011). p53: the attractive tumor suppressor in the cancer research field. *Journal of Biomedicine & Biotechnology*, 2011, 603925. <https://doi.org/10.1155/2011/603925>
- Pampfer, S., de Hertogh, R., Vanderheyden, I., Michiels, B., & Vercheval, M. (1990). Decreased inner cell mass proportion in blastocysts from diabetic rats. *Diabetes*, 39(4), 471–476. <https://doi.org/10.2337/diab.39.4.471>

- Pankiv, S., Clausen, T. H., Lamark, T., Brech, A., Bruun, J. A., Outzen, H., Øvervatn, A., Bjørkøy, G., & Johansen, T. (2007). p62/SQSTM1 binds directly to Atg8/LC3 to facilitate degradation of ubiquitinated protein aggregates by autophagy*[S]. *Journal of Biological Chemistry*, 282(33), 24131–24145. <https://doi.org/10.1074/jbc.M702824200>
- Pantaleon, M., Harvey, M. B., Pascoe, W. S., James, D. E., & Kaye, P. L. (1997). Glucose transporter GLUT3: Ontogeny, targeting, and role in the mouse blastocyst. *Proceedings of the National Academy of Sciences of the United States of America*, 94(8), 3795–3800. <https://doi.org/10.1073/PNAS.94.8.3795/ASSET/4C80AC9E-333A-4BEC-AD55-C1A59BB1AF90/ASSETS/GRAPHIC/PQ0771334006.JPEG>
- Pantaleon, M., & Kaye, P. L. (1998). Glucose transporters in preimplantation development. *Reviews of Reproduction*, 3(2), 77–81. <https://doi.org/10.1530/ROR.0.0030077>
- Pantaleon, M., Ryan, J. P., Gil, M., & Kaye, P. L. (2001). An unusual subcellular localization of GLUT1 and link with metabolism in oocytes and preimplantation mouse embryos. *Biology of Reproduction*, 64(4), 1247–1254. <https://doi.org/10.1095/BIOLREPROD64.4.1247>
- Pantaleon, M., Scott, J., & Kaye, P. L. (2008). Nutrient Sensing by the Early Mouse Embryo: Hexosamine Biosynthesis and Glucose Signaling During Preimplantation Development. *Biology of Reproduction*, 78(4), 595–600. <https://doi.org/10.1095/BIOLREPROD.107.062877>
- Pantaleon, M., Tan, H. Y., Kafer, G. R., & Kaye, P. L. (2009). *Toxic Effects of Hyperglycemia Are Mediated by the Hexosamine Signaling Pathway and O-Linked Glycosylation in Early Mouse Embryos I*. <https://doi.org/10.1095/biolreprod.109.076661>
- Paria, B. C., Huet-Hudson, Y. M., & Dey, S. K. (1993). Blastocyst's state of activity determines the “window” of implantation in the receptive mouse uterus. *Proceedings of the National Academy of Sciences of the United States of America*, 90(21), 10159. <https://doi.org/10.1073/PNAS.90.21.10159>

- Parzych, K. R., & Klionsky, D. J. (2014). An Overview of Autophagy: Morphology, Mechanism, and Regulation. *Antioxidants & Redox Signaling*, 20(3), 460.
<https://doi.org/10.1089/ARS.2013.5371>
- Patra, K. C., & Hay, N. (2014). The pentose phosphate pathway and cancer. *Trends in Biochemical Sciences*, 39(8), 347–354. <https://doi.org/10.1016/J.TIBS.2014.06.005>
- Peña-Blanco, A., & García-Sáez, A. J. (2018). Bax, Bak and beyond — mitochondrial performance in apoptosis. *The FEBS Journal*, 285(3), 416–431.
<https://doi.org/10.1111/febs.14186>
- Pizzino, G., Irrera, N., Cucinotta, M., Pallio, G., Mannino, F., Arcoraci, V., Squadrito, F., Altavilla, D., & Bitto, A. (2017). Oxidative Stress: Harms and Benefits for Human Health. *Oxidative Medicine and Cellular Longevity*, 2017, 8416763.
<https://doi.org/10.1155/2017/8416763>
- Płusa, B., & Piliszek, A. (2020). Common principles of early mammalian embryo self-organisation. *Development (Cambridge)*, 147(14).
<https://doi.org/10.1242/DEV.183079/224341>
- Pugsley, H. R. (2017). Assessing autophagic flux by measuring LC3, p62, and LAMP1 co-localization using multispectral imaging flow cytometry. *Journal of Visualized Experiments*, 2017(125). <https://doi.org/10.3791/55637>
- Ravikumar, B., Sarkar, S., Davies, J. E., Futter, M., Garcia-Arencibia, M., Green-Thompson, Z. W., Jimenez-Sanchez, M., Korolchuk, V. I., Lichtenberg, M., Luo, S., Massey, D. C. O., Menzies, F. M., Moreau, K., Narayanan, U., Renna, M., Siddiqi, F. H., Underwood, B. R., Winslow And, A. R., & Rubinsztein, D. C. (2010). Regulation of mammalian autophagy in physiology and pathophysiology. *Physiological Reviews*, 90(4), 1383–1435.
<https://doi.org/10.1152/PHYSREV.00030.2009/ASSET/IMAGES/LARGE/Z9J0041025580007.JPEG>

- Reubold, T. F., Wohlgemuth, S., & Eschenburg, S. (2011). Crystal Structure of Full-Length Apaf-1: How the Death Signal Is Relayed in the Mitochondrial Pathway of Apoptosis. *Structure*, 19(8), 1074–1083. <https://doi.org/10.1016/j.str.2011.05.013>
- Riley, J. K., Heeley, J. M., Wyman, A. H., Schlichting, E. L., & Moley, K. H. (2004). TRAIL and KILLER Are Expressed and Induce Apoptosis in the Murine Preimplantation Embryo. *Biology of Reproduction*, 71(3), 871–877. <https://doi.org/10.1095/BIOLREPROD.103.026963>
- Rossant, J. (1975). Investigation of the determinative state of the mouse inner cell massI. Aggregation of isolated inner cell masses with morulae. *Development*, 33(4), 979–990. <https://doi.org/10.1242/DEV.33.4.979>
- Runwal, G., Stamatakou, E., Siddiqi, F. H., Puri, C., Zhu, Y., & Rubinsztein, D. C. (2019). LC3-positive structures are prominent in autophagy-deficient cells. *Scientific Reports 2019 9:1*, 9(1), 1–14. <https://doi.org/10.1038/s41598-019-46657-z>
- Russell, R. C., Tian, Y., Yuan, H., Park, H. W., Chang, Y.-Y., Kim, J., Kim, H., Neufeld, T. P., Dillin, A., & Guan, K.-L. (2013). ULK1 induces autophagy by phosphorylating Beclin-1 and activating VPS34 lipid kinase. *Nature Cell Biology*, 15(7), 741–750. <https://doi.org/10.1038/ncb2757>
- Rusten, T. E., Lindmo, K., Juhász, G., Sass, M., Seglen, P. O., Brech, A., & Stenmark, H. (2004). Programmed autophagy in the Drosophila fat body is induced by ecdysone through regulation of the PI3K Pathway. *Developmental Cell*, 7(2), 179–192. <https://doi.org/10.1016/j.devcel.2004.07.005>
- Saikumar, P., Dong, Z., Patel, Y., Hall, K., Hopfer, U., Weinberg, J. M., & Venkatachalam, M. A. (1999). Role of hypoxia-induced Bax translocation and cytochrome c release in reoxygenation injury. *Oncogene 1998 17:26*, 17(26), 3401–3415. <https://doi.org/10.1038/sj.onc.1202590>

- Saraste, A. (2000). Morphologic and biochemical hallmarks of apoptosis. *Cardiovascular Research*, 45(3), 528–537. [https://doi.org/10.1016/S0008-6363\(99\)00384-3](https://doi.org/10.1016/S0008-6363(99)00384-3)
- Schaefer, U. M., Songster, G., Xiang, A., Berkowitz, K., Buchanan, T. A., & Kjos, S. L. (1997). Congenital malformations in offspring of women with hyperglycemia first detected during pregnancy. *American Journal of Obstetrics and Gynecology*, 177(5). [https://doi.org/10.1016/S0002-9378\(97\)70035-8](https://doi.org/10.1016/S0002-9378(97)70035-8)
- Schliwa, M., & Van Blerkom, J. (1981). Structural interaction of cytoskeletal components. *The Journal of Cell Biology*, 90(1), 222–235. <https://doi.org/10.1083/JCB.90.1.222>
- Schröder, B. A., Wrocklage, C., Hasilik, A., & Saftig, P. (2010). The proteome of lysosomes. *Proteomics*, 10(22), 4053–4076. <https://doi.org/10.1002/PMIC.201000196>
- Settembre, C., Di Malta, C., Polito, V. A., Arencibia, M. G., Vetrini, F., Erdin, S., Erdin, S. U., Huynh, T., Medina, D., Colella, P., Sardiello, M., Rubinsztein, D. C., & Ballabio, A. (2011). TFEB links autophagy to lysosomal biogenesis. *Science*, 332(6036), 1429–1433. https://doi.org/10.1126/SCIENCE.1204592/SUPPL_FILE/1204592.SETTEMBRE.SOM.PDF
- Sharma, N., Liu, S., Tang, L., Irwin, J., Meng, G., & Rancourt, D. E. (2006). Implantation serine proteinases heterodimerize and are critical in hatching and implantation. *BMC Developmental Biology*, 6(1), 1–11. <https://doi.org/10.1186/1471-213X-6-61/FIGURES/7>
- Sharpley, M. S., Chi, F., Hoeve, J. ten, & Banerjee, U. (2021). Metabolic plasticity drives development during mammalian embryogenesis. *Developmental Cell*, 56(16), 2329–2347.e6. <https://doi.org/10.1016/J.DEVCEL.2021.07.020>
- Shen, Han, Y.-J., Yang, B.-C., Cui, X.-S., & Kim, N.-H. (2009). Hyperglycemia Reduces Mitochondrial Content and Glucose Transporter Expression in Mouse Embryos Developing In Vitro. *Journal of Reproduction and Development*, 55(5), 20231.

- Shen, X., Zhang, N., Wang, Z., Bai, G., Zheng, Z., Gu, Y., Wu, Y., Liu, H., Zhou, D., & Lei, L. (2015). Induction of autophagy improves embryo viability in cloned mouse embryos. *Scientific Reports*, 5(1), 17829. <https://doi.org/10.1038/srep17829>
- Soliman, M. A., Abdel Rahman, A. M., Lamming, D. A., Birsoy, K., Pawling, J., Frigolet, M. E., Lu, H., Fantus, I. G., Pasculescu, A., Zheng, Y., Sabatini, D. M., Dennis, J. W., & Pawson, T. (2014). The adaptor protein p66Shc inhibits mTOR-dependent anabolic metabolism. *Science Signaling*, 7(313). https://doi.org/10.1126/SCISIGNAL.2004785/SUPPL_FILE/7_RA17_TABLE_S1.ZIP
- Strączyńska, P., Papis, K., Morawiec, E., Czerwiński, M., Gajewski, Z., Olejek, A., & Bednarska-Czerwińska, A. (2022). Signaling mechanisms and their regulation during in vivo or in vitro maturation of mammalian oocytes. *Reproductive Biology and Endocrinology*, 20(1), 1–12. <https://doi.org/10.1186/S12958-022-00906-5/FIGURES/1>
- Stroupe, C., Collins, K. M., Fratti, R. A., & Wickner, W. (2006). Purification of active HOPS complex reveals its affinities for phosphoinositides and the SNARE Vam7p. *The EMBO Journal*, 25(8), 1579–1589. <https://doi.org/10.1038/sj.emboj.7601051>
- Strumpf, D., Mao, C. A., Yamanaka, Y., Ralston, A., Chawengsaksophak, K., Beck, F., & Rossant, J. (2005). Cdx2 is required for correct cell fate specification and differentiation of trophectoderm in the mouse blastocyst. *Development (Cambridge, England)*, 132(9), 2093–2102. <https://doi.org/10.1242/DEV.01801>
- Sutton-McDowall, M. L., Gilchrist, R. B., & Thompson, J. G. (2010). The pivotal role of glucose metabolism in determining oocyte developmental competence. *Reproduction (Cambridge, England)*, 139(4), 685–695. <https://doi.org/10.1530/REP-09-0345>
- Sutton-McDowall, M. L., & Thompson, J. G. (2015). Metabolism in the pre-implantation oocyte and embryo. *Anim. Reprod.*, 12(3), 408–417.
- Takahashi, A., Alnemri, E. S., Lazebnik, Y. A., Fernandes-Alnemri, T., Litwack, G., Moir, R. D., Goldman, R. D., Poirier, G. G., Kaufmann, S. H., & Earnshaw, W. C. (1996). Cleavage

of lamin A by Mch2 alpha but not CPP32: multiple interleukin 1 beta-converting enzyme-related proteases with distinct substrate recognition properties are active in apoptosis.

Proceedings of the National Academy of Sciences, 93(16), 8395–8400.

<https://doi.org/10.1073/pnas.93.16.8395>

Thorens, B. (1996). Glucose transporters in the regulation of intestinal, renal, and liver glucose fluxes. *https://Doi.Org/10.1152/Ajpgi.1996.270.4.G541*, 270(4 33-4).

<https://doi.org/10.1152/AJPGI.1996.270.4.G541>

Thornberry, N. A., & Lazebnik, Y. (1998). Caspases: enemies within. *Science (New York, N.Y.)*, 281(5381), 1312–1316. <https://doi.org/10.1126/science.281.5381.1312>

Tonack, S., Fischer, B., & Navarrete Santos, A. (2004). Expression of the insulin-responsive glucose transporter isoform 4 in blastocysts of C57/BL6 mice. *Anatomy and Embryology*, 208(3), 225–230. <https://doi.org/10.1007/S00429-004-0388-Z>

Town, M., Jean, G., Cherqui, S., Attard, M., Forestier, L., Whitmore, S. A., Gallen, D. F., Gribouval, O., Broyer, M., Bates, G. P., Hoff, W. V. t., & Antignac, C. (1998). A novel gene encoding an integral membrane protein is mutated in nephropathic cystinosis. *Nature Genetics*, 18(4), 319–324. <https://doi.org/10.1038/NG0498-319>

Tsai, Yamauchi, Y., Riel, J. M., & Ward, M. A. (2020). Pregnancy environment, and not preconception, leads to fetal growth restriction and congenital abnormalities associated with diabetes. *Scientific Reports*, 10(1), 12254. <https://doi.org/10.1038/s41598-020-69247-w>

Tsukamoto, S., Kuma, A., Murakami, M., Kishi, C., Yamamoto, A., & Mizushima, N. (2008). Autophagy is essential for preimplantation development of mouse embryos. *Science*, 321(5885), 117–120. <https://doi.org/10.1126/SCIENCE.1154822>

Valverde, D. P., Yu, S., Boggavarapu, V., Kumar, N., Lees, J. A., Walz, T., Reinisch, K. M., & Melia, T. J. (2019). ATG2 transports lipids to promote autophagosome biogenesis. *The Journal of Cell Biology*, 218(6), 1787–1798. <https://doi.org/10.1083/JCB.201811139>

- van Engeland, M., Nieland, L. J., Ramaekers, F. C., Schutte, B., & Reutelingsperger, C. P. (1998). Annexin V-affinity assay: a review on an apoptosis detection system based on phosphatidylserine exposure. *Cytometry*, 31(1), 1–9. [https://doi.org/10.1002/\(sici\)1097-0320\(19980101\)31:1<1::aid-cyto1>3.0.co;2-r](https://doi.org/10.1002/(sici)1097-0320(19980101)31:1<1::aid-cyto1>3.0.co;2-r)
- van Vliet, A. R., Chiduza, G. N., Maslen, S. L., Pye, V. E., Joshi, D., De Tito, S., Jefferies, H. B. J., Christodoulou, E., Roustan, C., Punch, E., Hervás, J. H., O'Reilly, N., Skehel, J. M., Cherepanov, P., & Tooze, S. A. (2022). ATG9A and ATG2A form a heteromeric complex essential for autophagosome formation. *Molecular Cell*, 82(22), 4324–4339.e8. <https://doi.org/10.1016/J.MOLCEL.2022.10.017>
- Via y Rada, R., Daniel, N., Archilla, C., Frambourg, A., Jouneau, L., Jaszczyszyn, Y., Charpigny, G., Duranthon, V., & Calderari, S. (2022). Identification of the Inner Cell Mass and the Trophectoderm Responses after an In Vitro Exposure to Glucose and Insulin during the Preimplantation Period in the Rabbit Embryo. *Cells*, 11(23). <https://doi.org/10.3390/CELLS11233766/S1>
- Wales, R. G., & Du, Z. F. (1993). Contribution of the pentose phosphate pathway to glucose utilization by preimplantation sheep embryos. *Reproduction, Fertility, and Development*, 5(3), 329–340. <https://doi.org/10.1071/RD9930329>
- Wamelink, M. M. C., Struys, E. A., & Jakobs, C. (2008). The biochemistry, metabolism and inherited defects of the pentose phosphate pathway: A review. *Journal of Inherited Metabolic Disease*, 31(6), 703–717. <https://doi.org/10.1007/S10545-008-1015-6>
- Wang, L., Chen, M., Yang, J., & Zhang, Z. (2013). LC3 fluorescent puncta in autophagosomes or in protein aggregates can be distinguished by FRAP analysis in living cells. *Autophagy*, 9(5), 756–769. <https://doi.org/10.4161/auto.23814>
- Wang, T., Ming, Z., Xiaochun, W., & Hong, W. (2011). Rab7: role of its protein interaction cascades in endo-lysosomal traffic. *Cellular Signalling*, 23(3), 516–521. <https://doi.org/10.1016/j.cellsig.2010.09.012>

- Warburg, O. (1956). On the origin of cancer cells. *Science*, 123(3191), 309–314.
<https://doi.org/10.1126/SCIENCE.123.3191.309/ASSET/A8D38B53-799F-4009-AAD3-E77CEF33D301/ASSETS/SCIENCE.123.3191.309.FP.PNG>
- Watson, A. J. (1992). The cell biology of blastocyst development. *Molecular Reproduction and Development*, 33(4), 492–504. <https://doi.org/10.1002/MRD.1080330417>
- Wen, L. P., Fahrni, J. A., Troie, S., Guan, J. L., Orth, K., & Rosen, G. D. (1997). Cleavage of focal adhesion kinase by caspases during apoptosis. *The Journal of Biological Chemistry*, 272(41), 26056–26061. <https://doi.org/10.1074/jbc.272.41.26056>
- Winchester, B. (2005). Lysosomal metabolism of glycoproteins. *Glycobiology*, 15(6), 1R-15R. <https://doi.org/10.1093/glycob/cwi041>
- Würstle, M. L., & Rehm, M. (2014). A Systems Biology Analysis of Apoptosome Formation and Apoptosis Execution Supports Allosteric Procaspase-9 Activation. *Journal of Biological Chemistry*, 289(38), 26277–26289. <https://doi.org/10.1074/jbc.M114.590034>
- Wyman, A., Pinto, A. B., Sheridan, R., & Moley, K. H. (2008). One-cell zygote transfer from diabetic to nondiabetic mouse results in congenital malformations and growth retardation in offspring. *Endocrinology*, 149(2), 466–469. <https://doi.org/10.1210/EN.2007-1273>
- Xie, N., Zhang, L., Gao, W., Huang, C., Huber, P. E., Zhou, X., Li, C., Shen, G., & Zou, B. (2020). NAD⁺ metabolism: pathophysiologic mechanisms and therapeutic potential. *Signal Transduction and Targeted Therapy* 2020 5:1, 5(1), 1–37. <https://doi.org/10.1038/s41392-020-00311-7>
- Xie, Y., Kang, R., Sun, X., Zhong, M., Huang, J., Klionsky, D. J., & Tang, D. (2015). Posttranslational modification of autophagy-related proteins in macroautophagy. *Autophagy*, 11(1), 28–45. <https://doi.org/10.4161/15548627.2014.984267>
- Xu, Y.-N., Li, Y.-H., Hyun Lee, S., Kwon, J.-W., Ki Lee, S., Heo, Y.-T., Cui, X.-S., & Kim, N.-H. (2013). Hyperglycemia Influences Apoptosis and Autophagy in Porcine Parthenotes

Developing In Vitro. *Reprod Dev Biol*, 37(2), 65–73.

<https://doi.org/10.12749/RDB.2013.37.2.65>

Yang, H. W., Hwang, K. J., Kwon, H. C., Kim, H. S., Choi, K. W., & Oh, K. S. (1998).

Detection of reactive oxygen species (ROS) and apoptosis in human fragmented embryos.

Human Reproduction (Oxford, England), 13(4), 998–1002.

<https://doi.org/10.1093/HUMREP/13.4.998>

Yang, Y., Hu, L., Zheng, H., Mao, C., Hu, W., Xiong, K., Wang, F., & Liu, C. (2013).

Application and interpretation of current autophagy inhibitors and activators. *Acta*

Pharmacologica Sinica, 34(5), 625–635. <https://doi.org/10.1038/aps.2013.5>

Yao, Q., Chen, L., Liang, Y., Sui, L., Guo, L., Zhou, J., Fan, K., Jing, J., Zhang, Y., & Yao, B.

(2016). Blastomere removal from cleavage-stage mouse embryos alters placental function,

which is associated with placental oxidative stress and inflammation. *Scientific Reports*

2016 6:1, 6(1), 1–10. <https://doi.org/10.1038/srep25023>

Yen, W. C., Wu, Y. H., Wu, C. C., Lin, H. R., Stern, A., Chen, S. H., Shu, J. C., & Tsun-Yee

Chiu, D. (2020). Impaired inflammasome activation and bacterial clearance in G6PD

deficiency due to defective NOX/p38 MAPK/AP-1 redox signaling. *Redox Biology*, 28,

101363. <https://doi.org/10.1016/J.REDOX.2019.101363>

Yim, W. W. Y., & Mizushima, N. (2020). Lysosome biology in autophagy. *Cell Discovery* 2020

6:1, 6(1), 1–12. <https://doi.org/10.1038/s41421-020-0141-7>

Yoshinaga, K. (2013). A sequence of events in the uterus prior to implantation in the mouse.

Journal of Assisted Reproduction and Genetics, 30(8), 1017.

<https://doi.org/10.1007/S10815-013-0093-Z>

Yousif, M. D., Calder, M. D., Du, J. T., Ruetz, K. N., Crocker, K., Urquhart, B. L., Betts, D. H.,

Rafea, B. A., & Watson, A. J. (2020). Oleic Acid Counters Impaired Blastocyst

Development Induced by Palmitic Acid During Mouse Preimplantation Development:

- Understanding Obesity-Related Declines in Fertility. *Reproductive Sciences*, 27(11), 2038–2051. <https://doi.org/10.1007/S43032-020-00223-5/FIGURES/7>
- Yu, J., & Zhang, L. (2008). PUMA, a potent killer with or without p53. *Oncogene*, 27 Suppl 1(Suppl 1), S71-83. <https://doi.org/10.1038/onc.2009.45>
- Yu, S., & Melia, T. J. (2017). The coordination of membrane fission and fusion at the end of autophagosome maturation. *Current Opinion in Cell Biology*, 47, 92–98. <https://doi.org/10.1016/J.CEB.2017.03.010>
- Zenker, J., White, M. D., Gasnier, M., Alvarez, Y. D., Lim, H. Y. G., Bissiere, S., Biro, M., & Plachta, N. (2018). Expanding Actin Rings Zipper the Mouse Embryo for Blastocyst Formation. *Cell*, 173(3), 776-791.e17. <https://doi.org/10.1016/j.cell.2018.02.035>
- Zhang, Wan, X.-X., Hu, X.-M., Zhao, W.-J., -Xia Ban, X., Huang, Y.-X., Yan, W.-T., & Xiong, K. (2021). Targeting Programmed Cell Death to Improve Stem Cell Therapy: Implications for Treating Diabetes and Diabetes-Related Diseases. *Frontiers in Cell and Developmental Biology*, 9(809656). <https://doi.org/10.3389/fcell.2021.809656>
- Zhao, Y. G., Chen, Y., Miao, G., Zhao, H., Qu, W., Li, D., Wang, Z., Liu, N., Li, L., Chen, S., Liu, P., Feng, D., & Zhang, H. (2017). The ER-Localized Transmembrane Protein EPG-3/VMP1 Regulates SERCA Activity to Control ER-Isolation Membrane Contacts for Autophagosome Formation. *Molecular Cell*, 67(6), 974-989.e6. <https://doi.org/10.1016/J.MOLCEL.2017.08.005>
- Zhao, Y. G., & Zhang, H. (2019). Autophagosome maturation: An epic journey from the ER to lysosomes. *The Journal of Cell Biology*, 218(3), 757–770. <https://doi.org/10.1083/jcb.201810099>
- Zhen, Y., & Stenmark, H. (2023). Autophagosome Biogenesis. *Cells*, 12(4), 668. <https://doi.org/10.3390/cells12040668>

Zhou, C., Ma, K., Gao, R., Mu, C., Chen, L., Liu, Q., Luo, Q., Feng, D., Zhu, Y., & Chen, Q. (2017). Regulation of mATG9 trafficking by Src- and ULK1-mediated phosphorylation in basal and starvation-induced autophagy. *Cell Research*, 27(2), 184–201. <https://doi.org/10.1038/CR.2016.146>

Appendices

Appendix A: Canadian Council on Animal Care and Western University's Animal Care and Use Policies



2018-075:13

AUP Number: 2018-075

AUP Title: Mechanisms Controlling Preimplantation Development

Yearly Renewal Date: 08/01/2022

The **annual renewal** to Animal Use Protocol (AUP) 2018-075 has been approved by the Animal Care Committee (ACC), and will be approved through to the above review date.

Please at this time review your AUP with your research team to ensure full understanding by everyone listed within this AUP.

As per your declaration within this approved AUP, you are obligated to ensure that:

1. This Animal Use Protocol is in compliance with:
 - o [Western's Senate MAPP 7.12 \[PDF\]](#); and
 - o [Applicable Animal Care Committee policies and procedures](#).
2. Prior to initiating any study-related activities—as per institutional OH&S policies—all individuals listed within this AUP who will be using or potentially exposed to hazardous materials will have:
 - o Completed the appropriate institutional OH&S training;
 - o Completed the appropriate facility-level training; and
 - o Reviewed related (M)SDS Sheets.

Submitted by: Cristancho, Martha on behalf of the Animal Care Committee

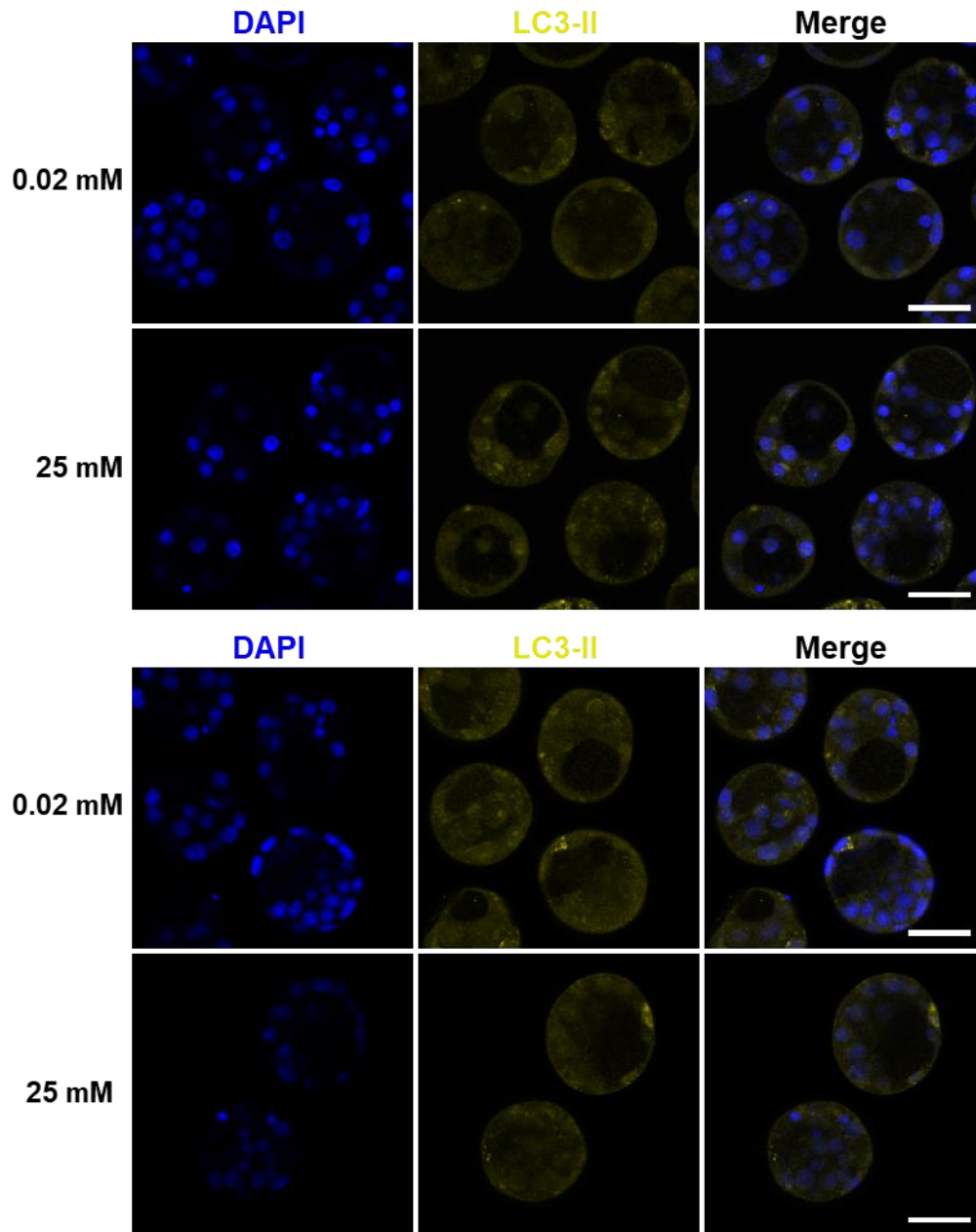


Animal Care Committee Chair

Animal Care Committee
The University of Western Ontario
London, Ontario Canada N6A 5C1

 | [ACC Website](#)

Appendix B: Supplementary Figure



Supplementary Figure 1: Raw (unprocessed) images of LC3 staining after early (36 hpi) and late (48 hpi) 2-cell culture in 0.2 mM (control) and 25 mM (high glucose) until the blastocyst

stage (E3.5; 96 hpi). Scale bars represent 50 μm . Figure created using QuickFigures (FIJI plugin). Figure corresponds with Figure 14 in results section.

Curriculum Vitae

Name:	Virginia Wolfe
Post-secondary Education and Degrees:	McMaster University Hamilton, Ontario, Canada 2016-2020 B.Sc.
Honours and Awards:	Trainee Award Childrens Health Research Institute July 2021 Western University Graduate Scholarships Obstetrics and Gynecology Graduate Scholarship August 2021 Physiology and Pharmacology Graduate Awards Stavraky Teaching Award November 2022
Related Work Experience	Teaching Assistant The University of Western Ontario January 2021- January 2023
Publications:	<i>Abstract:</i> Wolfe, V., Betts, D., & Watson, A. (2022). Investigating apoptosis and autophagy in hyperglycemic embryo culture. <i>Reproduction, Fertility and Development</i> , 35(2), 164-164.
Conferences:	London Health Research Day Western University, Canada (virtual) May 2022 Poster Child Health Research Day London ON, Canada May 2022 Poster Phys-Pharm Research Day London ON, Canada November 2022 Poster International Embryo Technology Society Lima, Peru January 2023 Poster Great Lakes Developmental Biology Meeting Toronto, ON, Canada June 2023